ACIT5900
MASTER THESIS
in
Applied Computer and Information Technology (ACIT)
May 2022

Robotics and Control

Control of wastewater overflow in Oslo

Halid Seyhan - s351671@oslomet.no

Supervisor: Tiina Komulainen – timako@oslomet.no

Department of Computer Science

Faculty of Technology, Art and Design

1 Preface

Being robotics and control specialization students, in our first semester, we took one robotics and one control subject as I shortly name them. Looking back, I can say that both were the hardest courses I had in my master's period. Ironically, they left the highest interest and satisfaction when I passed them. Especially, the control subject with its modelling and simulation aspects. Although, I tend to seek unfamiliar challenges if I can, a professor advised me to not attempt "artificial retina" since I have also chosen the short thesis which gives you roughly 4 months. Following his advice, also recalling the interest I had, I chose the "Control of Wastewater Overflow in Oslo". It was one of the better choices I made in life.

Although the initial focus was the control, this work was from the scratch. Therefore, it started with data collection with actually googling, revising previous works, reaching out to any technical data I could, continued with the modelling of the Oslo sewer network, finding and modelling rain event scenarios, lastly the control and running the simulations. Each step itself took quite the effort, but I enjoyed the challenge. My main focus was not finalizing the thesis. Instead, it was to put out a work that I could be satisfied with and realize the ideas I had within. Having these intentions, I made the model as realistic as possible I could, also efficient and flexible for any further work ideas from the beginning. In plain words, I still had ideas to go with which are mostly conveyed in the further work section. I should also point out the fact that what the developed model represents in real world is a very large and complex system. Reinforced with the restrictions to reach the data of the system and with the required simplifications to be able to model the system in a MATLAB/Simulink environment (Inc., 2021), a lot of assumptions were inevitable. I tried to clearly explain every assumption, simplification, and the method I used in the report. I sincerely wanted the artefact to also be relevant for any practical application. Therefore, the model is designed flexible and efficient for future calibrations and applications.

Overall, it was a nice journey that sometimes made me feel time passing faster and other times, vice versa. Master's thesis experience gave me a lot, which I will remember and probably be more aware of in the future. Firstly, I want to thank to my supervisor Tiina

Komulainen from my university Oslo Metropolitan for her valuable feedbacks, supporting and improving my ideas and occasionally clarifying the unsureness's, in other words, removing the knots in the pipes and restarting the steady flow of the work. Secondly, I want to thank to our collaboration partners that shared their valuable time and experiences with me in this work. Finn Aakre Haugen and Yongjie Wang from USN/Universitet i Sørøst Norge for providing me insights on how and where to start my work which is quite the concern in the beginning of any work. Christian Almestad, Berislav Tomicic and Ryan Walter Murray from DHI / Danish Hydraulic Institute for sharing their rich experiences from a business perspective, being helpful and transparent with the MIKE+ and the Future City Flow project. Johansen Hilde from VEAS/ Vestfjorden Avløpsselskap and Lars Olov Orre from Oslo VAV, Vann og avløpsetaten for giving me the red pill so I could wake up from my model and relocate myself in the real Oslo Sewer Network. Lastly special thanks to my dear wife Sena Uysun which is also a student for sharing similar struggles with me. I could also never end my text without thanking to my family in my homeland for supporting me when we speak on the phone by asking how my studies are going.

Halid SEYHAN 5 May 2022

2 Abstract/Summary

Purpose of this study was to obtain an accurate model of Oslo Sewer Network and to develop SISO and MIMO control strategies to minimize overflows. In Oslo, water quality in the fjord is a major concern. Extreme rain events cause untreated water spill to the Oslo fjord from the sewer network. Oslo Municipality is aiming to cut the overflow to Oslo fjord by 2035 and it is expected that with the climate change, Oslo region will face more extreme and frequent rain events in the future. Therefore, implementation of a real-time control strategy for the sewer network can contribute to have a cleaner water in the fjord. In this study, after a literature review on RTC and urban drainage systems, a model of the Oslo sewer network has been created in MATLAB/Simulink (Inc., 2021) environment. Second, SISO and MIMO control strategies are developed with the purpose of minimizing overflows. Third, historical rain events with varying intensity have been simulated and the performance of the control strategies have been tested with and without a real time optimization based on the weather forecast data. Accordingly, Research questions are: How much real-time control can reduce the overflows? How well SISO and MIMO control strategies perform in comparison? And how much will the real-time optimization with forecast data will improve their performances?

3 Table of Contents

4 List of Figures

5 List of Tables

6 Abbreviations, Symbols and Nomenclature

USN - Universitet i Sørøst Norge , University of Southeastern Norway

DHI - Danish Hydraulic Institute

Oslo VEAS - Vestfjorden Avløpsselskap / Westfjord Sewage Company

Oslo VAV - Vann og avløpsetaten / Water and Sewage Department

SN - Sewer Network

RTC - real time control

SISO – Single input single output

MIMO – Multiple input multiple output

Europe WFD – Water framework directive

WWTP - wastewater treatment plant

DO - dissolved oxygen

CSO - Combined sewer overflow

Overland flow: The transformation from resulting effective rainfall into a surface flow hydrograph.

Integrated modelling: modelling of the interaction between multiple systems having different governing equations.

Flooding – Condition where wastewater and/or surface water escapes from or cannot enter a drain or sewer system and either remains on the surface or enters buildings. EN752

Surcharge - Condition in which wastewater and/or surface water is held under pressure within a gravity drain or sewer system but does not escape to the surface to cause flooding. EN 752

RAS – Return activated sludge

Separate systems: meaning that stormwater and wastewater flows in distinct pipe systems.

Combined systems that convey both types of water in the same pipes.

NWP - numerical weather prediction

CV – Controlled variable

MV – Manipulated variable

DV – Disturbance variable

7 Introduction

As climate change puts its effects into action, northern Europe countries expect more frequent and intense precipitation in the future. Extreme weather will affect vulnerable urban drainage systems and cause larger and more frequent unwanted CSO events. Accordingly, many countries have initiated and accelerated scientific research and in parallel, infrastructure planning to prevent CSOs and other climate related problems in the future.

In 2015, Oslo city set the goal of becoming a climate resilient city. By 2030, city should have prepared itself for the expected changes until 2100. Today, Oslo city is already 1.5 degrees warmer and takes 15% more rain and the intensity and the frequency of extreme weather events have increased compared to previous century. (Department, 2020)

Oslo is the largest city in Norway as well as the capital of Norway. Metropolitan area with its surrounding municipalities hosts more than one million citizens which is around one fifth of the country's all population. The region takes a significant amount of precipitation each year, approximate value being 1010 mm. These factors exert a considerable pressure on the city's urban drainage system and CSOs happen throughout the year when it rains in Oslo. Regions receiving water body is the Oslo fjord. When CSOs happen, released untreated wastewater-rainwater mixture affects the water quality of the Oslo Fjord significantly. Occasionally, after such rain events, public is alerted against swimming in the fjord. Only in 2003, 3.79 million m^3 untreated water was spilled from the sewer network to the fjord at measured overflow points. (Kjell Terje Nedland, 2005) Since then, the capacity of the sewer network has been increased significantly yet, at the same time, population has been increasing and the climate change has been causing more intense and frequent rain events. Oslo municipality and partners have been on the subject for decades now. Infrastructural upgrades are ongoing, but they progress very slowly since they require exhaustive planning, budgeting, legal proceedings and especially, the constructing.

Rains do not always only result in untreated water spill to the fjord at overflow points. When extreme rain events hit, damage go beyond. In the last decade, Oslo city has faced several rain events resulting in floodings in some parts of the city. For example, on 12 June 2019, there were floodings in some basements. On 9 August 2017, which is one of the most extreme rain events in region's history, underground passages at Jernbanetorget station were filled with water and many basements were flooded. (Department, 2020) Four rain events, including these two extremities and more ordinary events are simulated in the developed Oslo SN model with control strategies in this study.

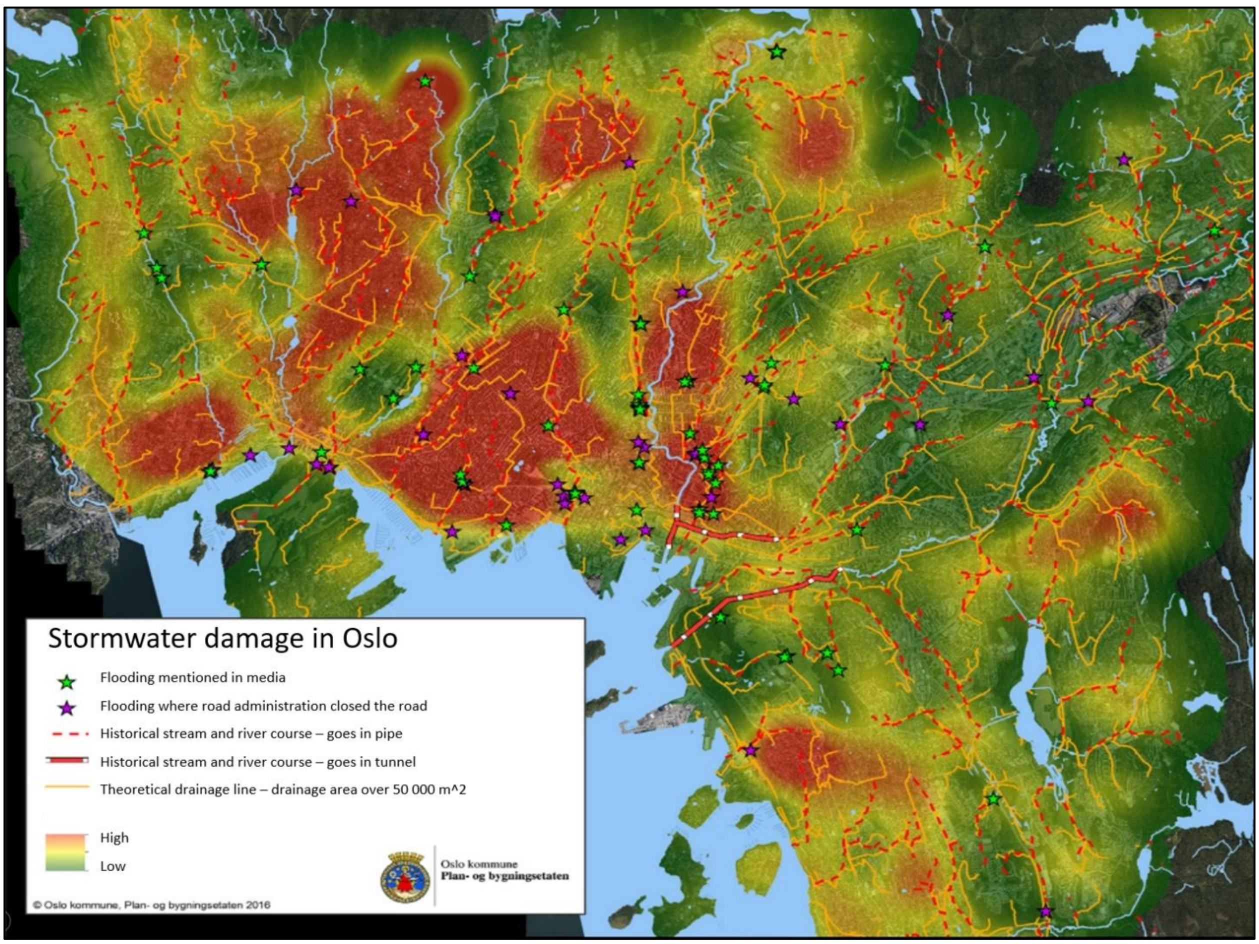

Figure 1 Registered damages in Oslo due to stormwater in the period 2008-2014

According to the report "Climate Change vulnerability Analysis for Oslo" by Oslo Municipality Climate Department (Department, 2020)

The Oslo fjord lies deep into the land and has close interactions with the Oslo city center and coastline municipalities. It has a long and narrow connection to open sea which limits the seawater circulation and make the fjord more vulnerable to any kind of pollution. It should be emphasized that rain induced CSOs are one of the many problems that affect the health of the fjord.

In parallel with the ongoing infrastructural improvements, an implementation of a real-time control strategy can further contribute to minimize the CSOs for Oslo. Advantage of an RTC compared to an infrastructural upgrade is that the performance of the system may jump up by simply effectively utilizing the volume of the sewer network and the already existing actuators in the system. Ensuring the optimal drift of the system with an RTC may provide the same improvement with much less cost and time.

Both the infrastructural upgrade and the RTC strategy cannot be simply implemented to a critical and vast urban drainage system without thorough investigations. In this case, modelling and simulation are very efficient and powerful tools to predict the effects of possible future projects on the system. Scope of this study has only covered the RTC aspect of the urban drainage systems with the case being the Oslo region. Modelling, simulation and visualization of results in this work are done in MATLAB/Simulink (Inc., 2021) environment.

The modelling in this work consists of three sub-models. Firstly, a simple ratio model is developed for rainfall-SN inlet inflow conversion. Conversion model accounts for the parameters of the catchments and dictates the portion of rainwater that should enter the SN. Inlet Inflows of the conversion model is not limited. Therefore, it is not possible to have surface overflows at the inlet points of the Oslo SN model. Supposed surface overflows are allowed to the Oslo SN but is spilled out of system at the first limited overflow point to the fjord. This principle cannot overload the model because rainfall input to the conversion model is always finite. Accordingly, for very extreme events' simulations, total overflow to the fjord deduced from the model can be interpreted as the total stormwater damage to the fjord and the city including surface and basement floodings etc. So, the total overflow generated by the model is always of relevance with respect to the actual rainfall of the simulated event and can be used to compare the performance of control strategies for the Oslo SN in a clearer picture. In plain words, all sorts of stormwater damages to the city and to the fjord are assumed as total overflow to the fjord in the model.

Second sub-model is the Oslo Sewer Network model itself. Network is approximated as 13 links and 5 magazines. A link basically is a pipe without a volume, so links are modelled as transport delays. Magazines on the other hand, are pipes with volumes. They are modelled as transport delays similar to the links but also with a volume in the end. Transport delays and magazine outflows are nonlinear properties of the model because they vary on how filled the related network sections are on each time step. Additionally, there are 3 pumps, 2 gates and a flow separator weir in the Oslo SN model. In an ideal scenario without any overflows, all flows into the model should end at the two wastewater treatment plants of the Oslo region.

Third and last sub-model is the overflow model. In this work, a unique approach has been created to model the overflow of the Oslo SN. 5 fixed magazine volumes are where the overflows are modelled. For each magazine, there is a virtual magazine which has infinite volume. Virtual and real magazine couples take the exact same input from the Oslo SN model and the volume differences between the couples at the end of the simulations are interpreted as the overflows.

Outflow from a magazine is either strictly dictated by a pump or a combination of a gate and how filled the magazine is. For the overflow model, possible maximum outflows from the magazines are very decisive of the overflow volume in the model. These critical constraints are computed with tracing the flow loads across the network back to their catchment origins. Maximum flow input capacity of the two WWTPs, in other words, maximum outflow capacity of the Oslo SN without an overflow is weighed against the total flow load at these end points. Founded weight has been interpolated backwards in the system to find the maximum outflows from the gated magazines. Under simulations, the interpolation assumption made it harder to get overflows in the later magazines (Esp. VEAS magazine). The constraints in the model were flexible for any calibration but the change was evaluated unnecessary since the later feedback revealed that indeed, it is quite hard to get overflows in the later section magazines of the Oslo SN. Overflows and storm water damages are more frequent around the city center.

For the control of the model, governing equations of the model were linearized and transfer functions to be used in control applications were derived. 6 inlet flows are disturbance variables. Pumps, gates and separation weir are 6 manipulated variables in total. 5 controlled variables are the water levels in the 5 magazines. Each CV is paired with the magazine's outflow MV. Fagerlia separation weir on the other hand, has its own independent control for allocating the northern main inflow to the SN between the two WWTPs.

In the case of an urban drainage system control, a feedforward control should theoretically perform very well, since the rainfall disturbance to the system can be anticipated with weather forecast and the process has a lot of delays (from the rainfall to the actual overflows from the SN). Feedforward control can prepare the system by maximizing available volume in the Oslo SN before the rain hits. The same strategy however can also be achieved by implementing real-time optimization of CV set-points using the forecast data in a feedback control strategy. The latter is tested in this study.

A SISO control strategy with PI controllers and a MIMO control strategy with an MPC will be compared. Both control strategies are tested with and without a real-time optimization with forecast data as well. Tests are done with simulation of rain events selected from the rainfall historical data of the region. The model itself has strong nonlinearities yet, the tested controllers are based on the linearized transfer functions. Accordingly, this study will also provide an answer to the research question; how effective are linear PI and MPC controllers to control a non-linear urban drainage system model. Tuning of the PI controllers were done according to Skogestad rules. (Skogestad, 2002) Tuning of the MPC was done according to the book 'Process Dynamics and Control' (Dale E. Seborg, 2004) and findings in the literature review about MPC of urban drainage systems. Specifically: (Nadia Schou Vorndran Lund, 2018)

Oslo SN like most SNs, is controlled by a rather conventional way. Actuators are deployed by operators which simply can be approximated as a rule-based control. VAV and VEAS have had collaboration with universities USN and Oslo Met for research addressing a potential real time control for Oslo SN. For a professional solution to the problem business contract with the DHI initiated the Future City Project (DHI, 2022) for Oslo and a high-fidelity MIKE modelling of the SN. MIKE model is finished and calibrated, ongoing step is the RTC for the Oslo SN. Accordingly, this study has been completed in collaboration with Oslo VAV, VEAS and DHI.

8 Literature Review

Urban drainage systems are very large and established in a way that projects on them require very through investigations, planning and legislation. Infrastructure projects are long-term and costly which makes urban drainage modeling very indispensable.

Solely modeling the hydrodynamic processes within an urban drainage system may not be sufficient because, urban drainage systems are known to have strong interactions with their environments. Early phases of urban-drainage modeling revealed that modelling of urban drainage systems require modules or even separate models that describe dominant processes around the system. Such processes can be for example rainfall-surface runoff or other hydrological processes. First one is more dominant in impervious city catchments, whereas the latter process is more dominant in rural catchment areas. Accordingly, most urban drainage models are integrated models by necessity.

Which processes to integrate in your model depends on the environment of the subject drainage system and the problem to be addressed. Modelling of an integrated urban wastewater system, starting point, the principles and the problems to address are clearly and extensively illustrated by (Wolfgang Rauch, 2002):

8.1 Three typical problems:

8.1.1 Toxic impact due to unionized ammonia discharged mainly from CSOs.

CSO discharge is caused by short-term hydrodynamic effects in the sewer system which requires hydrodynamic instead of hydrologic transport modelling.

8.1.2 Hygienic problems caused by faecal coliforms.

8.1.3 Oxygen depletion in river

Problems in water environments could be simplified as either the quality of the subject water is inadequate, or the placement of the water volume is undesired. Since one can easily affect the other, combinations of the two are common.

In the case of an urban drainage system, both problems are strongly present. Floodings are unwanted in the catchment areas of the SN, also the quality of the receiving water body that intakes the overflows and the treated water should be adequate.

8.2 Prerequisite for modelling of drainage systems dynamics

In a modeling work, based on the scope, required integrity, dominant processes, and the problems to be addressed, the modules to be included are listed below (Wolfgang Rauch, 2002):

8.2.1 Rainfall-runoff modeling

A model should generally include some type of conversion model to convert the rainfall to surface runoff. Catchments' surface runoff concentrates with time and enter as inflows to the SN model thorough nodes (manholes etc.). There are several methods to model these processes. (J. Sitterson, 2018)

8.2.2 Hydraulics in sewer systems

Either an unsteady open channel flow model (based on Saint Venant equations) or simpler flow routing models (reservoirs in series with the water being routed downstream) should be used to model hydraulics in a SN.

8.2.3 Water quality and pollution transport in sewer systems

In cases where a closer look to the quality of water is required, pollutant accumulation, pollutant wash off, pollutant transport transfer and pollutant processes should be included in the modeling.

8.2.4 Wastewater treatment

Treatment process at the plants itself is a very complex process with several steps and should require a separate module or a model. There are available modeling software's in the field that are specifically specialized for modeling of wastewater treatment plants. Included processes in the model should be:

Flow propagation and mixing

Usually, instantaneous flow propagation is assumed. Mixing is typically modelled using the continuous stirred tank reactors (CSTR) in series approach.

Unit process descriptors

Clarifiers, activated sludge, biofilms, anaerobic digestion

8.2.5 Rivers (and other receiving waters)

Dominant receiving water impacts are single event or accumulative effects. Single events refer to short term simulations for example a rain event and the consequential CSOs or river flow/level increases. Accumulative effects are on the other hand refer to the pollutants which make progress under relatively long periods of time.

8.3 Dual drainage modelling of flooding in urban areas

A relatively early example of integrated modelling can be "coupled dual drainage modelling" where surface-flow and drainage system dynamics interact with each other:

Presented RisUrSim is in the European research project EUREKA. Surcharged sewer systems lead to the necessity of dual drainage models to analyze urban floods. Dual drainage modeling is described as the distinct surface flow and its interaction with sewer flow in surcharged sewer systems. (Theo G. Schmitt, 2004)

According to European Standard EN 752, approved by European Committee for Standardization, urban drainage systems should be designed to withstand with periods of flooding in range of 10 to 50 years dependent on the type of the area. EN752 specifies the design of storm and flooding frequencies varying for rural, residential and industrial/commercial areas. (Theo G. Schmitt, 2004)

Dual modeling should accurately describe the hydraulic phenomena: (Theo G. Schmitt, 2004)

- Transition from free surface flow to pressure flow to the sewer system
- Rise of the water above ground level leading to water escaping from sewer system
- Surface flow created by flooding
- Interaction between surface flow and pressurized sewer flow

Urban drainage modelling specifies system components as: (Theo G. Schmitt, 2004)

- Single drainage areas (roofs, streets, parking lots, yards etc.) where rainfall is transformed into runoff
- Distinct surface drainage components (street gutters) where surface runoff is lead into the sewer system through inlets
- Surface areas where surface flow might occur in case of flooding
- Closed underground sewer (manholes, control structures and outlets) forming the sewer network

In simulation, single areas are implemented as mostly sub-catchments that are linked to sewer network via input elements, mostly manholes represented as nodes. (Theo G. Schmitt, 2004)

RisUrSim is composed of three modules. Module RisoReff defines areas where surface flow, flooding and sewer flow are excluded. (e.g. roofs) Here, surface runoff enters the sewer system at specific inlets with a uni-directional manner. Module RisoSurf computes surfaceflow according to shallow water equations (Navier-Stokes) and dynamic sewer flow (Saint-Venant-Equations) is within the module HamokaRis. Underground sewer system is represented by a set of nodes and conduits (sewer segments between nodes). There is a bi-directional exchange of flow between surface flow module and the sewer flow module. (Theo G. Schmitt, 2004)

A case study with dual drainage modelling is applied for Kaiserslautern, Germany and surface flooding could be reproduced realistically. (Theo G. Schmitt, 2004)

8.4 Coupled hydrologic-hydraulic modelling for mixed-urban areas

A higher integration level model compared to “dual drainage modeling” is for example, the “coupled hydrologic-hydraulic modeling” in which, the rainfall-runoff, hydrologic processes

State-of-the-art urban flood modelling is done by a coupled 1D pipe and 2D overland flow to simultaneously represent pipe and surface flows. This method is useful with highly paved urban areas, but it is questionable for rural areas where land hydrology processes are strong. (e.g., evatransportation, infiltration and flow exchange between surface and groundwater). Initially, hydrologic-hydraulic models were used for problems related to groundwater infiltration into sewers. Today, a new method with a 3D hydrologic model and a 1D drainage network coupled can be used for mixed-urban areas. Specifically, a MIKE SHE model can be used for simulating land-phase hydrology, MOUSE for urban drainage (with a fully hydrodynamic pipe flow module and a conceptual surface run-off module for simulating pipe flows). (N. D. Sto Domingo, 2010)

Impervious areas such as houses, roads and walkways are included in the runoff module of the pipe model. Station-based precipitation is applied over the area. In hydrological model, land surface properties such as vegetation cover, roughness and landuse are described based on GIS and national database data. These pervious areas are subject to precipitation, evaporation and infiltration processes. (N. D. Sto Domingo, 2010)

The interaction between the pipe network and the hydrology is modelled through flow exchange at certain linking points and segments defined with head differences and exchange coefficients. (N. D. Sto Domingo, 2010)

8.4.1 Coupled modeling Cases:

8.4.1.1 Greve municipality in Denmark

City center is highly built-up along the coast and has large green areas which are mostly agriculture areas in the upper catchments. City center is prone to flooding which is known with historical data. New coupled hydrologic-hydraulic method is considered effective for such semi-urban areas. City center had already been modelled with a traditional 1D-2D method before and the results were in agreement with the flooding observed in the past. (N. D. Sto Domingo, 2010)

8.4.1.2 Olsbakken

Hydrologic-hydraulic model was also applied to mixed-urban catchment of Olsbakken north of the city center. (N. D. Sto Domingo, 2010)

Results of the newly implemented hydrologic-hydraulic model for both cases were in par with the state-of-the-art methods. In addition, new model provides insight to hydrologic process while describing flooding in mixed-urban areas. (N. D. Sto Domingo, 2010)

8.5 Integrated urban water modelling

Many other urban drainage modelling names with different integration levels and properties can be found in literature. Aforementioned two studies were only examples of the progression of integrated modelling. In order to get a clear picture of the integrated urban drainage modeling a classification can be useful.

Since water management field requires modelling of the interaction between multiple systems having different governing equations, integrated models and program platforms are developed. In integrated modelling, the primary focus has been the interaction between overall systems components.

8.5.1 Modelling based on integration Level

According to Bach and colleagues, urban drainage models can be classified based on four 'degrees of integration' levels. A higher integration level can be interpreted as a model with larger extent where more components and their interactions of the real system are included in the modeling work. (Peter M. Bach, 2014)

8.5.1.1 Integrated component-based models (ICBMs)

Integration of components within the local urban water sub-system (e.g. coupling several treatment processes within a wastewater treatment plant.) These are analogous to plant-wide models.

8.5.1.2 Integrated urban drainage models (IUDMs) or integrated water supply models (IWSMs)

Integrating sub-systems of either IUDMs or IWSMs

8.5.1.3 Integrated urban water cycle models (IUWCs)

Linking IUDMs and IWSMs into a single framework also known as 'total urban water cycle'.

8.5.1.4 Integrated urban water system models (IUWSMs)

While focus remains on the urban water, these models combine the urban water cycle with different disciplines (e.g. climate, economics).

From category 1 to 4, system scope becomes broader and creates a higher-level managerial problem and work becomes more interdisciplinary. Integrated Urban Water Systems themselves stay under the broader field of Environmental Decision Support Systems (EDSSs). (Peter M. Bach, 2014)

8.5.2 Classification and specifications of urban drainage system software packages

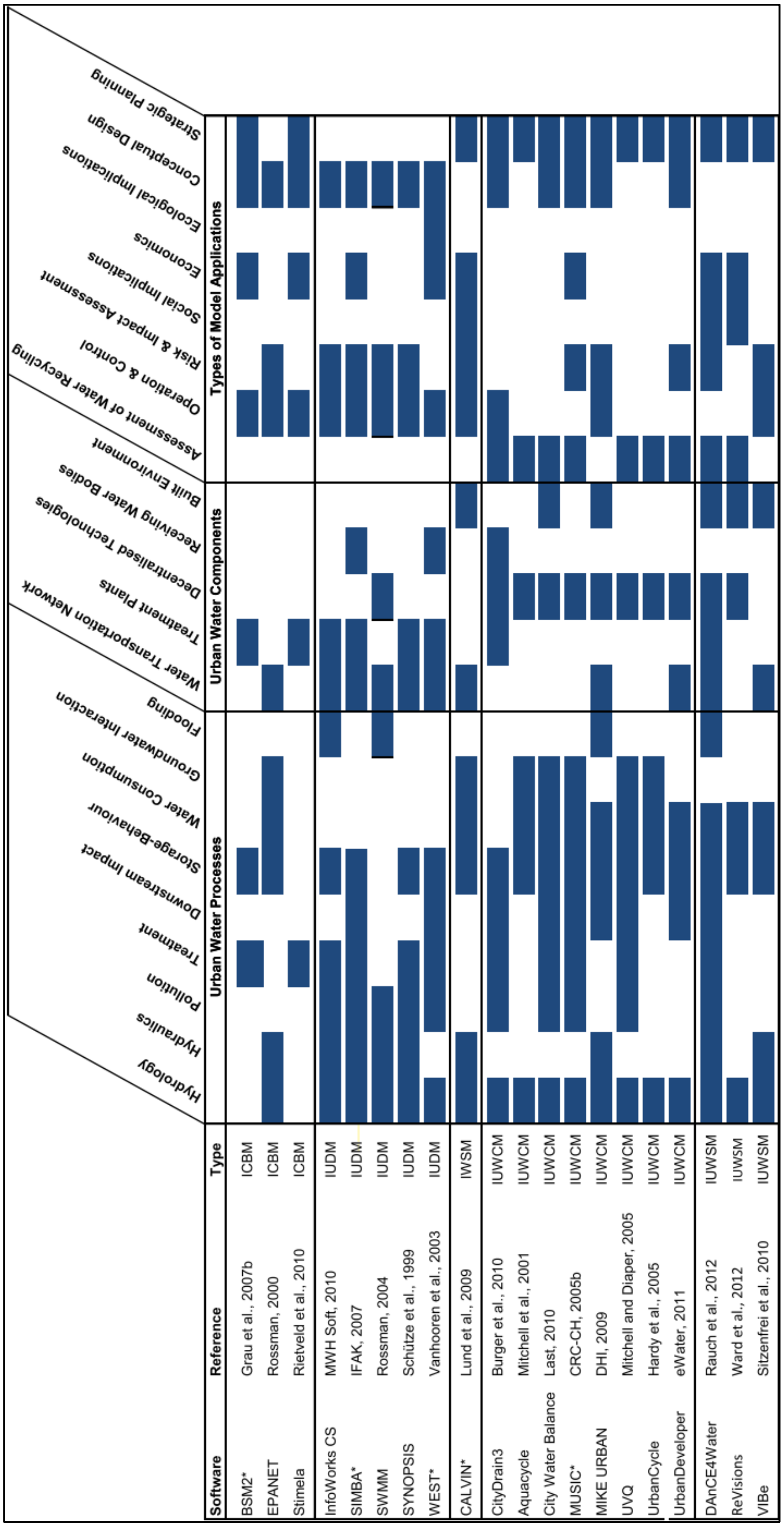

Figure 2 Urban drainage modeling packages (Peter M. Bach 2014)

In addition to the integration level classification, in Figure 2 Urban drainage modeling packages (Peter M. Bach 2014), a nice overview over available urban drainage software packages and their capabilities are presented.

Bach and the colleagues pointed out the problems we face with the integrated modelling. Accordingly, we still lack sound knowledge on feedback loops in integrated models. We do not have access to suitable algorithms and sub-models for integration because of their excessive complexity, different purposes of development at their times and having incompatible parameters and variables. (Peter M. Bach, 2014)

8.6 Integrated modelling cases:

8.6.1 Congost in Spain (Lorenzo Benedetti, 2013)

Models were Infoworks CS for sewer systems, GPS-X for WWTPs and Infoworks RS for the river. An integrated model was built in WEST. The expert knowledge together with rules generated from an interpretation of the simulation results is integrated in an environmental decision support system that is helping water managers to take decisions.

8.6.2 Copenhagen and Aarhus in Denmark (Lorenzo Benedetti, 2013)

In the case of Copenhagen, for modeling, a MIKE model of 76 km2 catchment was integrated with a WEST model of the Lynetten WWTP. Major infrastructural investments were combined with the implementation of integrated RTC systems for the SN. RTC was developed in detailed hydrodynamic MIKE models and supported with weather radar nowcasting.

In the city of Aalborg, control of WWTP based on catchment flow forecasting is currently applied and it is in the testing phase for the Lynetten WWTP. (Lorenzo Benedetti, 2013)

8.6.3 Eindhoven in Netherlands (Lorenzo Benedetti, 2013)

For the case of Eindhoven, main issue was the water quality. In 2006, an integrated monitoring network was implemented in the sewer, WWTP and river (The Dommel). Models for sewer, WWTP and river were integrated in WEST.

8.6.4 Trondheim in Norway (Wolfgang Rauch, 2002)

A SIMBA model for Trondheim consists of 83 sub-catchments and 72 other installations such as pumping stations, overflows, and retention tanks. After model calibration, simulations with remedial measures (increased pump capacity, revised overflow settings, installation of storage tanks, separation of sewers, reduction of groundwater infiltration and dynamic regulation of tunnel storage.) were conducted. Findings predicted reduced hydraulic load for possible future treatment plant by 10-20%. Also, for some overflows, discharges reduced up to 80%.

8.7 Climate change impacts on urban drainage systems

Climate change has started to increase the intensity and frequency of extreme weather events all around the world. Specifically, in Nordic countries of Europe, reports indicate more intense rainfalls and increased mean sea-level at coastal municipalities. Urban drainage systems are known to be vulnerable to these conditions. Accordingly, many Nordic countries have initiated research on how they can mitigate the impact of climate change on sewer systems with cost-efficient and timely manageable methods. (O. Mark, 2008)

8.7.1 Denmark

In accordance with the climate change, in Denmark, high intensity rain fall events will increase in summer and the mean sea level will increase as well. The Danish Water and Wastewater Association (DANVA) has taken the decision to carry out research directly applicable to Danish municipalities for adaptation to climate change. (O. Mark, 2008)

8.7.2 Sweden

The report from the Swedish Association for Water and Wastewater states that the climate change may affect the drinking water systems as well as the wastewater system. Climate change scenarios show less rain fall for summer, but at least 40-50% more rain fall during winter and autumn. (O. Mark, 2008)

8.7.3 Norway

According to the report issued by The Ministry of Environment in 2006, Norway must except higher frequencies of intensity and volume for stormwater in accordance with the climate change. This will cause more surcharge events, increased sewer overflow events and volume, more stormwater overflows also increased load to the treatment plants. In addition, rising sea levels can cause backwater in the discharge pipes causing pollution of receiving waters. Over the next 50 years, precipitation volume will increase between 5% and 20% and heavy rain events will happen more often.

8.8 Modelling of Climate Change for Urban Drainage systems

A widespread usage of modelling for urban drainage is to investigate the effects of potential projects and future scenarios on the system. A worthwhile project should not only address the current issues of the system but also cover the expected scenarios with a safety margin into the future. Accordingly, modeling should include possible population increase and the effects of climate change.

An example of modeling climate change for urban drainage systems with implemented cases is presented by (O. Mark, 2008). First, rain gauge measurement history data are converted into rainfall grids as a climate model of the region. Then, expected growth in rain density is applied to climate model and converted back to the gauge measurements. For Denmark, rains used today are multiplied with a factor of 1.2-1.5 for climate change model. An upgrade today to comply with the worst-case climate change scenerio and a safety factor to the systems were estimated to be very costly. Therefore, municipalities are recommended to not invest heavily today for an upgrade and not to wait and see the full effects of climate change to act. Instead, they should get an assessment of impacts and develop a plan for timely management incorporated with their maintenance plans.

8.8.1 Climate change modelling cases:

8.8.1.1 Helsingborg: Lussebäcken catchment

Current situation with increased population and an upgraded system scenarios were applied to the model. According to results, city growth would slightly increase the flood risk.

Combination of city growth and the worst climate change scenario can cause worst drainage problems and upgraded system may not be enough to eliminate these combined impacts. (O. Mark, 2008)

8.8.1.2 Kalmar: Lindsdal catchment, Sweden

Higher rainfall intensities as a result of climate change would cause higher water flow in the pipes and consequently result in more frequent floods with also longer flooding durations. (O. Mark, 2008)

8.8.1.3 Odense, Denmark

Danish municipality have been experiencing floods. A combination of a 2-D surface flow model and a 1-D sewer system model was utilized. Volume exchange between the models were described depending on the flow conditions. Worst case climate change scenarios and a 20% safety factor were applied to the computation and results showed the predicted increase in floods. A local consultant proposed a solution which solves the main flooding, but other local solutions still should be applied. (O. Mark, 2008)

8.9 RTC applications of urban drainage systems

Research regarding real-time control of urban drainage systems, specifically MPC have gained a lot of attention recently. Real applications of advanced RTC in urban drainage systems are not in par with the papers yet, promising implementation examples keep emerging around the globe.

8.9.1 Review-MPC applications of urban drainage systems

Control of urban drainage systems consist of passive control (a certain static setting) or RTC (converting real-time measurements into operational decisions by rules and algorithms of varying complexity). RTC requires sensors and controllers, a telemetry system and a supervisory control and data acquisition (SCADA) system. (Nadia Schou Vorndran Lund, 2018)

Most urban water systems are controlled by passive control, rule based (local) control or manually by an operator. A global RTC system should be better than these methods meaning suboptimal control is very pervasive in urban water systems. Implementation of RTC has been limited due to unreliable sensors, actuators, communication systems supplemented with insufficient computational power. Implementation problems include uncertainty of input forecasts, lack of consensus on best practice within MPC, a confusing MPC terminology at the interface between many disciplines, crippling technology adaptation mostly due to trust issues and the lack of institutional capacity. (Nadia Schou Vorndran Lund, 2018)

Number of studies addressing MPC for urban drainage systems are increasing very rapidly over the years. For example, publication number between 2013-2017 is more than two times of the number between years 2008-2012. Yet, operational implementations are still very rare but MPC for urban drainage is a promising technology in the decades to come. (Nadia Schou Vorndran Lund, 2018)

MPC is an advantageous control strategy for complex urban water systems. MPC is suitable for a global control scheme but can also be applied locally. Provided with input predictions MPC can also anticipate potential problems arising in the system. (Nadia Schou Vorndran Lund, 2018)

Control of urban water systems mostly consist of minimizing CSOs in the system, and it is found that the minimization of CSO is highly dependent on the quality of the input forecasts for MPC. (Nadia Schou Vorndran Lund, 2018)

Main constraints for urban drainage systems can be for example, maximum and minimum basin volumes, flow through certain actuators and locations and maximum rate of change of actuator flows. (Nadia Schou Vorndran Lund, 2018)

Optimization model can either be a convex program or a non-linear program. Convex program is fast to solve with a guarantee of finding the global optimum however, system dynamics should be profoundly simplified. A non-linear model accounts for non-linearities in the system but can handle fewer optimization variables, no guarantee to find the global optimum and is computationally heavy. (Nadia Schou Vorndran Lund, 2018)

Previously, high fidelity models (for example MIKE URBAN from DHI and SWMM from EPA) were considered very suitable for design and analysis purposes but not suitable to be used as internal MPC models. (Elliott and Trowsdale, 2007). However, developments in non-linear MPC and advanced RTC of urban drainage systems enabled up-to-date advanced control toolboxes within high fidelity modeling software's. Newsworthy attempts are relatively fresh and there is still little consensus about how to conceptualize reality or a detailed HiFi model into an internal MPC model that is computationally feasible but still sufficiently accurate. (Nadia Schou Vorndran Lund, 2018)

Model should include complex phenomena; free flow to pressurized flow, internal overflows, external overflows, backwater effects. They are mostly non-linear and depend on the state of the system. (Nadia Schou Vorndran Lund, 2018)

8.9.2 Inputs to the MPC models

Input to the internal MPC model includes rain, runoff, and/or sewage from other part of the urban drainage system. Rainfall forecasts can be obtained from extrapolated radar rainfall estimates (Nowcast) or from NWP models. Radar nowcasts should perform better for short time periods (up to a couple of hours), whereas NWP is more reliable for longer time periods. Occasionally, large deviations occur between the nowcast and the NWP. Therefore, an input model is essential to tolerate uncertainties in predictions and to effectively converge two input systems. (Nadia Schou Vorndran Lund, 2018)

8.9.3 Advantages and disadvantages of MPC for urban drainage systems

Current findings indicate a slight positive correlation between catchment size and average CSO reduction for MPC applications. And homogenously long-time distributed rain scenarios with MPC are not likely to provide performance improvement. As a result, study shows that MPC for CSO mitigation may work better for larger catchments and that it is efficient for small and medium-sized events where storage is sufficient for optimization, whereas large events are mostly unaffected by MPC." (Nadia Schou Vorndran Lund, 2018)

8.9.4 MPC of urban drainage cases

8.9.4.1 The Astlingen system implemented in SIMBA# (Manfred Schuetze, 2021).

SIMBA# is developed by the Water & Energy department at ifak e.V., a private non-for-profit research institute in Magdeburg, Germany.

Most sewer operators already have a simplified (hydrologic) model of their system which can be used for a starting point of internal model of the MPC. (Manfred Schuetze, 2021)

MPC routine: An optimizer is called which also calls the internal model every 5 minutes. Control horizon was set for 30 minutes (with a typical receding horizon approach). (Manfred Schuetze, 2021)

A wide range of different optimizers are available in Simba# simulator (including local and global optimization routines). For Astlingen system, the BOBYQA algorithm (A constrained local derivative-free method) has been chosen and proven to be very effective. In comparison, an efficient global routine, Controlled Random Search did not yield better results. (Manfred Schuetze, 2021)

8.9.4.2 Kolding, Denmark MPC implementation (P. A. Stentoft, 2020)

Aim of this study was to minimize the electricity cost of the urban drainage system by minimizing actuator usage and maximizing available water volume in the system under dry weather conditions with an MPC.

Sewer systems are in dry-weather conditions for most of the time and have excess storage capacity. In (P. A. Stentoft, 2020) MPC strategy was to utilize this storage to delay the power consumption for pumping and treatment. After a simulation study, MPC had the actual operation for a total of 7-days trial period (2+5).

Aim was to control the power consumption and the effluent quality of a water resource recovery facility (WRRF). Electricity prices were known 12 to 36 hours ahead so, this price based MPC could react to electricity prices and forecasted pollutant loads 24 hours ahead. (Prediction horizon=24 hours). This MPC only operated in dry-weather conditions. (P. A. Stentoft, 2020)

A QP (Quadratic Programming) solver (from the R library quadprog) was used. (Which finds the optimal x that minimizes the objective function.) (P. A. Stentoft, 2020)

The strategy resulted in approximately 200 DKK savings per day. (P. A. Stentoft, 2020)

A water quality-based model predictive control approach was developed by (Congcong Sun, 2021).

8.10 Basic mathematical modelling of different elements in sewer network

In catchment/sewer modelling the main distinction is between models with full hydrodynamics (de Saint-Venant equations) in terms of partial differential equations (PDEs) and models with simplified hydrodynamics (tanks-in-series (TIS) approach) written as ordinary differential equations (ODEs). Simplified ODE models usually are of sufficient quality. (Lorenzo Benedetti, 2013)

HiFi models are suitable to represent quality dynamics and processes in sewer networks but not ideal for optimization due to computational requirements. Control-oriented quality models which can describe complex dynamics with simpler equations are a necessity for optimization in real-time. (Congcong Sun, 2021)

8.10.1 Detention tank

$$vol(k+1) = vol(k) + \Delta t\left(\sum_{i=1}^{n_{in}} f_{in}^{i}(k) - \sum_{i=1}^{n_{out}} f_{out}^{i}(k)\right) \qquad (1)$$

Δt is sampling time and k is time step.

Constraints:

$0 \leq f(k) \leq f^{max}$ maximum flow at certain locations (2)

$0 \leq vol(k) \leq vol^{max}$ maximum volume of the tank (3)

8.10.2 Gates or pumps

$$u(k) \leq u^{max}(k) \quad (4)$$

U is the vector of controlled variables and umax includes the maximum constraints.

8.10.3 Junction node

Mass balance is used for water in and out of a junction.

$$\sum_{i=1}^{n_{out}} f_{out}^{i}(k) = \sum_{i=1}^{n_{in}} f_{in}^{i}(k) \qquad (5)$$

8.10.4 Overflow

CSO occurs when the downstream element is exceeded by the flow in the upstream element.

$$f_{out}(k) = \max\{0, f_{in}(k) - maxcap(k)\} \qquad (6)$$

$$f_{out}(k) = f_{in}(k) - f_{CSO}(k) \qquad (7)$$

Total CSO:

$$f_{environment}(k) = \sum_{i=1}^{n_{CSO}} f_{CSO}^{i}(k) \qquad (8)$$

8.10.5 Sewer

Sewer or a collection of sewers in the network can be assumed as a tank which collects water based on the volumetric difference between input and output flows. (Equation 1)

Outflow vector f_{out} should comply with defined constraints but also should be proportional to the sewer volume $vol(k)$ at the current time step k:

$$f_{out}(k) = c_{int} * vol(k) \quad (9)$$

c_{int} is a vector of parameters which relates to the outflow of a sewer with the water volume stored in it.

Hydraulic transport in a sewer (combining equations 1 and 9):

$$f_{out}(k+1) = (1 - c_{int}\Delta t) f_{out}(k) + c_{int}\Delta t f_{in}(k) \quad (10)$$

8.10.6 Case study: Badalona, Spain (Congcong Sun, 2021)

HiFi model:

Figure 3 Badalona SN

Model is simulated in InfoWorks Integrated Catchment Modelling (InfoWorks ICM).

Blue cylindrical is detention tank. The WWTP is located on the side of the coast. Red colored outfall points along the coast are CSO locations. P1, P2 and P3 are rain gauges. (Congcong Sun, 2021)

Simplified model:

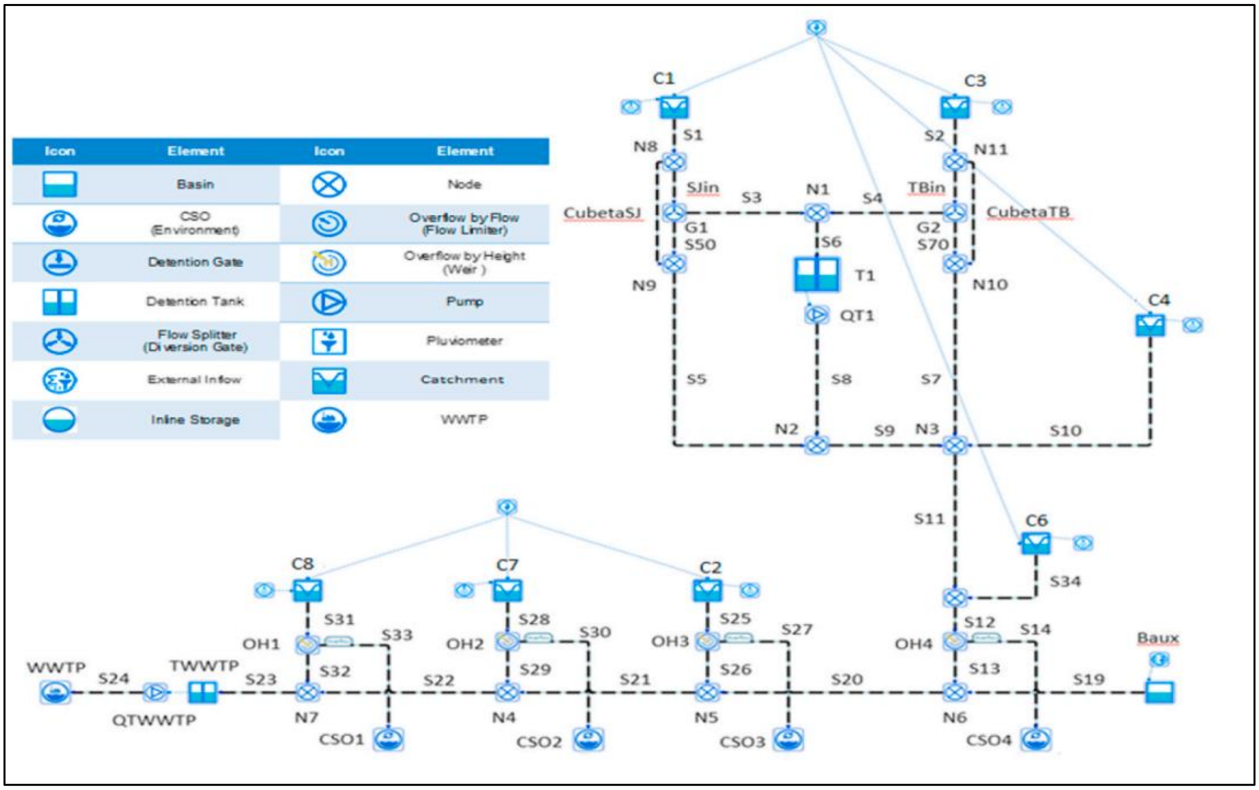

Figure 4 Simplified Badalona SN

7 catchments (C1,C2,C3,C4,C6,C7,C8) and a basin (Baux) connected by 35 links and 5 outfalls. There are 2 gates (G1,G2) operating water input to detention tank, one pump station (QT1) to empty the detention tank and another pump (QTWWTP) to schedule flows to the WWTP. (Congcong Sun, 2021)

The GAMS optimization library is used as a solver for the implemented MPC. (Rosenthal, 2007)

Compared to local control, MPC for some rain scenarios provided more than 20% CSO reduction and more than 12% reduction in TSS pollution. (Congcong Sun, 2021)

9 Method

9.1 Oslo urban drainage system

Sewage system of Oslo was constructed over a period of 150 years. Average age of the system is 53 years. Post 1965 constructions are mainly separated sewers. Today, 57% is combined and 43% is separated. (Oslo, 2019)

Oslo sewer network consists of 2350 km of sewers, 57 pumping stations, 11 retention basins and two WWTPs. The plants are connected to the network by 45 km of tunnels. (Oslo, 2019)

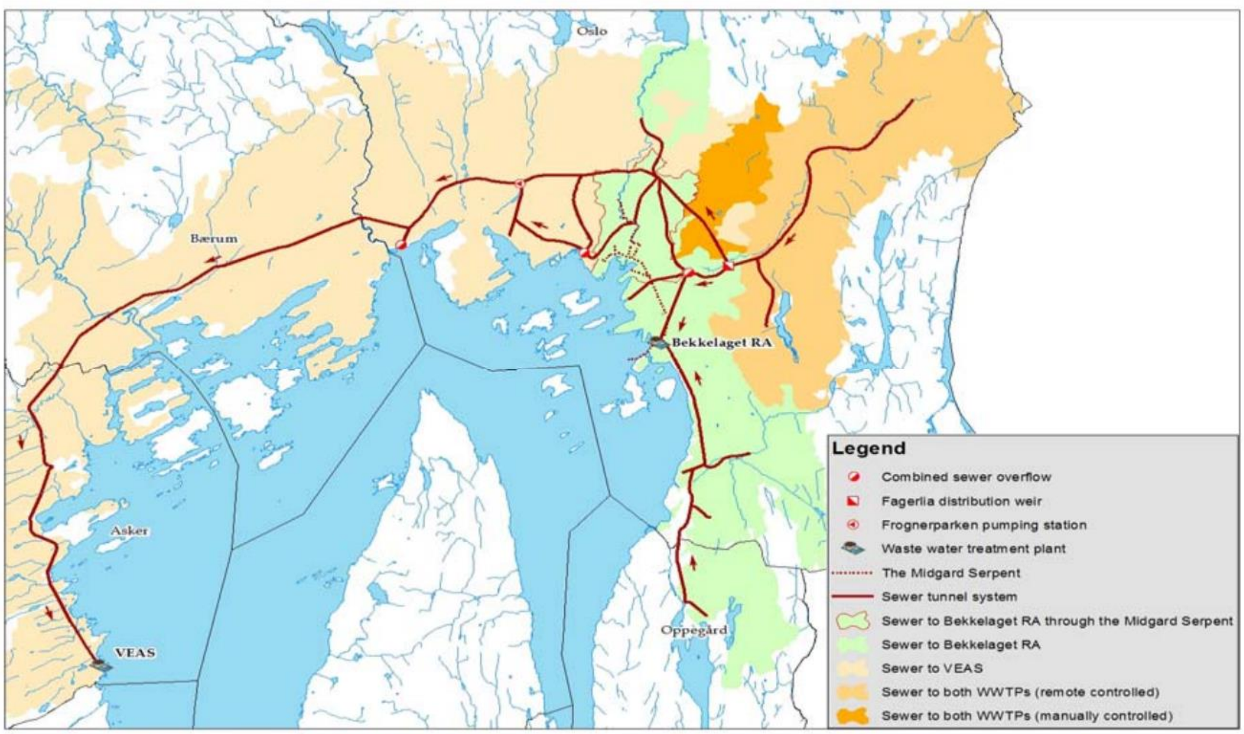

The map shows the sewage system in the city and the 45 km tunnel transporting 70 percent of the load to the VEAS WWTP.

Figure 5 Oslo sewer network

Figure 5 Oslo sewer network is from the report "Application Form for the European Green Capital Award 2019, 9 Wastewater management" of Oslo city. (Oslo, 2019) The Midgard Serpent is newly established sewage after investing 140 million Euro in 2014.

9.2 Oslo region wastewater treatment plants

9.2.1 VEAS WWTP

VEAS tunnel capacity 200,000,000 liters. On a day with no rainfall, VEAS treats 2300-3000 liters of wastewater each second. Maximum plant capacity is 11000 liters a second. Each year, the WWTP treats 100-110 million m^3 wastewater. (VEAS, 2022)

Taking approximately 2650 liters per second as base, on dry weather conditions, inflow to the VEAS plant is approximately 159 m^3/min. On a rainy day, taking maximum capacity of 11000 liters per second as base, maximum possible inflow to the VEAS plant is approximately 660 m^3/min. (VEAS, 2022)

9.2.2 Bekkelaget WWTP

In 2021, Bekkelaget WWTP increased its capacity from 270,000 people to 500,000 people. Now, the wwtp can handle %40 of Oslo municipal water. Lately, this improvement leaded to a more varying control of Fagerlia valve to optimize the flows into the two wwtps. (gruppen, 2022)

In our MATLAB/Simulink (Inc., 2021) model, 1,211,000 people are included from Oslo region. In steady state/dry weather conditions, 793,000 people's wastewater goes to VEAS WWTP and 418,000 people's wastewater goes to Bekkelaget WWTP.

Assuming those 793,000 people causing 159 m^3/min wastewater inflow to VEAS WWTP, one person is responsible for 0,0002005 m^3/min wastewater flow. Accordingly, 418,000 people would create 83.81 m^3/min wastewater inflow to the Bekkelaget wwtp.

Input to the Oslo SN model is inlet flows. An inlet flow takes in municipal wastewater and rain inflow when it rains. From a rainfall to a rain inflow to the sewer network, computation is done by a conversion model.

9.3 Modeling

9.3.1 Rainfall – Oslo SN inflow conversion model

9.3.1.1 Catchments

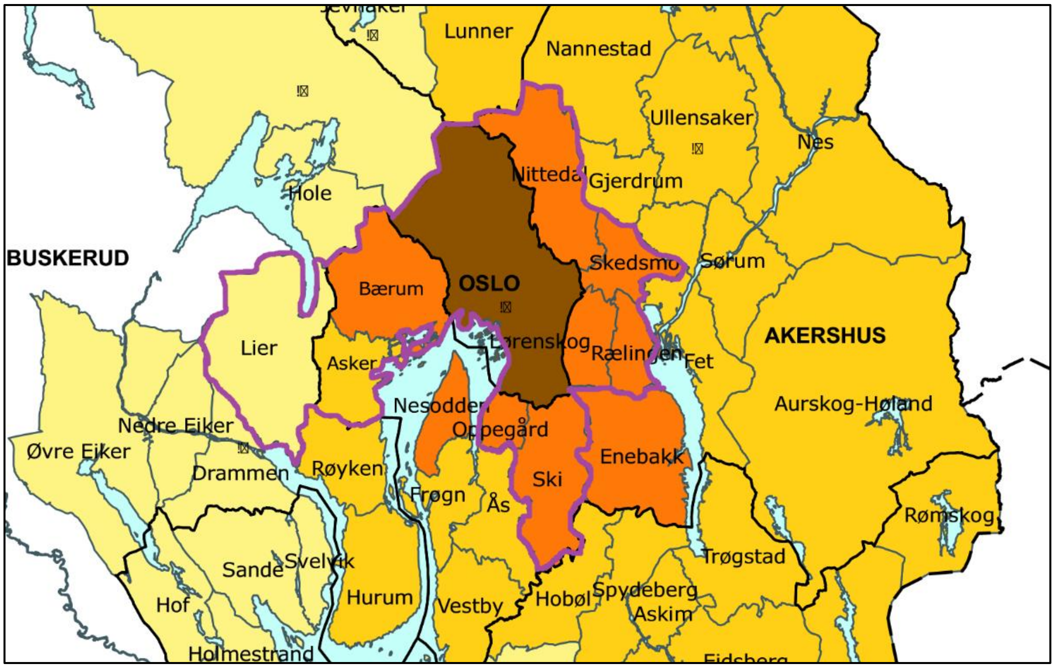

Figure 6 Included Oslo municipalities in the catchments/conversion model

A total of 1455300000 m^2 area and 1211000 people have been included from Oslo region as 9 catchment areas in the model.

A simple model will be used to convert rainfall to surface runoff for catchments.

- Rainfall intensity is assumed uniform over an entire catchment.
- Water moves with constant velocity to the network inlet that the catchment is connected to. Larger catchment area creates longer concentration time.
- Reduction factor will be 1 for all catchments meaning no water loss in rainfall – runoff conversion.
- Initial loss and all the other losses (evaporation, interception etc.) will be 0, meaning no loss.

- Catchment area imperviousness will directly affect the rainfall – runoff conversion ratio. For urban catchments, imperviousness is %20 and above and for rural catchments, it is under 20%.

Approximated values of the catchment parameters follow in the Table 1 Catchment parameters 1.

Table 1 Catchment parameters 1

Catchment	Regions	Population	Area [m^2]	Flows into
Catchment_1	Festning	150 000	77 000 000	Festning inlet
Catchment_2	Østensjø	125 000	77 000 000	East inlet
Catchment_3	Furuset	150 000	115 000 000	North inlet
Catchment_4	Torshov	150 000	115 000 000	Torshov inlet
Catchment_5	Nordstrand	125 000	77 000 000	Nordstrand inlet
Catchment_6	Lillestrøm+Lorenskog +Nittedal+Raelingen	181 000	415 800 000	North inlet
Catchment_7	Baerum	135 000	192 000 000	Baerum inlet
Catchment_8	Asker+Lier	130 000	192 000 000	Asker inlet
Catchment_9	Ski+Oppegård	65 000	192 000 000	Søndre Nordstrand inlet

9.3.1.2 Catchment data acquisition from MIKE+ Oslo SN model developed by DHI

There are 108 catchments in Oslo MIKE model ranging from 8.36 ha to 3150 ha. On the other hand, there are 9 catchments in our simpler model. Accordingly, it can be assumed that 1 catchment in our model represents a total of 12 catchments in MIKE model.

Values presented below will be a rounded approximation value of 12 catchment batches with highest and lowest values of the given parameter.

Imperviousness of catchments range from 0% to 40% with entire region being approximately 5%.

Concentration time of catchments range from 30 to 240 minutes with entire region being approximately 60 minutes.

Based on MIKE+ high fidelity model and the information given above, our simple rainfall – rain inflow model has been calibrated. 9 catchments' time of concentration and area imperviousness are approximated accordingly, and results are presented in Table 2 Catchment parameters 2.

Approximate catchment area is 2.1*77 million m^2. Assuming 60 minutes of concentration time for 2.1*77 million m^2 area, all 9 catchments' values are interpolated.

High population density areas will be assumed to have higher ratio of imperviousness. Whole Oslo regions population density is 64 thousand people/x area (77 million m^2). Assuming 5% imperviousness for the whole Oslo region, individual catchments' values are interpolated.

Table 2 Catchment parameters 2

Catchment	Regions	Area [77 million m^2]	Time of concentration [min]	Population density [Thousand people/77 million m^2]	Area imperviousness [%]
Catchment_1	Festning	1	28.6	150	11.72
Catchment_2	Østensjø	1	28.6	125	9.77
Catchment_3	Furuset	1.5	42.9	100	7.81
Catchment_4	Torshov	1.5	42.9	100	7.81
Catchment_5	Nordstrand	1	28.6	125	9.77
Catchment_6	Lillestrøm+ Lorensko+ Nittedal+ Raelingen	5.4	154	33.5	2.62
Catchment_7	Baerum	2.5	71	54	4.22
Catchment_8	Asker+	2.5	71	52	4.06

	Lier				
Catchment_9	Ski+ Oppegård	2.5	71	26	2.03

As a result, rainfall – rain inlet flow model can be expressed as:

F_?r = R_d * C?_a * C?_i * (1/1000) (11)

F_?r: Rain induced inlet flow [m^3/min]

R_d: rain density [mm/min]

C?_a: catchment area [m^2]

C?_i: catchment imperviousness [0-1]

1/1000: unit control

With concentration times from Table 2 Catchment parameters 2 as time delays of the equation 11.

9.3.2 Oslo SN model

Actual Oslo SN depicted in Figure 5 Oslo sewer network is approximated as 13 links, 5 magazines, 5 overflows, 3 pumps, 2 gates and a separation weir in the Oslo SN model.

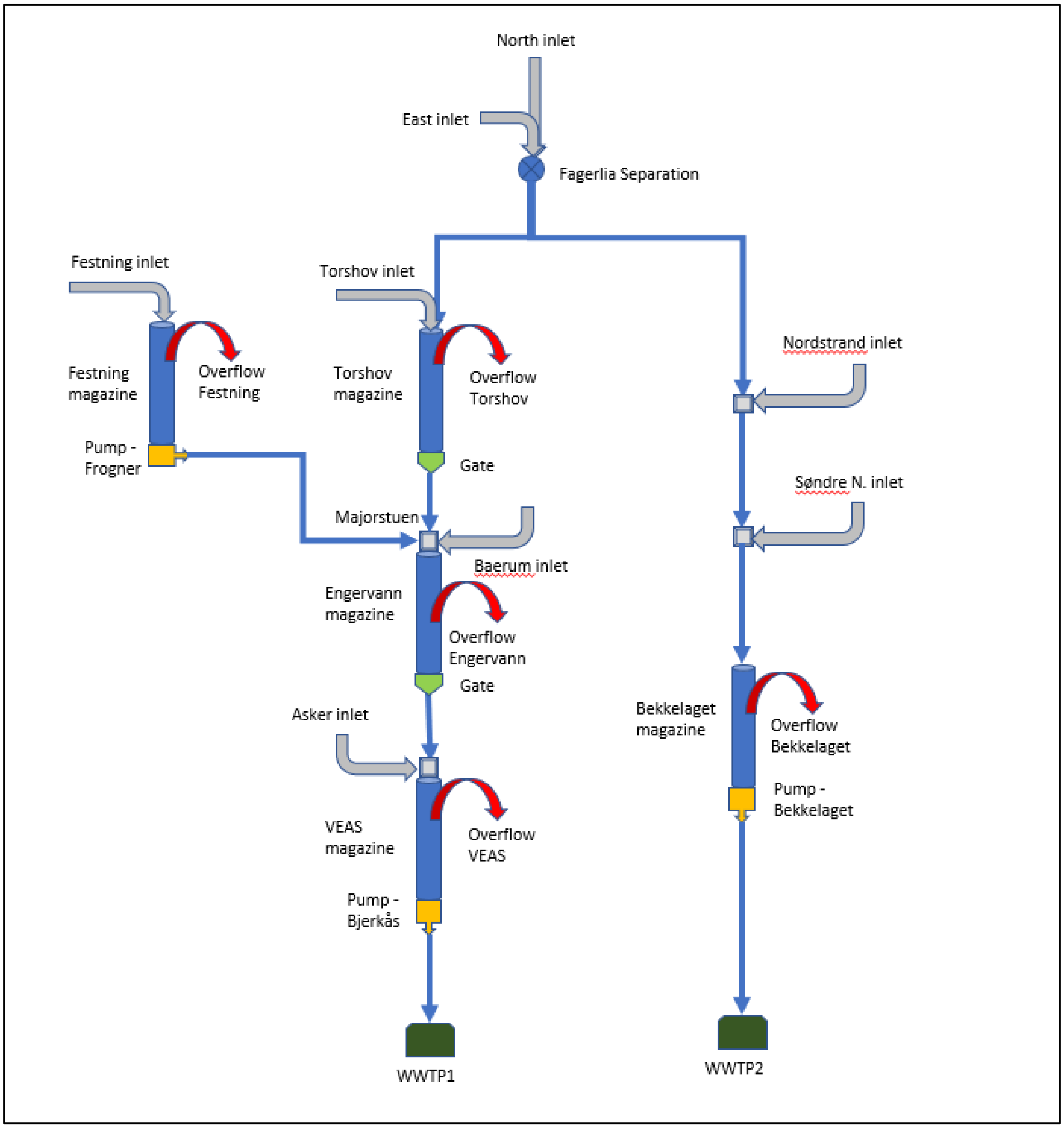

Figure 7 Oslo SN model schematic diagram

9.3.2.1 Oslo SN model schematic diagram

Structural data for Oslo SN for the sections where Oslo VEAS is responsible were found from the modelling work (Haugen, 2018).

9.3.2.2 Municipal wastewater

Inlets are flow connections to the links. (Table 3 Links) Steady state/dry weather flow of an inlet into the Oslo SN is modelled as a product of catchment population that the inlet is connected to and the person equivalent wastewater amount per minute, 0.0002005 m^3/min.

$$F\_?m = C?\_p*pe\_wwf \qquad (12)$$

F_?m: Municipal wastewater inlet flow [m^3/min]

C?_p: Population of the catchment area

Pe_wwf: Person equivalent wastewater flow [m^3/min]

9.3.2.3 Diurnal pattern

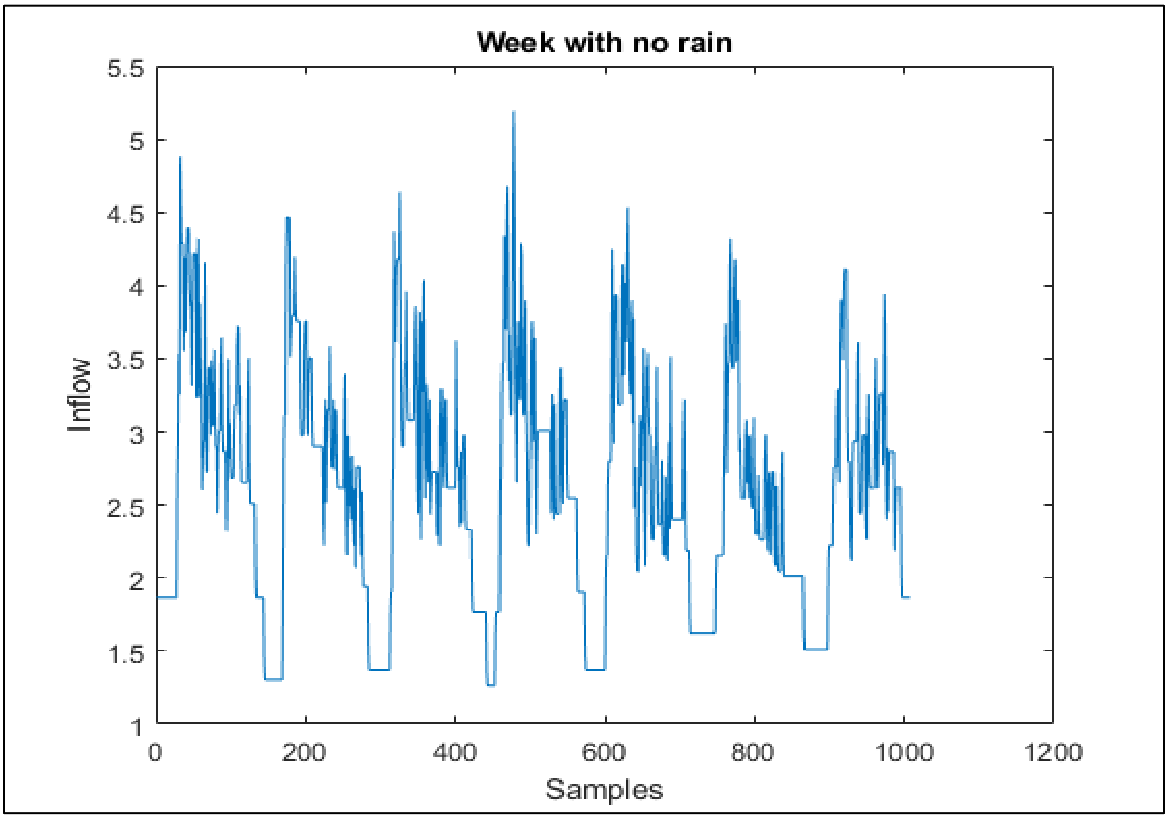

Figure 8 Municipal wastewater trend in Bjørnegrad

A week of municipal wastewater inflow from 16 September 00:00 to 22 September 23:50 in Bjørnegrad. A typical municipal wastewater flow trend can be observed with bottom levels in the night and higher levels with multiple peaks in the daytime.

In the model, an approximation has been done and a sinus wave has been implemented for the diurnal pattern. Wave ranges from 0 to 2 and has a one-day period (1440 min). It reaches value 0 at hour 5 am and value 2 at hour 17 pm everyday throughout the simulation period. Approximate value of the wave is 1.

Diurnal pattern is modelled as a product of sinus wave shown in Figure 9 Diurnal pattern trend approximated as a sin wave in the model in 3 days period (4320 min). and the steady state flow of an inlet flow from the equation 12.

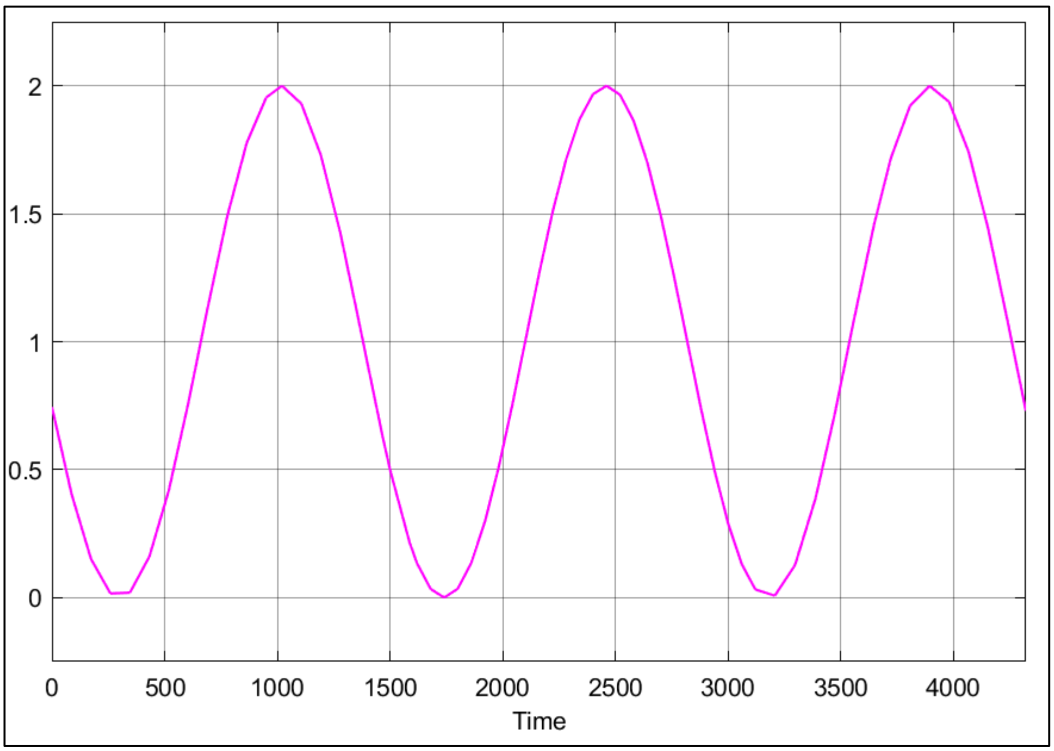

Figure 9 Diurnal pattern trend approximated as a sin wave in the model in 3 days period (4320 min).

Combining dry (eq.12) and wet weather (eq.11) inlet flow equations gives the total dynamic flow of an inlet in the Oslo SN model:

F_?t = F_?m*d_u + F_?r (13)

F_?t: Total inlet flow [m^3/min]

F_?m: Municipal wastewater inlet flow [m^3/min]

d_u: sinus wave of the diurnal pattern

F_?r: Rain induced inlet flow [m^3/min]

Total inlet flows of the 9 catchments are the main inputs to the Oslo SN MATLAB/Simulink (Inc., 2021) model. For the modelling of the Oslo sewer network, tanks in series approach was used. Water flow is modelled as volume transport through links(pipes) and magazines with transport delays.

A magazine is a link/pipe with also some volume to store wastewater. Pipes are only delays, whereas magazines are delays and a storage volume after the delay.

9.3.2.4 Links/Pipes in the model

Links are assumed to have no volume to store water. They are only transport delays as specified in equation 15. The magazine in the equation 15 is the magazine that the link flows into.

Table 3 Links

Link	from	to	Length [m]
Link_1	Festning inlet	Festning magazine - Majorstuen	4400
Link_2	East inlet (Østensjø)	Fagerlia separation	3500
Link_3	North inlet (Furuset)	Fagerlia separation	7100
Link_4	Fagerlia separation	Torshov magazine - Majorstuen	7300
Link_5	Torshov inlet	Torshov magazine - Majorstuen	3000
Link_6	Majorstuen	Vaekerø	5400
Link_7	Vaekerø	Engervann magazine	7600
Link_8	Baerum inlet	Engervann magazine	6000
Link_9	Engervann magazine	VEAS magazine - WWTP	15000
Link_10	Asker inlet	VEAS magazine - WWTP	8000
Link_11	Fagerlia separation	Bekkelaget magazine - WWTP	5500
Link_12	Nordstrand inlet	Bekkelaget magazine - WWTP	1000
Link_13	Søndre N. inlet	Bekkelaget magazine - WWTP	7500

9.3.2.5 Magazines in the network

There are 5 magazines in the Oslo SN model, Torshov, Festning, Engervann, Bekkelaget and VEAS magazine. Magazines have circular cross shapes with known diameters and lengths. In the model they are assumed to have rectangular cross shapes with given diameters taken as their heights. Assumed rectangular cross shapes have the same areas with the circular cross shapes and magazines' bottom areas are calculated accordingly. In the model, these bottom areas are used to convert water level to volumes and vice versa in the magazines.

Festning magazine represents the main flow, length and the volume of the Oslo SN from Festning, through Frognerpark pump station and ends at Majorstuen.

Torshov magazine represents the main flow, length and the volume of the Oslo SN from Fagerlia separation, through Torshov and ends at Majorstuen.

Engervann magazine represents the main flow, length and the volume of the Oslo SN from Majorstuen, through Vaekerø and ends at Engervann.

VEAS magazine represents the main flow, length and the volume of the Oslo SN from Engervann, through Bjerkås and ends at Slemmestad WWTP.

Bekkelaget magazine represents the main flow, length and the volume of the Oslo SN from Fagerlia separation, through Bekkelaget and ends at Bekkelaget WWTP.

Table 4 Magazines

Magazine	Diameter[m]	Assumed rec. height [m]	Cross section area [m^2]	Length [m]	Bottom area [m^2]	Volume [m^3]
Festning	3	3	7.0686	4400	1.03e+04	3.11e+04
Torshov	3	3	7.0686	7300	1.72e+04	5.16e+04
Engervann	3.35	3.35	8.8141	7600	1.99e+04	6.69e+04
Bekkelaget	3	3	7.0686	5500	1.29e+04	3.88e+04
VEAS	3.5	3.5	9.6211	15000	3.94e+04	1.44e+05

Minimum water level in all magazines are 0.1 meters to ensure the flow continuity in the model.

Steady state/dry weather water level in a magazine is taken as half of the height of the magazine.

Total volume of the magazines/Oslo sewer network is 3.3288e+05 m^3.

Transport delays in the magazines are as specified in the equation 15.

9.3.2.6 Transport delays

In Oslo sewer network, time of wastewater to travel from Fagerlia separation to the VEAS WWTP varies between 5 to 7 hours. Length is approximately 35300 meters. This gives a speed of between 84.05 m/min and 117.667 m/min.

Vfmin=84.05 [m/min]

Vfmax=117.667 [m/min]

Vfdif=Vfmax-Vfmin=33.617 [m/min] (14)

Outflow speed from a magazine should be proportional to the occupied magazine volume as shown in equation. Higher flow speed should result in lower delays through links and magazines.

Time delay [min] in a link/magazine in the model:

Td=L_?/(Vfmin+(H_?m/Hmax_?m)*Vfdif) (15)

Td: time delay [min]

L_?: length of the link/magazine [m]

H_?m: steady state/dry weather water level in the magazine [m]

Hmax_?m: Maximum possible water level in the magazine [m]

Vfmin: Minimum flow speed through a link/magazine specified in eq. 14. [m/min]

Vfdif: Differentiation of maximum and minimum flow speed in a link/magazine specified in eq. 14. [m/min]

Table 5 Transport delays

Delay	Symbol	Link	Length [m]	Steady state value [min]	Unit
Time delay Festning inlet	tdfi	Link_1	4400	44	min

(Festning magazine)					
Time delay East inlet	tdei	Link_2	3500	35	min
Time delay North inlet	tdni	Link_3	7100	70	min
Time delay Torshov inlet	tdti	Link_5	3000	30	min
Time delay Baerum inlet	tdbi	Link_8	6000	59	min
Time delay Asker inlet	tdai	Link_10	8000	79	min
Time delay Nordstrand inlet	tdnsi	Link_12	1000	10	min
Time delay Søndre Nordstrand inlet	tdsnsi	Link_13	7500	74	min
Time delay Torshov magazine	tdtm	Link_4	7300	72	min
Time delay Engervann magazine	tdem	Link_7	7600	75	min
Time delay VEAS magazine	tdvm	Link_9	15000	149	min
Time delay Bekkelaget magazine	tdbm	Link_11	5500	55	min
Time delay Majorstuen - Vaekerø	tdmv	Link_6	5400	54	min

Dynamic values of the delays in the model vary according to equation 15.

9.3.3 Overflow model

In the model, based on dynamic equations of wastewater mass conservation, (equations 25, 26, 27, 28, 29) total inflows and outflows to a magazine are integrated to find the occupying water volume. Volumes are then converted to the water levels in the magazines. Naturally, water levels cannot exceed magazine levels as integrators are limited. For overflow modelling however, parallel integrators have been implemented. They create virtual copies of the magazines which in theory can be filled to infinity since the parallel integrators are not limited. At the end of each simulation run, water level differences between the virtual and real magazines are converted back to the water volumes. These differential volumes are the untreated wastewater overflows from the Oslo SN to the Oslo Fjord.

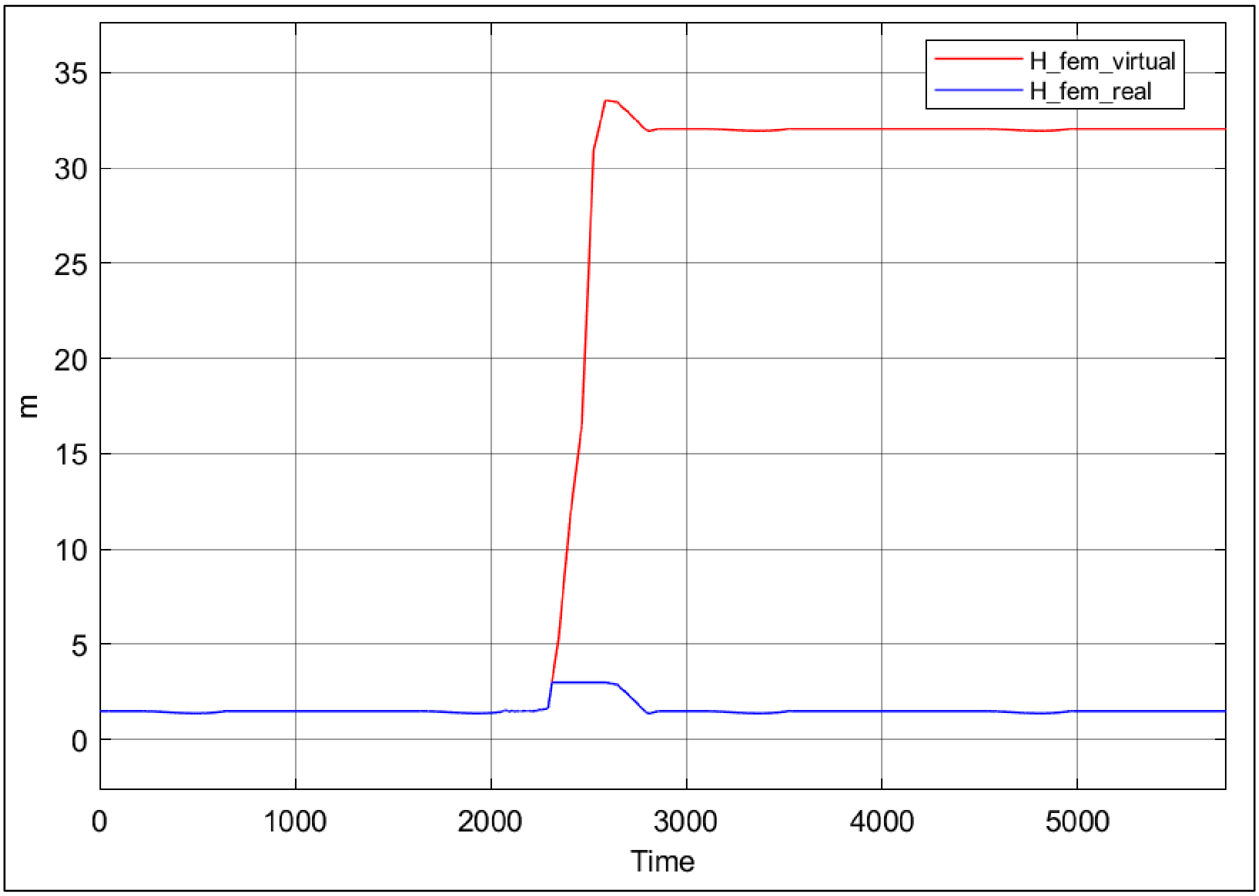

Figure 10 Virtual and real Festning magazines wastewater levels

Example in Figure 10 Virtual and real Festning magazines wastewater levels: PI control in rain event 3 without forecast data.

Initial testing of this unique overflow modeling method revealed an issue where negative overflows were observed in some control periods. Negative overflow is naturally unacceptable for Oslo SN model. Excessive water volume spilled to the fjord cannot re-enter to the SN.

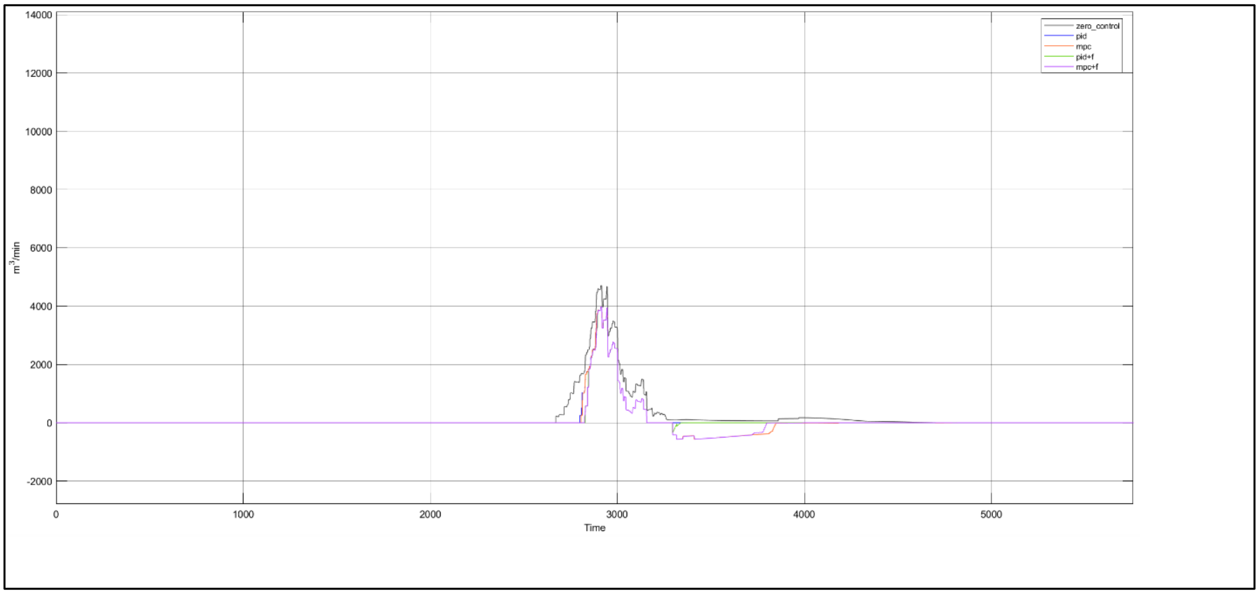

Figure 11 Initial overflow model testing, observed negative overflows, event 1

During and sometime after rain events end, control strategies maintain the highest outflow conditions for the MVs (actuators) to prevent delayed overflows in the system. However, if the control strategy prolongs these MV conditions longer than needed, CVs (Levels in the real magazines) hit their minimum limits and stay at minimums until MVs are changed. Because of the rain event, unlimited virtual magazines have higher volumes/water levels and when the real magazines hit the minimums, they continue to decrease. Since overflow model measures the difference between the real and virtual magazines, negative overflows may happen under special circumstances. Ideally, control algorithms should no longer force the MVs when the CVs are at their minimums. Especially, the MPC strategy exhibited this behavior.

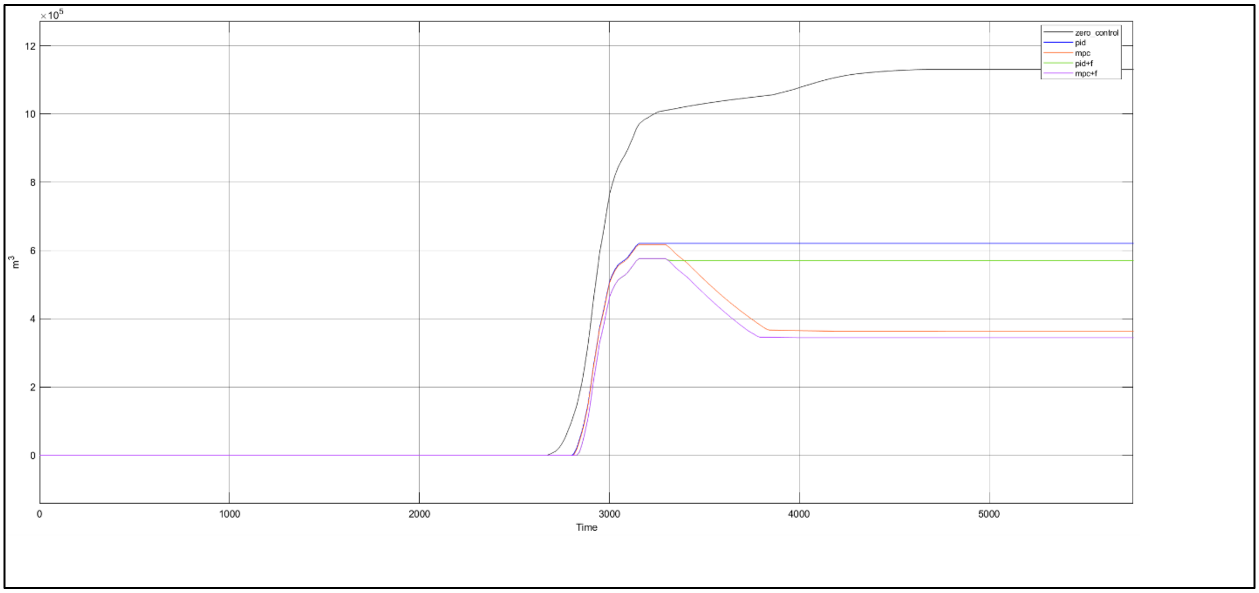

Figure 12 Initial overflow model testing, observed decreases in overflow volumes, event 1

Negative overflow conditions in the model only occur after the rain event ends and the levels in the real magazines hit their minimum limits. It is evident in the simulation results that no overflows happen in and after these conditions. Accordingly, finalized overflow model should only accept positive overflow values from the system. Negative overflow values are neglected, and the overflow volume is kept constant. As a result, overflow model visualizes the maximum volume difference between the real and the virtual magazines as an accurate measure of the real overflow volume.

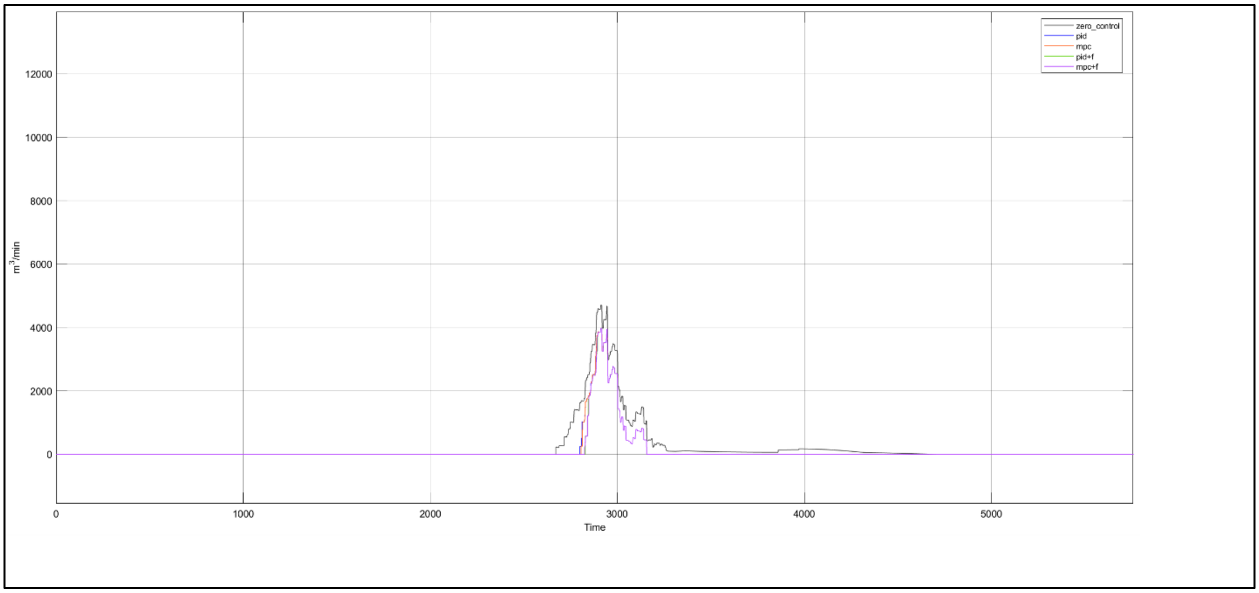

Figure 13 Finalized overflow model, observed overflow, event 1

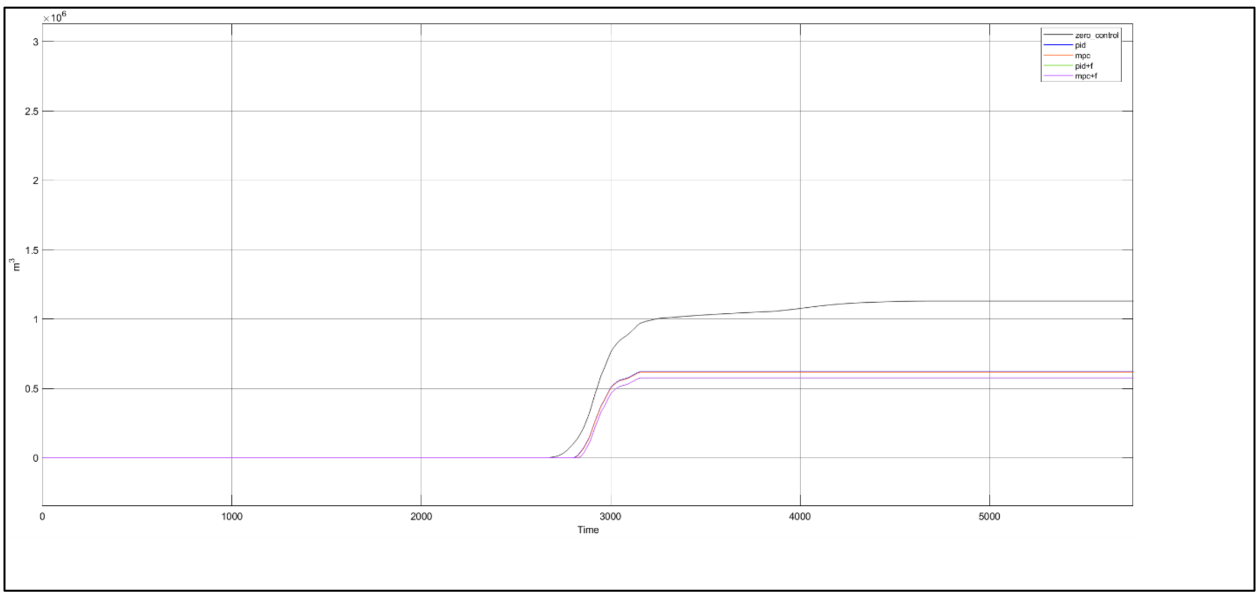

Figure 14 Finalized overflow model, overflow volume, event 1

9.3.3.1 Flow loads across the Oslo SN model

Magazines are where overflows happen in the Oslo SN model. When high inflows outrun the possible maximum outflow from a magazine, water starts to fill up the available volume. If this condition persists a certain amount of time, volume gets filled and overflow starts. Assuming only one directional flow in the Oslo SN model, it is possible to trace these flows back to their origins for any section in the network. Flows are products of rainfall density, catchment parameters and the network structure.

No overflows are assumed, and variable x is introduced to define the flow loads. X is the rain inflow to the model per 77 million m^2 catchment area times the catchment imperviousness based on the dynamic rainfall density per minute. Taking the catchment parameters from Table 1 Catchment parameters 1 and running the flows along Oslo SN with its default structure and without any real time control control gives dynamic flow loads across the network.

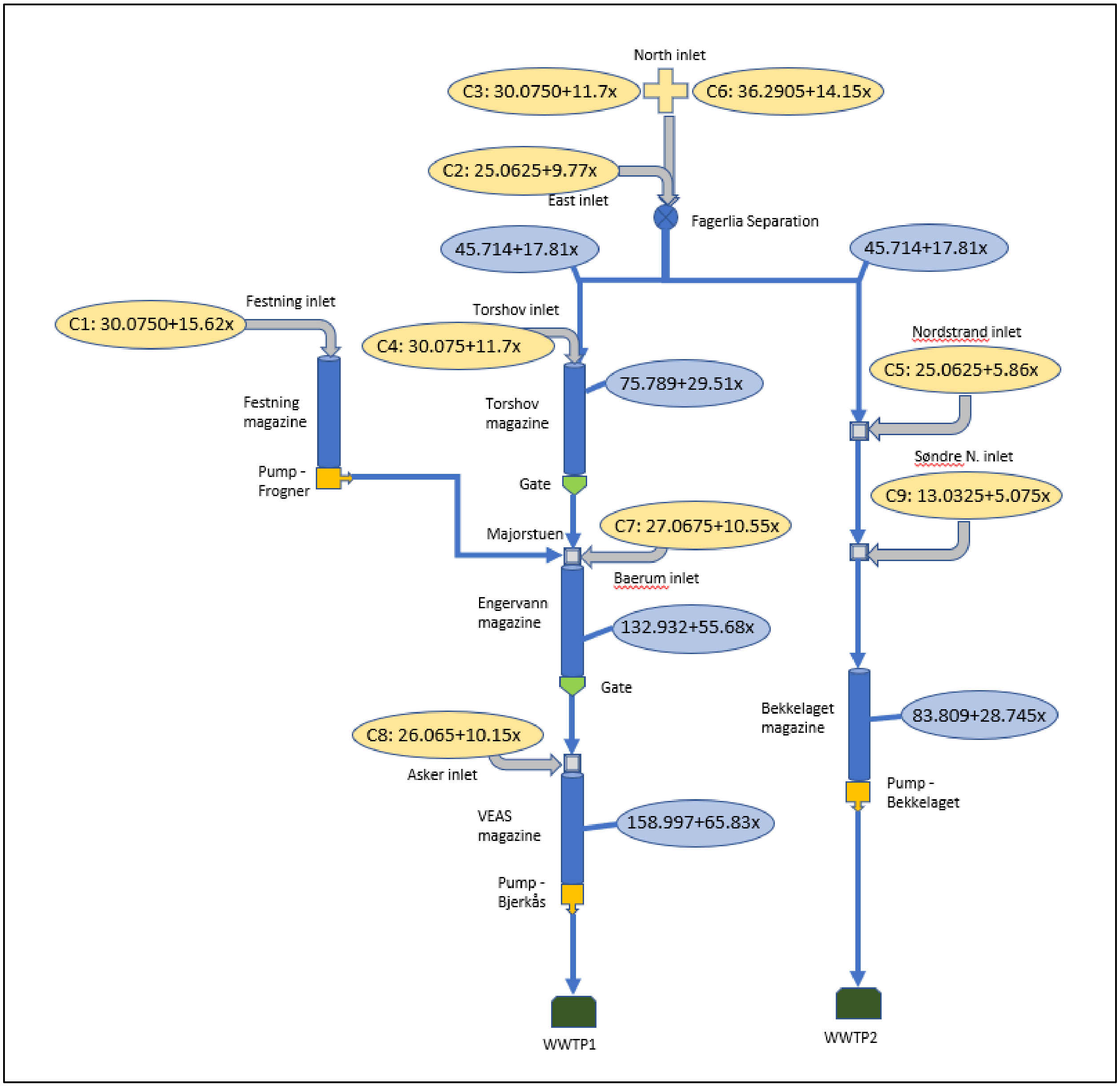

Figure 15 Flow loads across the Oslo SN model

Eclipsed numbers represent the flow loads. First variable is the approximated municipal wastewater flow and the second parameter with x is the rain induced flow. Yellow loads are initial loads from the catchments and the blue loads are the consequential loads at the specified locations of the Oslo SN.

These flow loads can help to determine some critical constraints in the model. Constraints of the model are very important to have right amount of overflows in the model.

Also, choosing constraints proportional to the flow loads may contribute positively to the consistency of overflows across the network.

9.3.3.2 Constraints

Magazine levels and volumes are fixed constants. (Table 4 Magazines) Maximum outflows from the magazines VEAS, Festning and Bekkelaget are simply the maximum flow capacities of their pumps. Outflows from the magazines Torshov and Engervann can be controlled by their gates however, their maximum outflow value can be found according to specific flow loads at these magazines.

9.3.3.2.1 Pumps

Outflows from Festning, VEAS and Bekkelaget magazines are controlled by pumps. Pumps' maximum capacities are independent of flow loads.

Table 6 Pumps

Pump	from	to	Minimum flow [m^3/min]	Steady state flow [m^3/min]	Maximum flow [m^3/min]
P1 – Frognerparken pump	Festning magazine	Majorstuen (Link_6)	6	30.1	150
P2 – Bjerkås pump	VEAS magazine	VEAS WWTP1	32	159	660
P3 – Bekkelaget pump	Bekkelaget magazine	Bekkelaget WWTP2	17	83.8	440

Any water the pump is not able to deliver when the magazine is full is converted to overflow in the model with the second integrator.

Since P2 Bjerkås pump and P3 Bekkelaget pump maximum flows are the constraints to the flows to the two WWTPs of the model, maximum treatment capacity of the model is then; P2max+P3max m^3 per minute. Applying this to the total flow load at the two WWTPs from the Figure 15 Flow loads across the Oslo SN yields the equation:

$$P2\ max. + P3\ max. = P2\ steady\ state + P3\ steady\ state + 94.575*x \quad (16)$$

Analyzing the maximum drift in the model can be used to assume the maximum X value (before the overflows). Taking the values from Table 6 Pumps:

X = 9.0636 m^3/min rain inflow per 77 million m^2*imperviousness. Rainfall densities that generate rain inflows over this X value would cause overflows at the flow load dependent constraints of the model (Torshov and Engervann maximum outflows).

9.3.3.2.2 Torshov magazine outflow

Steady state outflow from Torshov magazine is equal to the total of steady state inflows to the Torshov magazine, in accordance with equation 1.

$$P4=((F\_n+F\_e)/2)+F\_t \qquad (17)$$

P4: Steady state outflow from Torshov magazine [m^3/min]

F_n: North inlet steady state inflow [m^3/min]

F_e: East inlet steady state inflow [m^3/min]

F_t: Torshov inlet steady state inflow [m^3/min]

Maximum Outflow from Torshov magazine:

$$P4max=((F\_n+F\_e)/2)+F\_t+29.51*x \quad (18)$$

P4max: Maximum outflow from Torshov magazine [m^3/min]

F_n, F_e, F_t: North, East and Torshov inlet flows [m^3/min]

X: rain inflow per 77 million m^2*imperviousness [m^3/min]

9.3.3.2.3 Engervann magazine outflow

Steady state outflow from Engervann magazine is equal to the total of steady state inflows to the Engervann magazine, in accordance with equation 1.

$$P5=((F\_n+F\_e)/2)+F\_t+F\_f+F\_b \qquad (19)$$

P5: Steady state outflow from Engervann magazine [m^3/min]

F_n, F_e, F_t: North, East and Torshov inlet flows [m^3/min]

F_f: Festning inlet steady state inflow [m^3/min]

F_b: Baerum inlet steady state inflow [m^3/min]

Maximum Outflow from Engervann magazine:

$$P5max=((F_n+F_e)/2)+F_t+F_f+F_b+55.68*x \qquad (20)$$

P5max: Maximum outflow from Engervann magazine [m^3/min]

F_n, F_e, F_t: North, East and Torshov inlet flows [m^3/min]

F_f, F_b: Festning and Baerum inlet flows [m^3/min]

X: rain inflow per 77 million m^2*imperviousness [m^3/min]

9.3.3.2.4 Gates

Torshov and Engervann magazines outflows are controlled by gates. In the model, gates take a value between 0 and 1. This is an indicator of how much open the gate is, and the magazines outflow has a linear correlation with this value.

Table 7 Gates

Gate	Magazine outflow	Steady state value	Allowed values	Allowed flow range
G4	Torshov magazine	0.4416	0 - 1	0 – P4max (Eq.18)
G5	Engervann magazine	0.4170	0 - 1	0 – P5max (Eq.20)

Steady state G4 value:

$$G4=P4/(P4max*(H\_tm/Hmax\_tm) \qquad (21)$$

G4: Steady state Torshov magazine gate value

P4max: Maximum outflow from Torshov magazine [m^3/min]

H_tm: steady state/dry weather water level in the Torshov magazine [m]

Hmax_tm: Maximum possible water level in the Torshov magazine [m]

Steady state G5 value:

$$G5=P5/(P5max*(H\_em/Hmax\_em)) \quad (22)$$

G5: Steady state Engervann magazine gate value
P5max: Maximum outflow from Engervann magazine [m^3/min]
H_em: steady state/dry weather water level in the Engervann magazine [m]
Hmax_em: Maximum possible water level in the Engervann magazine [m]

In the dynamic Oslo SN model, outflows from Torshov and Engervann are not only affected by the gate values but also affected by how much volume is occupied in the tunnel in each time step in accordance with equation 9.

Dynamic outflow from Torshov magazine:

$$G4*P4max*(H\_tm/Hmax\_tm) \quad (23)$$

G4: Dynamic Torshov gate value between 0-1
P4max: Maximum outflow from Torshov magazine [m^3/min]
H_tm: Dynamic water level in the Torshov magazine [m]
Hmax_tm: Maximum possible water level in the Torshov magazine [m]

Dynamic outflow from Engervann magazine:

$$G5*P5max*(H\_em/Hmax\_em) \quad (24)$$

G5: Dynamic Engervann gate value between 0-1

P5max: Maximum outflow from Engervann magazine [m^3/min]

H_em: Dynamic water level in the Engervann magazine [m]

Hmax_em: Maximum possible water level in the Engervann magazine [m]

Dynamic outflow equations coincide with the values given in Table 7 Gates.

9.3.3.3 Overflows

Table 8 Overflows

Overflow	From magazine	Equation
Engervann overflow (Lysaker)	Engervann magazine	En_o
VEAS overflow	VEAS magazine	V_o
Bislettbekken overflow		Bi_o = 0.25*T_o + F_o
Ekeberg overflow		Ek_o = 0.75*T_o + Be_o
Festning overflow	Festning magazine	F_o
Torshov overflow	Torshov magazine	T_o
Bekkelaget overflow	Bekkelaget magazine	Be_o

First four overflows do reach the fjord directly. Last three are added to the other overflows as defined in the equations of Table 8 Overflows.

9.3.4 Simulation Scenarios

9.3.4.1 Rain events

Typically, a simulation covers a four-day period and rain event is placed in the second day. First, third and fourth days have dry weather conditions. First dry day provides enough time for control algorithm to get forecast data and maximize the available volume in the network before rain hits. Last two dry days on the other hand, allows model to demonstrate the full-scale transport delay behaviors in the network and also to settle down before simulation period ends.

Historical rain events with varying impacts have been chosen from the Oslo region rainfall data from database (Meteorologisk institutt, 2021) served by the Norwegian Meteorological Institute and NRK, Norsk Rikskringkasting AS. Hourly raining data is converted to rainfall per minute values and fed to the system with step input blocks.

Negligible precipitation before and after the event are not included in the event. (Table 9 Rain events)

Table 9 Rain events

Scenario	Date	Rain duration	Simulation duration	Total rainfall [mm]
Event 1	2019 June 11th 20:00 pm – 12th 5:00 am	9 hours	4 days	18
Event 2	2019 August 29th 4:00 am – 9:00 pm	5 hours	4 days	22.7
Event 3	2017 August 9th 13:00 am – 20:00 pm	7 hours	4 days	41.5
Event 4	2016 May 9th 12:00 am – 20:00 pm	8 hours	4 days	8.2

In rain event 1, there were floodings in some basements. In rain event 3, which is one of the most extreme rain events in region's history, underground passages at Jernbanetorget station were filled with water and many basements were flooded. Rain event 4 on the other hand, is a common moderate event with its evenly time-distributed low rainfall intensity.

In this modeling work, all rain events are assumed unchanging for all catchments of the Oslo region.

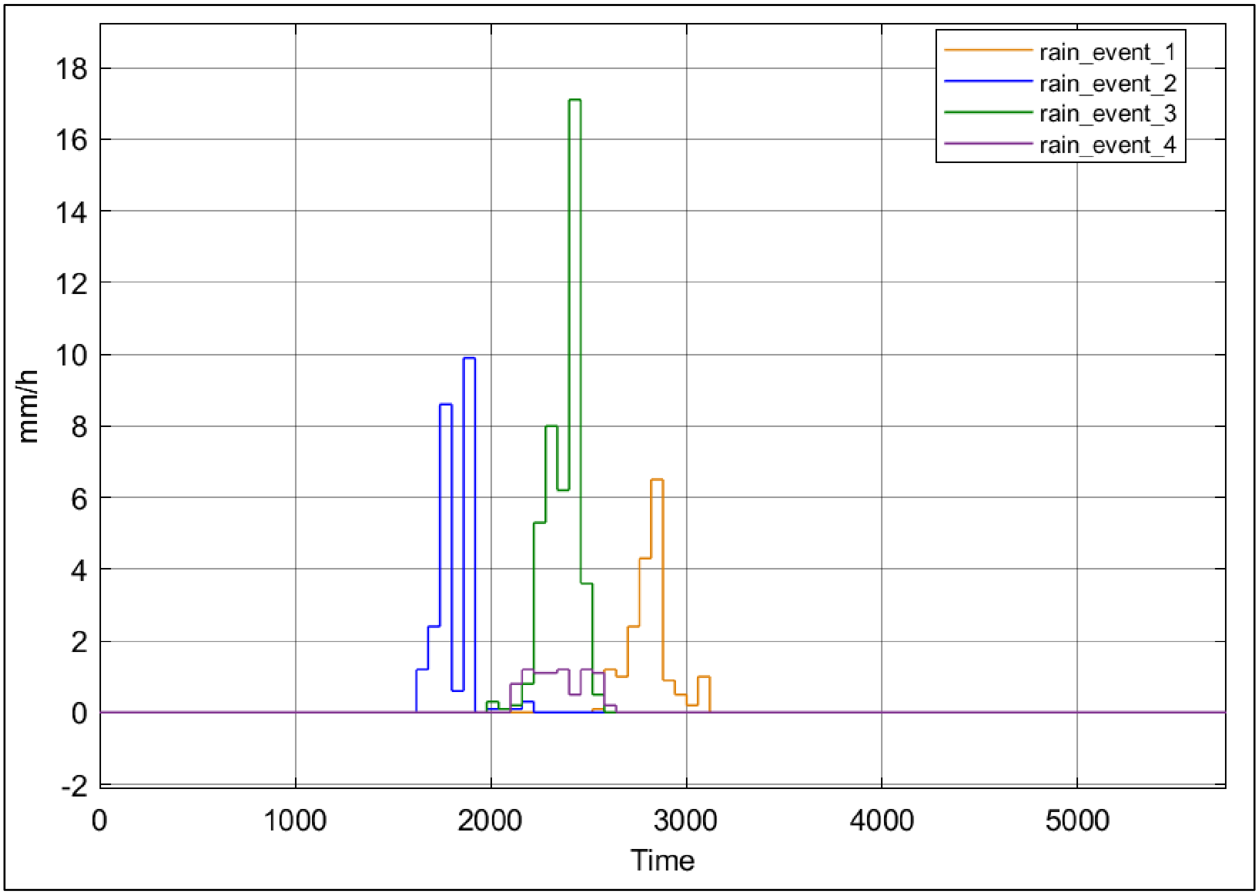

Figure 16 Rain events

9.4 Control of Oslo SN model

Considering its magnitude, daily municipal wastewater variation is quite manageable for the Oslo SN. However, rainfall events are the main concerns for the Oslo SN model. Significant escalations at the inlet flows created by the rainfall are main disturbances of the dynamic control scheme.

9.4.1 Parameters of the model

9.4.1.1 Inlet flows – DVs, disturbance variables

Table 10 Inlet flows/Disturbance variables

Name	Symbol	Unit
North inlet	F_n	m^3/min
East inlet	F_e	m^3/min

Festning inlet	F_f	m^3/min
Torshov inlet	F_t	m^3/min
Baerum inlet	F_b	m^3/min
Asker inlet	F_a	m^3/min
Nordstrand inlet	F_ns	m^3/min
Søndre Nordstrand inlet	F_sns	m^3/min

In the model and in the control scheme:

North and East inlets are 1 disturbance variable. Nordstrand and Søndre Nordstrand inlets are also 1 disturbance variable since they are added together before fed to the model as inputs. This approach reduces the number of DVs from 8 to 6 which may enable simpler and more optimal control.

9.4.1.2 Gates and pumps – MVs, manipulated variables

Gates and pumps are the actuators of the system. Since they can already be controlled by operators, an RTC strategy can utilize these actuators to maximize the performance of the Oslo SN.

Table 11 Gates, pumps and separation/Manipulated variables

Name	Symbol	Unit
Frognerparken pump (Festning magazine outflow)	P1	m^3/min
Torshov magazine outflow gate	G4	ratio
Engervann magazine outflow gate	G5	ratio
Bjerkås Pump (VEAS magazine)	P2	m^3/min
Bekkelaget Pump (Bekkelaget magazine)	P3	m^3/min
Fagerlia Separation	Vv	ratio

9.4.1.3 Magazine levels – CVs, controlled variables

It is assumed that controlling levels in the magazines should achieve the goal of minimizing overflows.

Table 12 Magazine water levels/Controlled variables

Name	Symbol	Unit

Festning magazine level	H_fem	m
Torshov magazine level	H_tm	m
Engervann magazine level	H_em	m
VEAS magazine level	H_vm	m
Bekkelaget magazine level	H_bm	m

9.4.1.4 Constant parameters of the model

Table 13 Constant parameters

Name	Symbol	Value	Unit
Bottom area Festning magazine	B_fem	1.03e+04	m^2
Bottom area Torshov magazine	B_tm	1.72e+04	m^2
Bottom area Engervann magazine	B_em	1.99e+04	m^2
Bottom area VEAS magazine	B_vm	3.94e+04	m^2
Bottom area Bekkelaget magazine	B_bm	1.29e+04	m^2
Fagerlia separation steady state value	Vv	0.5	ratio
Torshov magazine maximum outflow	P4max	343.26	m^3/min
Engervann magazine maximum outflow	P5max	637.6	m^3/min
Maximum level Festning magazine	Hmax_fem	3	m
Maximum level Torshov magazine	Hmax_tm	3	m
Maximum level Engervann magazine	Hmax_em	3.35	m
Maximum level VEAS magazine	Hmax_vm	3.5	m
Maximum level Bekkelaget magazine	Hmax_bm	3	m

9.4.2 Dynamic equations of the model

It is assumed that the water in the Oslo SN model is incompressible. Accordingly, conservation of mass and volume is one and the same.

Festning magazine, conservation of wastewater mass

$$B_{fem} * \frac{dH_{fem}}{dt} = F_{f(t-tdfi)} - P1(t) \quad (25)$$

Torshov magazine, conservation of wastewater mass

$$B_{tm} * \frac{dH_{tm}}{dt} = \left[F_{n(t-tdni-tdtm)} + F_{e(t-tdei-tdtm)}\right] * Vv(t - tdtm) + F_{t(t-tdti)} - G4(t) * P4max * \frac{H_{tm(t)}}{Hmax_{tm}} \quad (26)$$

Engervann magazine, conservation of wastewater mass

$$B_{em} * \frac{dH_{em}}{dt} = F_{b(t-tdbi)} + P1(t - tdmv - tdem) + G4(t - tdmv - tdem) * P4max * \frac{H_{tm(t-tdmv-tdem)}}{Hmax_{tm}} - G5(t) * P5max * \frac{H_{em(t)}}{Hmax_{em}} \quad (27)$$

VEAS magazine, conservation of wastewater mass

$$B_{vm} * \frac{dH_{vm}}{dt} = F_{a(t-tdai)} + G5(t - tdvm) * P5max * \frac{H_{em(t-tdvm)}}{Hmax_{em}} - P2(t) \quad (28)$$

Bekkelaget magazine, conservation of wastewater mass

$$B_{bm} * \frac{dH_{bm}}{dt} = \left[F_{n(t-tdni-tdbm)} + F_{e(t-tdei-tdbm)}\right] * [1 - Vv(t - tdbm)] + \left[F_{ns(t-tdnsi)} + F_{sns(t-tdsnsi)}\right] - P3(t) \quad (29)$$

For delays see Table 5 Transport delays.

9.4.2.1 Simplified equations for the control algorithms

Converting non linearities which are time delays, and Q-h related outflows to their steady state values in the equations 25, 26, 27, 28 and 29:

Festning magazine, conservation of wastewater mass

$$B_{fem} * \frac{dH_{fem}}{dt} = F_{f(t-43.62)} - P1(t-0) \qquad (30)$$

Torshov magazine, conservation of wastewater mass

$$B_{tm} * \frac{dH_{tm}}{dt} = (F_n + F_e)(t - 124.92) * Vv + F_{t(t-29.74)} - G4(t-0) * \frac{P4max}{2} \qquad (31)$$

Engervann magazine, conservation of wastewater mass

$$B_{em} * \frac{dH_{em}}{dt} = F_{b(t-59.48)} + P1(t - 128.89) + G4(t - 128.89) * \frac{P4max}{2} - G5(t-0) * \frac{P5max}{2} \qquad (32)$$

VEAS magazine, conservation of wastewater mass

$$B_{vm} * \frac{dH_{vm}}{dt} = F_{a(t-79.32)} + G5(t - 148.72) * \frac{P5max}{2} - P2(t-0) \qquad (33)$$

Bekkelaget magazine, conservation of wastewater mass

$$B_{bm} * \frac{dH_{bm}}{dt} = (F_n + F_e)(t - 107.12) * (1 - Vv) + (F_{ns} + F_{sns})(t - 42.13) - P3(t-0) \qquad (34)$$

Applying Laplace transform to the equations 30, 31, 32,33 and 34 (Shown without the delays):

$$B_{fem} * s * H'_{FEM}(s) = F'_F(s) - P1'(s) \qquad (35)$$

$$B_{tm} * s * H'_{TM}(s) = \overline{Vv} * (F_{N+E})'(s) + (\overline{F_N + F_E}) * VV'(s) + 1 * F'_T(s) - G4'(s) * \frac{P4max}{2}$$
(36)

$$B_{em} * s * H'_{EM}(s) = 1 * F'_B(s) + 1 * P1'(s) + \frac{P4max}{2} * G4'(s) - \frac{P5max}{2} * G5'(s) \quad (37)$$

$$B_{vm} * s * H'_{VM}(s) = 1 * F'_A(s) + \frac{P5max}{2} * G5'(s) - 1 * P2'(s) \qquad (38)$$

$$B_{bm} * s * H'_{BM}(s) = (1 - \overline{Vv}) * (F_{N+E})'(s) - (\overline{F_n + F_e}) * VV'(s) + 1 * (F_{NS+SNS})'(s) - 1 * P3'(s) \qquad (39)$$

Deriving transfer functions from equations 35, 36, 37, 38 and 39 gives:

9.4.2.2 Transfer functions CVs and MVs

Table 14 Transfer functions CVs and MVs

TF	CV	MV	Process gain	Time constant 1	Time constant 2	(Steady state) Delay [min]
TF01	H_fem	P1	-1	B_fem= 1.04e+04	0	0
TF02	H_fem	G4	0	1	0	0
TF03	H_fem	G5	0	1	0	0
TF04	H_fem	P2	0	1	0	0
TF05	H_fem	P3	0	1	0	0
TF06	H_fem	Vv	0	1	0	0
TF11	H_tm	P1	1	1	0	0

TF12	H_tm	G4	-P4max/2= -172	B_tm= 1.72e+04	0	0
TF13	H_tm	G5	0	1	0	0
TF14	H_tm	P2	0	1	0	0
TF15	H_tm	P3	0	1	0	0
TF16	H_tm	Vv	F_n+F_e= 91	B_tm= 1.72e+04	0	72
TF21	H_em	P1	1	B_em= 1.99e+04	0	129
TF22	H_em	G4	P4max/2= 172	B_em= 1.99e+04	0	129
TF23	H_em	G5	-P5max/2= -319	B_em= 1.99e+04	0	0
TF24	H_em	P2	0	1	0	0
TF25	H_em	P3	0	1	0	0
TF26	H_em	Vv	0	1	0	0
TF31	H_vm	P1	0	1	0	0
TF32	H_vm	G4	0	1	0	0
TF33	H_vm	G5	P5max/2= 319	B_vm= 3.95e+04	0	149
TF34	H_vm	P2	-1	B_vm= 3.95e+04	0	0
TF35	H_vm	P3	0	1	0	0
TF36	H_vm	Vv	0	1	0	0
TF41	H_bm	P1	0	1	0	0
TF42	H_bm	G4	0	1	0	0
TF43	H_bm	G5	0	1	0	0
TF44	H_bm	P2	0	1	0	0
TF45	H_bm	P3	-1	B_bm= 1.3e+04	0	0
TF46	H_bm	Vv	-(F_n+F_e)= -91	B_bm= 1.3e+04	0	55

9.4.2.3 Transfer functions CVs and DVs

Table 15 Transfer functions CVs and DVs

TF	CV	DV	Process gain	Time constant 1	Time constant 2	(Steady state) Delay [min]
TF51	H_fem	F_n+F_e	0	1	0	0
TF52	H_fem	F_f	1	B_fem= 1.0367e+04	0	44
TF53	H_fem	F_t	0	1	0	0
TF54	H_fem	F_b	0	1	0	0
TF55	H_fem	F_a	0	1	0	0
TF56	H_fem	F_ns+F_sns	0	1	0	0
TF61	H_tm	F_n+F_e	Vv= 0.5	B_tm= 1.72e+04	0	125
TF62	H_tm	F_f	0	1	0	0
TF63	H_tm	F_t	1	B_tm= 1.72e+04	0	30
TF64	H_tm	F_b	0	1	0	0
TF65	H_tm	F_a	0	1	0	0
TF66	H_tm	F_ns+F_sns	0	1	0	0
TF71	H_em	F_n+F_e	0	1	0	0
TF72	H_em	F_f	0	1	0	0
TF73	H_em	F_t	0	1	0	0
TF74	H_em	F_b	1	B_em= 1.99e+04	0	59.48
TF75	H_em	F_a	0	1	0	0
TF76	H_em	F_ns+F_sns	0	1	0	0
TF81	H_vm	F_n+F_e	0	1	0	0
TF82	H_vm	F_f	0	1	0	0
TF83	H_vm	F_t	0	1	0	0
TF84	H_vm	F_b	0	1	0	0
TF85	H_vm	F_a	1	B_vm= 3.95e+04	0	79
TF86	H_vm	F_ns+F_sns	0	1	0	0
TF91	H_bm	F_n+F_e	1-Vv= 0.5	B_bm= 1.3e+04	0	107
TF92	H_bm	F_f	0	1	0	0

TF93	H_bm	F_t	0	1	0	0
TF94	H_bm	F_b	0	1	0	0
TF95	H_bm	F_a	0	1	0	0
TF96	H_bm	F_ns+F_sns	1	B_bm= 1.3e+04	0	42

9.4.3 Degrees of freedom analysis

Degrees of freedom analysis presented in chapter 2.3 in (Dale E. Seborg, 2004) will be used.

Oslo SN model has:

13 constant parameters (Table 13 Constant parameters)

6+6+5=17 variables (Table 10 Inlet flows/Disturbance variables; 8 inlet flows are reduced to 6 MVs, Table 11 Gates, pumps and separation/Manipulated variables, Table 12 Magazine water levels/Controlled variables)

5 independent differential equations (Equations 25, 26, 27, 28 and 29)

The degrees of freedom are thus:

17-5=12

The dependent variables are controlled output variables on the left side of the differential equations 25, 26, 27, 28 and 29; 5 magazine levels H_fem, H_tm, H_em, H_vm and H_bm.

Because all degrees of freedom have been utilized, the differential equations are exactly specified and can be solved.

9.4.4 Fagerlia separation weir

From a wastewater management perspective for Oslo SN, Fagerlia separation plays a very critical role. Dynamic control of Fagerlia separation makes it possible that, unlike other inlet flows, East and North inlet flows can be strategically allocated between the two WWTPs enabling a more flexible and optimal Oslo SN deployment.

Fagerlia separation point collects the flows from Link 2 - East inlet and Link 3 - North inlet. Collected flows are separated between the Link 4 reaching Torshov magazine and the Link 11 reaching the Bekkelaget magazine. The flow directed to Link 4 eventually reaches VEAS WWTP and the flow directed to Link 11 eventually reaches Bekkelaget WWTP. See Figure 7 Oslo SN model schematic diagram.

Efficient deployment of this Fagerlia separation feature can further improve the performance of Oslo SN specifically under uneven rainfall events in Oslo region which is suggested in the further work section.

Under dry weather/steady state conditions, at Fagerlia point, half of the flow is directed to Link 4 and the other half is directed to Link 11.

9.4.4.1 Control of Fagerlia separation

Fagerlia separation steady state/dry weather value, Vv = 0.5

Fagerlia separation minimum value, Vvmin = 0.3

Fagerlia separation maximum value, Vvmax = 0.7

In the Oslo SN model, Fagerlia separation is governed by an independent proportional control. This control balances out the volume occupancy ratio of Torshov and Bekkelaget magazines. Implementation in the dynamic model:

$$Vv=0.2*[(H\_bm/Hmax\_bm)-(H\_tm/Hmax\_tm)]+0.5 \qquad (40)$$

Vv: Fagerlia separation value

H_bm: Dynamic water level in the Bekkelaget magazine [m]

Hmax_bm: Maximum possible water level in the Bekkelaget magazine [m]

H_tm: Dynamic water level in the Torshov magazine [m]

Hmax_tm: Maximum possible water level in the Torshov magazine [m]

9.4.5 Real-time optimization using forecast data

Each rain event data also has its forecast data. In parallel to the rainfall data, this forecast data is also fed to the model every minute. Rain event periods (Assuming 10 hours for each), 12 hours before and 6 hours after events were forecasted as rainy. Value 1 is sent to the model in case of positive rain forecast whereas value 0 is sent to the model in case of no rain forecast. With forecast data, Oslo SN control algorithm is expected to prepare itself to an incoming event by maximizing its available volume and further reducing possible overflows.

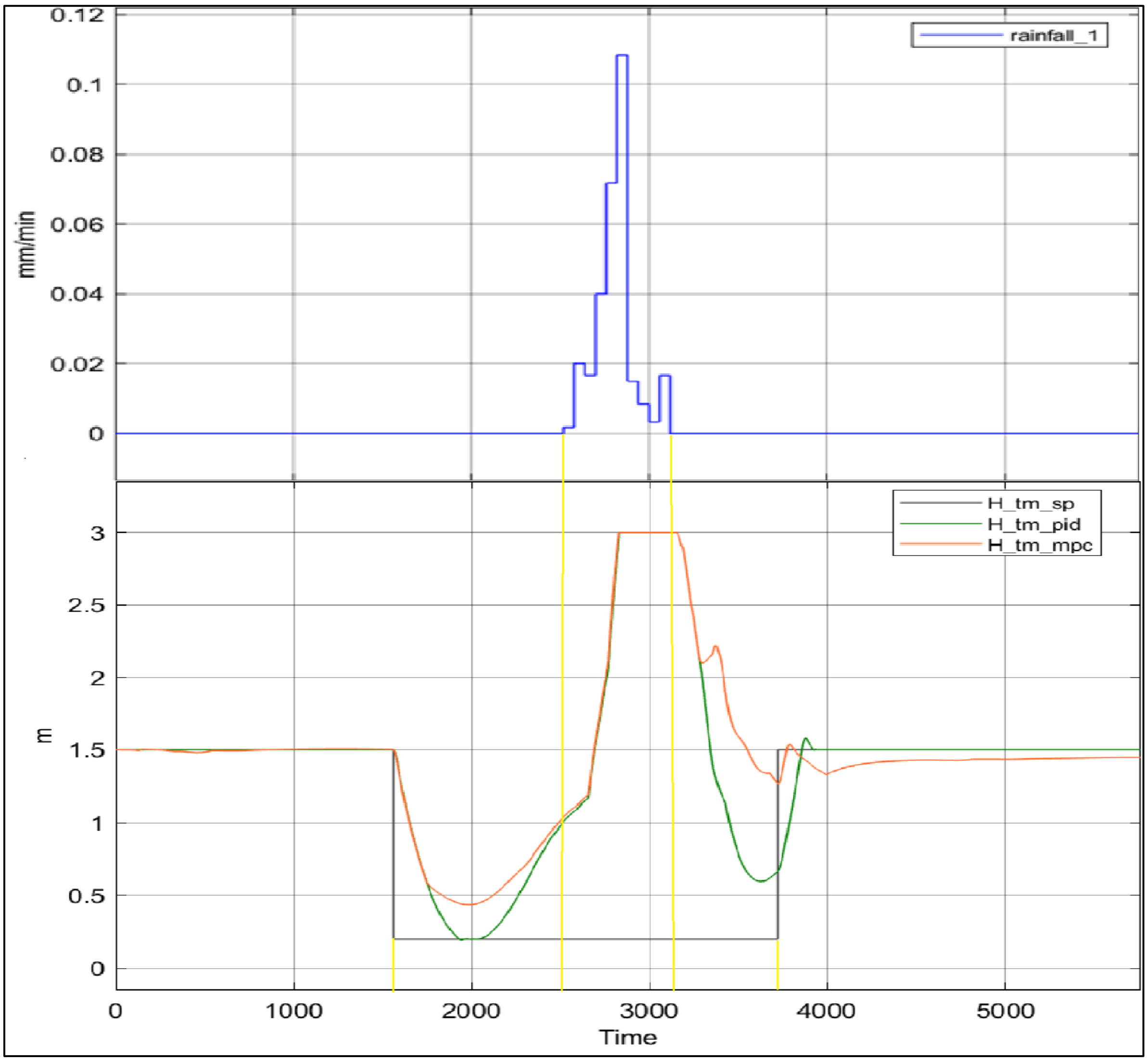

Figure 17 Real-time Optimization using Forecast Data

Figure 17 Real-time Optimization using Forecast Data shows the example of rain event 1 and step changes applied to the CV-Torshov magazine level set-point.

12 hours before the rain event starts, forecast feed to the model step changes from 0 to 1. This change triggers a circuit in the model where set point levels of all magazines are reduced to 0.2 meters to maximize the available volume before the rain hits. Control algorithms should

easily be able adopt the set point change in 12 hours. In addition, on account of long delays in the model, reduced set point levels persist even 6 hours after the rain event ends. This is to ensure that the control algorithm continues to minimize the delayed overflows in the network.

It is suspected that this prior control setup will largely compensate for an integrated feedforward control of the model.

9.4.6 Hardware and software

Modeling and simulations were carried out with a Lenovo Ideapad L340 Gaming laptop and MATLAB version R2021b was used. For PI control, MPC and visualization of results, separate MATLAB m files and Simulink model couples were created. Simulink models and m files are included in the digital artifact of this master's thesis work.

9.4.7 PI control, SISO strategy

For single input single output control strategy, PI controllers will be implemented to the Oslo SN model.

PID control algorithm in series form; (Skogestad, 2002)

$$c(s) = K_c * \left(\frac{\tau_i s+1}{\tau_i s}\right) * (\tau_D s + 1) \qquad (41)$$

9.4.7.1 Skogestad PID controller tuning rules

First order transfer function:

$$g(s) = \frac{K_p * e^{-\theta s}}{(\tau_1 s+1)} \qquad (42)$$

Kp process gain, $\tau 1$ time constant, θ time delay

(Skogestad, 2002) controller tuning parameters:

$$\tau_c \approx \theta \; (43)$$

$$K_c = \frac{\tau_1}{K_p(\tau_c+\theta)} \; (44)$$

$$\tau_i = \min \{\tau_1, 4 * (\tau_c + \theta)\} \quad (45)$$

9.4.7.2 Control pairs

For instance, Bristol's relative gain array method is a systematic approach that can be used for the analysis of multivariable process control problems. Given steady state information, the method can provide a measure of process interactions and recommendations of most effective pairings of CVs and MVs. (Dale E. Seborg, 2004)

In Oslo SN control, MVs are the magazine outflow controllers which are pumps and gates (There is also Fagerlia separation as an MV, but it has its own independent control.) and CVs are the water levels in the magazines. It should be evident that each magazine level should be paired with that magazines outflow controller for the best control. Accordingly, Bristol's RGA method for the pairings of the CVs and MVs, in this case, evaluated unnecessary.

9.4.7.3 Control pair transfer functions

TFs from Table 14 Transfer functions CVs and MVs

Table 16 Control pair TFs

Control loop	TF	CV	MV	Process gain	Time constant 1	Time constant 2	Delay
1	TF01	H_fem Festning M. level	P1 Forgnerparken pump	-1	B_fem= 10367	0	0
2	TF12	H_tm Torshov M. level	G4 Torshov outflow gate	-P4max/2= -172	B_tm= 17200	0	0
3	TF23	H_em Engervann M. Level	G5 Engervann outflow gate	-P5max/2= -319	B_em= 19996	0	0
4	TF34	H_vm VEAS M. level	P2 Bjerkås pump	-1	B_vm= 39466	0	0
5	TF45	H_bm Bekkelaget M. level	P3 Bekkelaget pump	-1	B_bm= 12959	0	0

9.4.7.4 PI parameters of Oslo SN model

Applying Skogestad controller tuning rules to the control loop TFs yields the parameters for the PI controllers:

Table 17 PI parameters

Control loop	TF	CV	MV	PI controller	Proportional	Integral
1	TF01	H_fem	P1	PI1	-1.0367e+04	0.25
2	TF12	H_tm	G4	PI2	-1.0021e+02	0.25
3	TF23	H_em	G5	PI3	-62.7241	0.25
4	TF34	H_vm	P2	PI4	-3.9466e+04	0.25
5	TF45	H_bm	P3	PI5	-1.2959e+04	0.25

PI controller outputs are added to the steady state values of the inputs and sent to the Oslo SN model. Constraints on the MVs are applied to the output saturation of the controllers. (Table 18 PI controller limitations)

Since MVs are pumps and gates, it naturally should take some time for them to change their values. It is assumed that all MVs can reach from their minimum values to their maximum values in 30 minutes and vice versa. For these rate of change limitations, rate limiter blocks are applied to PI outputs. (Table 18 PI controller limitations)

Anti-windup method, clamping is applied to the output saturation of the controllers.

Table 18 PI controller limitations

PI controller	Maximum output	Minimum output	MV	Steady state input to the model	Minimum input to the model	Maximum output to the model	Rising rate of change limit (per minute)	Falling rate of change limit (per minute)
PI1	119.9	-24.075	P1	30.1	6	150	4.8	-4.8
PI2	0.5584	-0.4416	G4	0.4416	0	1	0.033	-0.033
PI3	0.583	-0.417	G5	0.4170	0	1	0.033	-0.033
PI4	501	-127	P2	159	32	660	20.93	-20.93

PI5	356	-67	P3	83.8	17	440	14.1	-14.1

For more information about MVs and their values, see Table 6 Pumps and Table 7 Gates.

9.4.8 Mpc control, MIMO strategy

For multiple input multiple output control strategy, a linear MPC will be implemented to the Oslo SN model. For the linear internal model of MPC, control pair TFs from Table 16 Control pair TFs were used.

9.4.8.1 Principles of Model Predictive Control

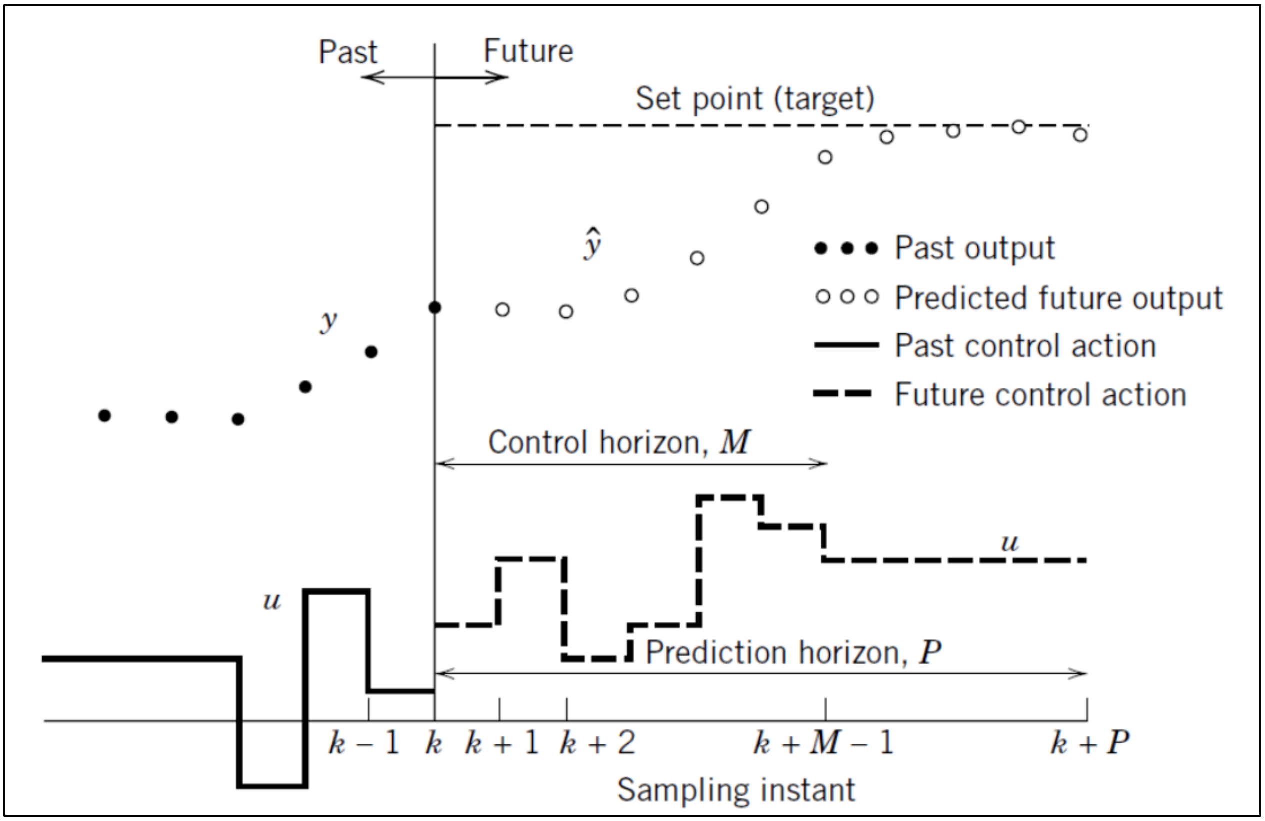

Figure 18 MPC algorithm

Figure 18 MPC algorithm is from the book (Dale E. Seborg, 2004).

$y_{sp} = set\ point\ (target)$

$y = measured\ output$

$\hat{y} = predicted\ future\ output$

$u = control\ action$

$k = current\ time\ step\ (discrete\ time)$

$M = control\ horizon$

$P = rediction\ horizon$

Linear process model:

$$x(k+1) = Ax(k) + Bu(k), y(k) = Cx(k) + Du(k) \qquad (46)$$

MPC optimizes future control actions u for M steps forward to achieve:

$$\hat{y}(k+P) = y_{sp}(k+P) \qquad (47)$$

MPC predicts future output $\hat{y}$ for P steps forward. Control actions are based on linear process model (equation 46) and all the previous inputs and outputs and future setpoint trajectory. All calculations are repeated each time step. (Dale E. Seborg, 2004)

9.4.8.2 MPC tuning rules

General MPC tuning rules from (Dale E. Seborg, 2004).

Sampling time, $Tsampling < T/10$

Settling time, $Tsettling \approx 4T + \theta$

Model horizon N, $N = Tsettling/Tsampling$

Typically; $30 \leq N \leq 120$.

If $N > 120$ increase Tsampling, If $N < 30$ decrease Tsampling

Control horizon M, $N/3 \leq M \leq N/2$

Typically, $5 \leq M \leq 20$, Increasing M makes controller more aggressive

Prediction horizon P, $P = N + M$

Decreasing P makes controller more aggressive

Output weighting matrix Q for CVs (y)

Controlled output variables yi are weighted according to their relative importance Initial value is 1. More important variables have larger numbers.

Input weighting matrix R for MVs (u)

Initial value is 0.1. Larger values will reduce the rate of change for MVs.

9.4.8.3 Urban drainage systems' MPC tuning from literature

Literature has no consensus about the optimal MPC parameterization for urban drainage systems. Many MPC parameterization examples based on their specific applications in urban drainage systems have been reviewed and some optimal tuning values are presented in reference (Nadia Schou Vorndran Lund, 2018).

Sampling interval 1-10 min, mostly 5 minutes.

Settling duration < sampling interval

Collective horizon 30-120 min (should coincide with forecast ability of many radar nowcast products). An example of 13 hr. with an NWP model also exists. Collective horizon is when control horizon and prediction horizon are of equal length.

Examples: Sampling intervals of 10, 5 and 2 min, respectively setting durations of 10, 5 and 120 min, and all applied a collective horizon of 2hr.

In theory, a long collective horizon and a short sampling interval and settling duration will increase the performance of the model (up to a limit. 60 and 100 minutes found by two studies. Lower limit found by 25 minutes by another study to prevent myopic control.). Based on model dynamics, sampling interval may have a bigger effect (3-9 minutes). (Nadia Schou Vorndran Lund, 2018)

9.4.8.4 MPC tuning of Oslo SN model

Model horizon is 120 minutes. Collective horizon approach was adopted. So, prediction and control horizons are 60 minutes. Sampling time is 5 minutes.

Table 19 MPC limitations

CV	MV	Minimum output	Maximum output	Steady state input to the model	Minimum input to the model	Maximum output to the model	Rising rate of change limit (per minute)	Falling rate of change limit (per minute)
H_fem	P1	-24.075	119.9	30.1	6	150	4.8	-4.8
H_tm	G4	-0.4416	0.5584	0.4416	0	1	0.033	-0.033
H_em	G5	-0.417	0.583	0.4170	0	1	0.033	-0.033
H_vm	P2	-127	501	159	32	660	20.93	-20.93
H_bm	P3	-67	356	83.8	17	440	14.1	-14.1

MPC outputs are added to the steady state values of the inputs and sent to the Oslo SN model. MPC output limitations in Table 19 MPC limitations are the same as PI controllers' limitations in Table 18 PI controller limitations.

Weight Matrices

Q matrix, equal weighting between the CVs:

$$Q = [1\ 1\ 1\ 1\ 1] \qquad (48)$$

Ru matrix, equal weighting for the MVs

$$Ru = [0\ 0\ 0\ 0\ 0] \qquad (49)$$

Rd matrix, equal weighting for the changes in the MVs

$$Rd = [0\ 0\ 0\ 0\ 0] \qquad (50)$$

No rate of change limitation is applied to the internal model of MPC. However, output of the MPC is limited by rate limiter blocks in the model. Rate of change for the MPC is the same as PIs from Table 18 PI controller limitations. Applying the exact same rate of change limitation to both control strategies further validates the comparison between them in this work.

Oslo SN Model predictive controller is structured with the simplified linear TFs from Table 16 Control pair TFs and hence is a linear MPC. Linear Oslo SN MPC will be tested in Oslo SN which has non-linear flows and delays in the system. Results will show how a simplified linear MPC performs in a non-linear urban drainage system control.

10 Results and Discussion

10.1 Controller testing and results

For each simulation, first, inputs to the model are presented which are the rainfall data of the specific event and its effects on the inlet flows/DVs. The four control strategies are tested against the same rain event and its inlet flows/disturbances. They are PI, PI+F, MPC and MPC+F. “+F” notation means the upgrade: real-time optimization with forecast data on PI and MPC control strategies.

Next, control results of the control strategies under the same rain event conditions are presented which are pumps and gates values/MVs, magazine levels/CVs and WWTP inflows. Last, overflows and overflow volume results are presented.

Result reading:

- Variable name with 0 in the end is the steady state value of the variable shown as a reference point
- Maximum water levels for the magazines are shown in results. When the level hits the maximum, the overflow period of a magazine can visually observed on the CV result figures.
- Parameters were grouped and each group is presented in a compact form to not overpopulate the report. Result figures’ variables may not be very clear to the eye yet, numerical results and comparisons will be presented in tables additionally.

In dry weather periods of the simulations, for the management of municipal wastewater, MV controls are very similar between the control strategies, except not when PI control occasionally has some small overshooting’s. (Figures 21, 24, 29, 32, 37, 40, 45 and 48)

MV results with the forecast data show expected maximum MV values, 12 hours before the rain event hits and a decrease to minimum values a short time after. (Figures 24, 32, 40 and 48) With this action, volumes in the magazines are maximized before the rain hits, by reducing set-points and adjusting the CVs with the real-time optimization with forecast data. (Figures 25, 33, 41 and 49)

PI control exhibits some oscillatory periods in MV results. Less than PI, but MPC also exhibits similar oscillatory periods. These oscillatory periods are mostly when rain events hit and leave. Rate of change for both control strategies for MV movements are hardly limited and these oscillations are naturally within these limits. Since the simulation period is 4 days, oscillations look more obvious. Regardless, it is not an ideal control behavior. (Figures 21, 24, 29, 32, 37, 40, 45 and 48)

During events, PI and MPC controls maximize the MV values as expected. However, MPC is more reluctant than PI control to reduce back the MV values after the event ends. Especially for MVs: Frognerparken pump, Bekkelaget pump and Bjerkås pump. (Figures 21, 24, 29, 32, 37 and 40) In rain event 3 (figures 37 and 40) the decreases in MVs are even more delayed. In rain event 4 (figures 45 and 48) however PI and MPC control have more similar MV behaviors with little to none delay for decrease in MVs for MPC compared to PI controllers. It seems that the more extreme the event is, the longer the delay in MV decreases for MPC.

As for the CVs, because of the previously mentioned MPC behavior, MPC simulations end up with less wastewater in the Oslo SN and sometimes even hit the minimum level limits. The levels take much longer times to reach set-points after the rain events end for the MPC control. Especially for Festning, Bekkelaget and Veas magazines. (Figures 22, 25, 30, 33, 38, 41, 46) This was not the case for moderate rain event 4 with forecast data. (Figure 49)

Fagerlia separation independent control is included in the MV result figures. Independent control seems to have taken more actions while running with the MPC. (Figures 21, 24, 29, 32, 37, 40 and 45) Exception is moderate rain event 4 with forecast data. (Figure 48)

As expected, results show that it is very unlikely to get overflows from later magazines in the network especially the Veas magazine. (Figures 22, 25, 30, 33, 41, 46 and 49) Only in rain event 3 and without forecast data, overflow was observed from Veas magazine. (Figure 38)

Rain event 3 resulted in the most unreliable control. Additionally, the control without forecast being worse than the control with forecast. Overflows were observed from all magazines and some magazines alone had several overflowing periods. (Figure 38) The problem that MPC overly deploying MVs after the rain event ends, was the longest in rain event 3, and specifically without forecast. (Figure 37) For the MV Bjerkås pump, it persisted so long that 4 days of simulation were not enough for it to settle down. (Figure 37 and 39) Since Bjerkås pump is the inflow to the Veas WWTP, inflow to the WWTP was at its maximum starting from rain event and to the end of simulation. (Figure 39) Bjerkås pump takes the wastewater from Veas magazine. Approximately 12 hours after rain event 3 ends, Veas magazine has hit its minimum limit and stays at minimum until the end of simulation. (Figure 38) However, the pump continues to take wastewater with its maximum capacity from a magazine which has already hit its minimum level limit. The integrity of the model becomes questionable at this period for MPC control, rain event 3, without forecast. This could have been avoided with an implementation of logic switch between the tank level and the controller output in the model where if the level hits minimum, the pump stops in a further work. It is obvious that the results of MV behavior, WWTP inflows and treated water volume for this period is not realistic. Regardless, overflow measurements from these simulations are still accurate reason being MV over deployment cannot increase nor decrease the overflow amount after the rain event ends and the level in the magazine has hit zero.

It was expected that the more extreme the event is, the less reliable the MATLAB/Simulink model becomes. Rain event 3 is one of the most extreme events in the regions history and it was the most extreme event in the simulations of this work. Accordingly, it was not a surprise that the event 3 has forced the limits of both the model's integrity and the control strategies. Not empowering the control with forecast also made the scenario even harder to manage for the model and the control. (Figures 37, 38, 39 compared to figures 40, 41, 42)

Rain event 1 and 2 are also extreme and rare events, rain event 4 is however a moderate event. Since light/moderate events like rain event 4 happen many times every year and are very common for all times, rain event 4 is the most important example scenario of this work. The performance of the model and the control strategies should especially be evaluated based on the most frequent events in the historical data of the region and the urban drainage system of the Oslo city.

Rain event 4 exhibited the smoothest controls as expected and it was even more smooth with forecast data. MPC and PI controllers had similar MV results only with some oscillations more with PI, less with MPC. (Figures 45 and 48) Integrity of the model is not violated. (Figures 46, 47, ,49 and 50)

10.1.1 Simulation 1

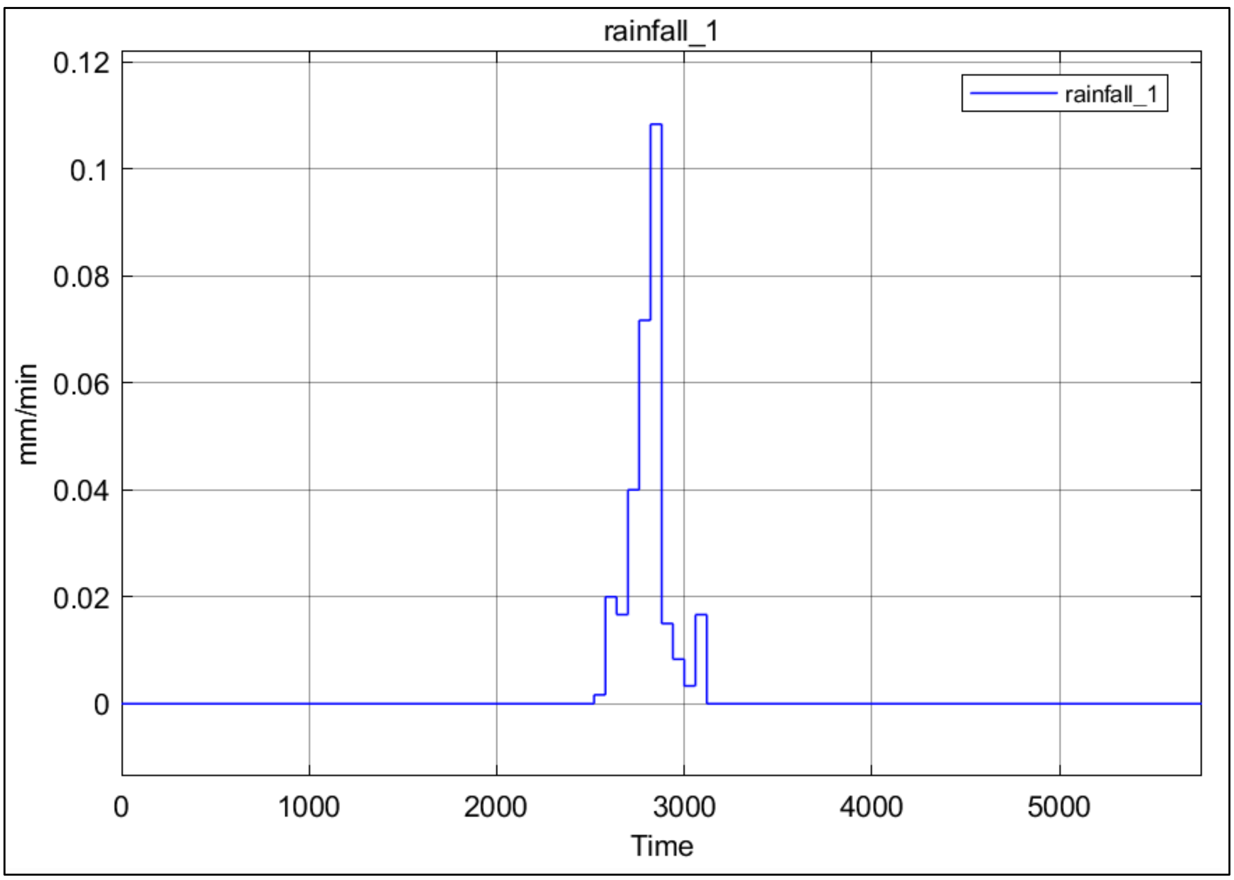

Figure 19 Simulation 1, Rain event 1

10.1.1.1 Inputs to the model, Rain event 1:

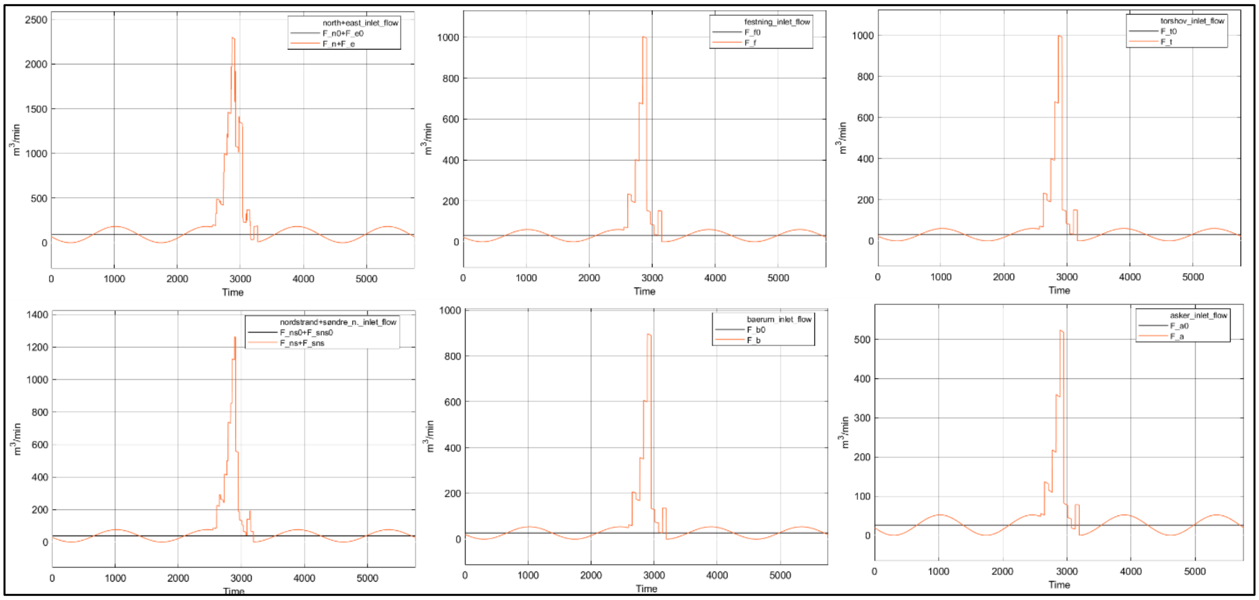

Figure 20 Rain event 1, Inlet flows/DVs

10.1.1.2 Rain event 1 without forecast data, controller results

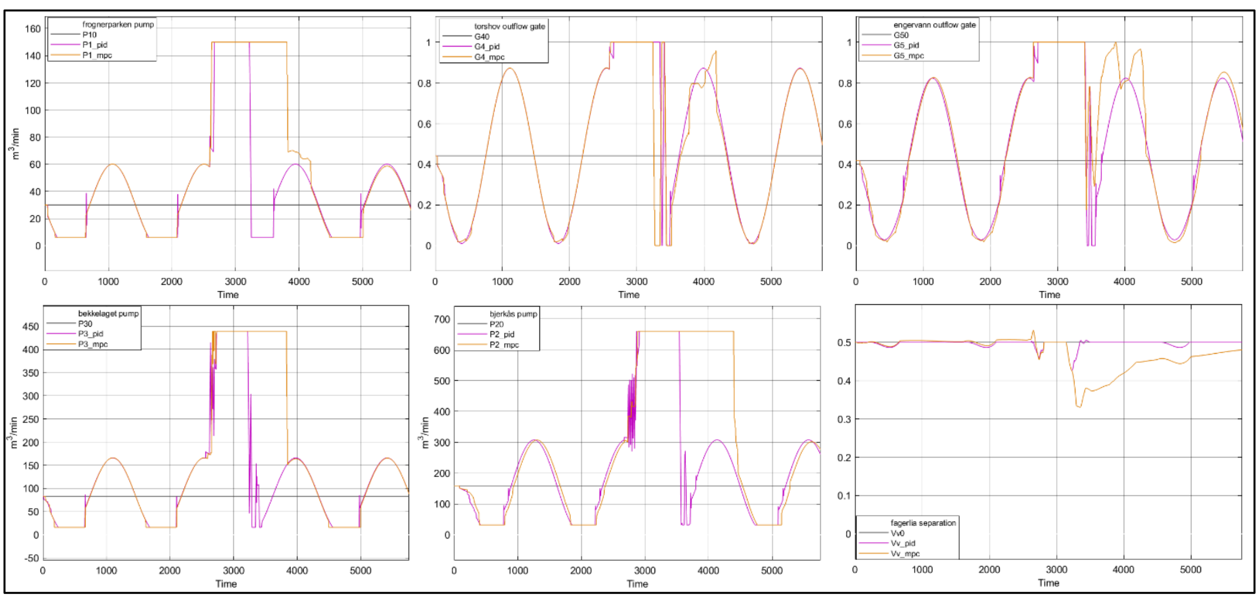

Figure 21 Rain event 1, without forecast, MV results

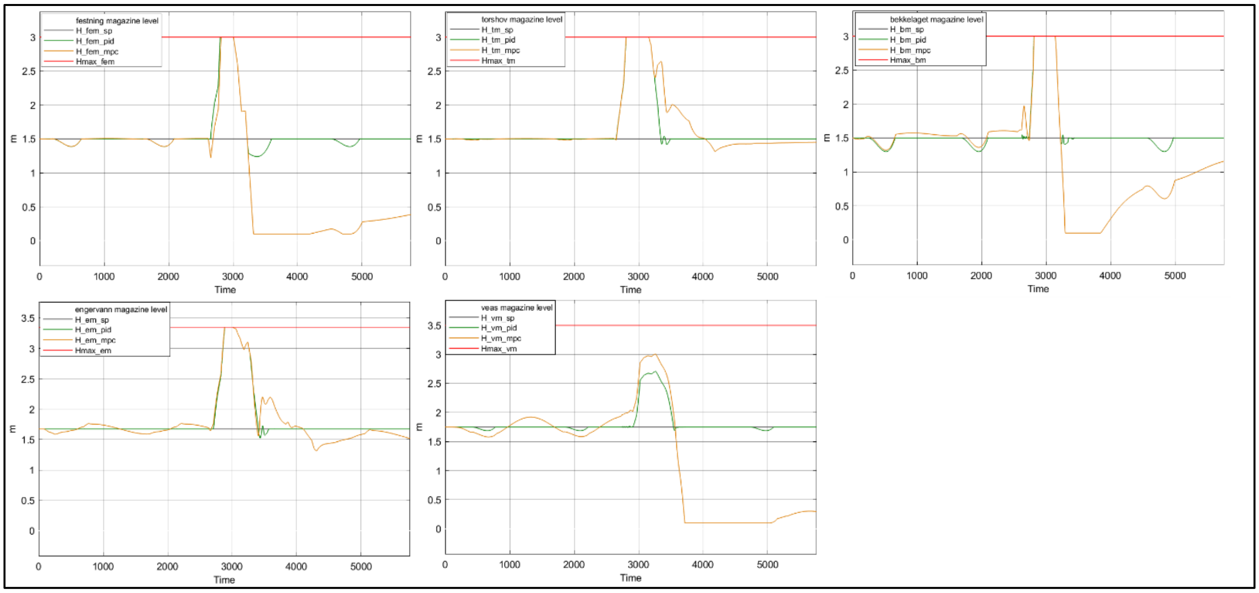

Figure 22 Rain event 1, without forecast, CV results

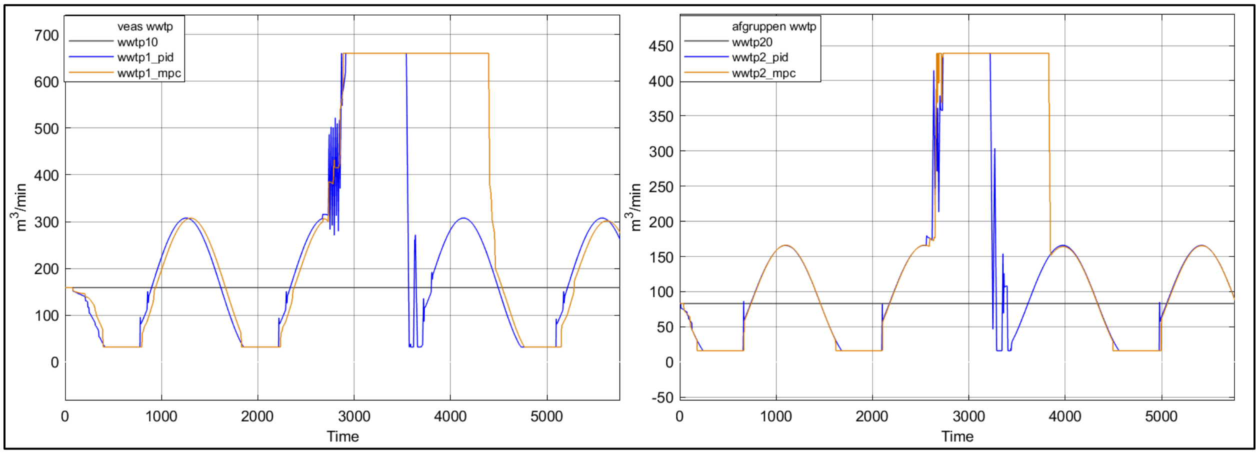

Figure 23 Rain event 1, without forecast, WWTP inflows

10.1.1.3 Rain event 1 with forecast data, controller results

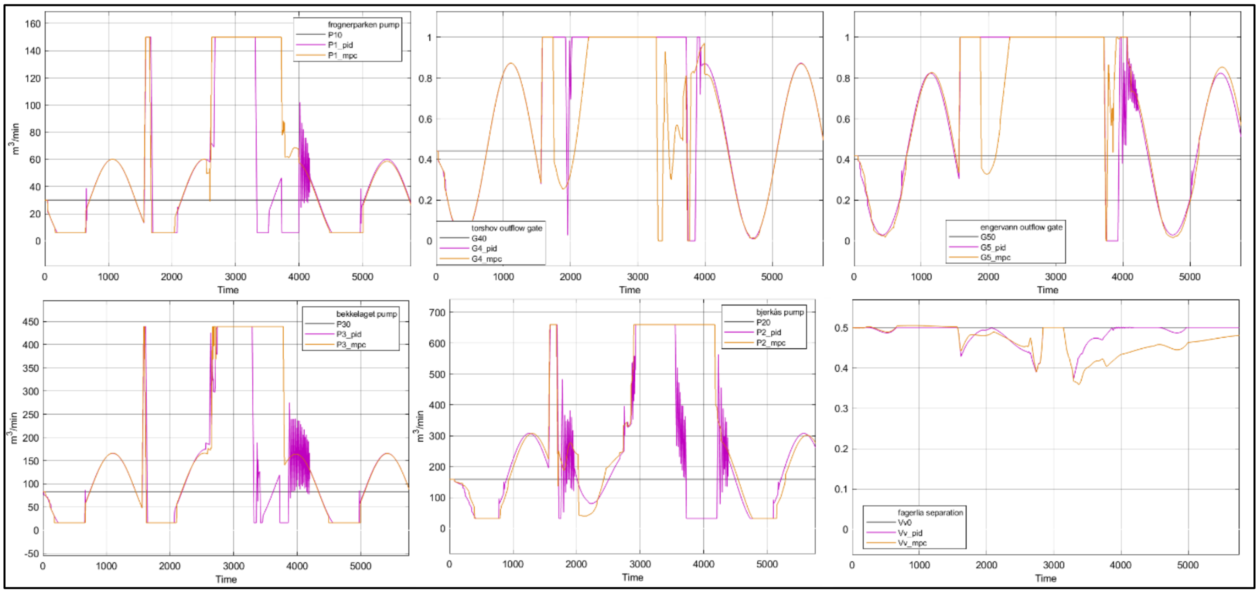

Figure 24 Rain event 1, with forecast, MV results

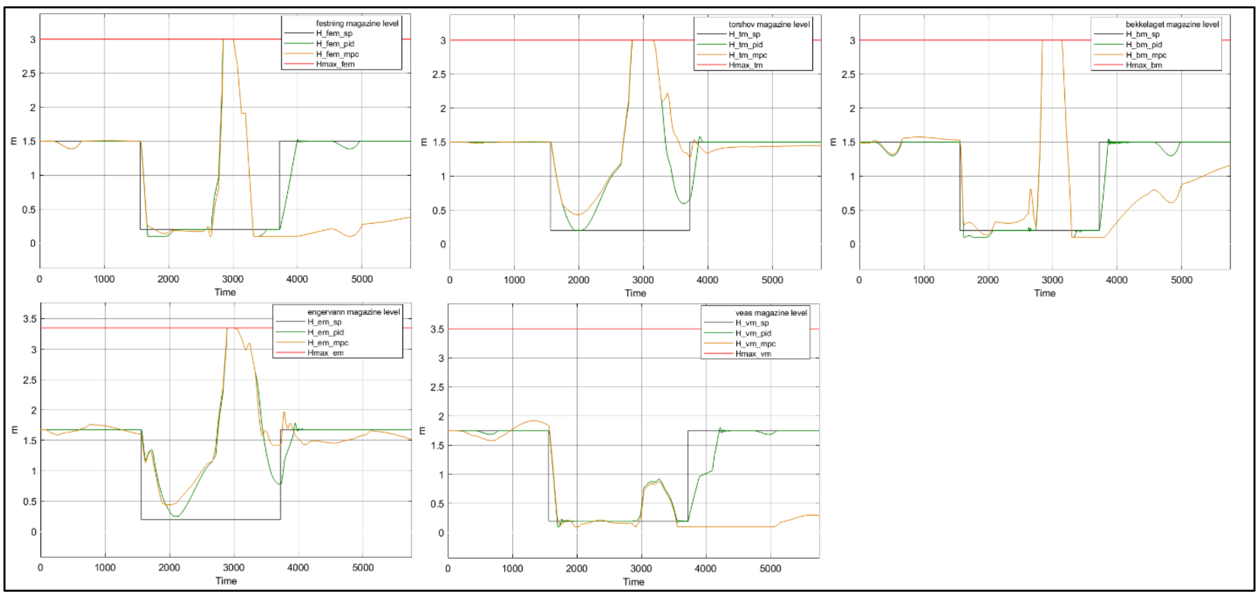

Figure 25 Rain event 1, with forecast, CV results

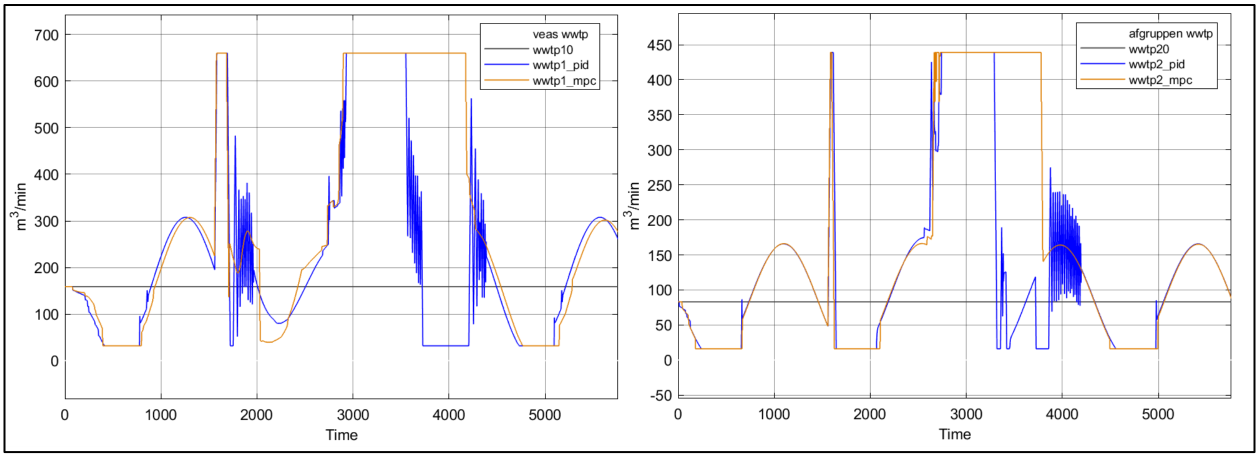

Figure 26 Rain event 1, with forecast, WWTP inflows

10.1.2 Simulation 2

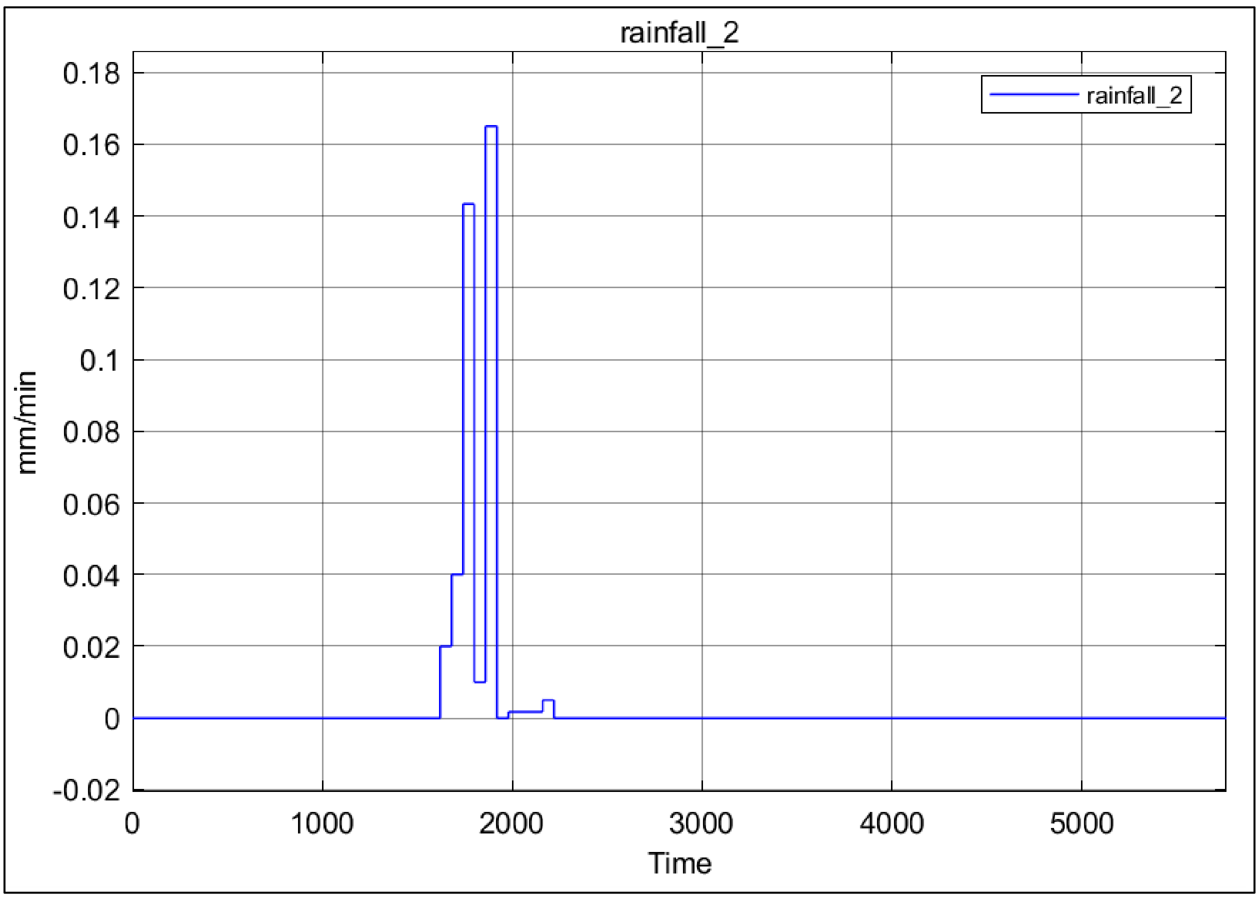

Figure 27 Simulation 2, Rain event 2

10.1.2.1 Input to the model, Rain event 2:

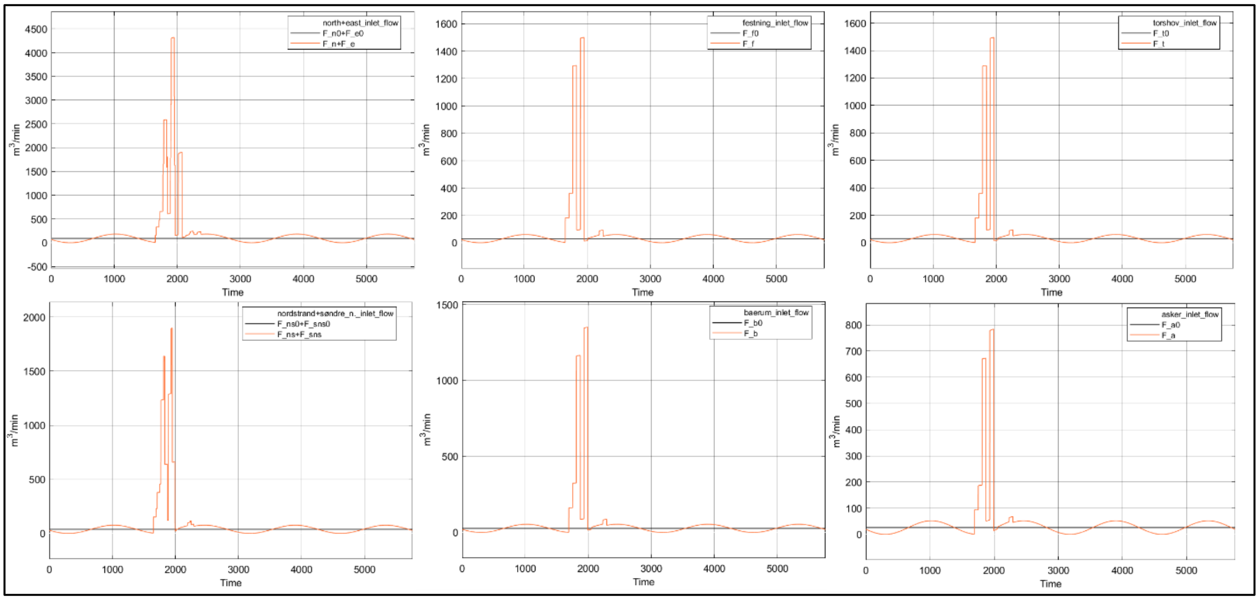

Figure 28 Rain event 2, Inlet flows/DVs

10.1.2.2 Rain event 2 without forecast data, controller results

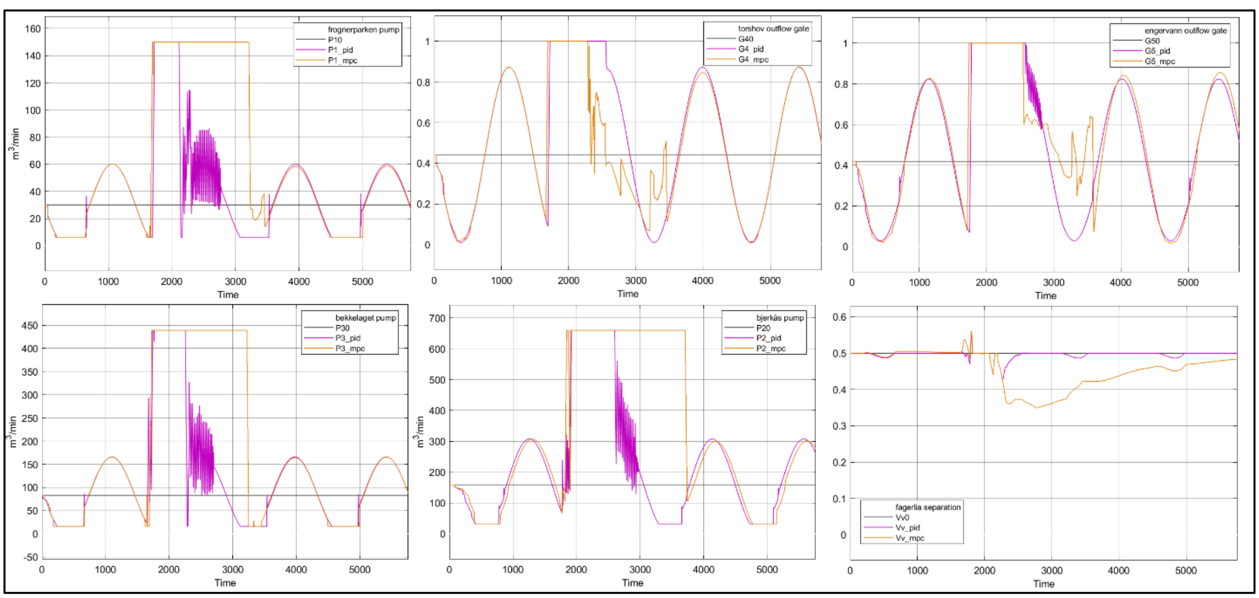

Figure 29 Rain event 2, without forecast, MV results

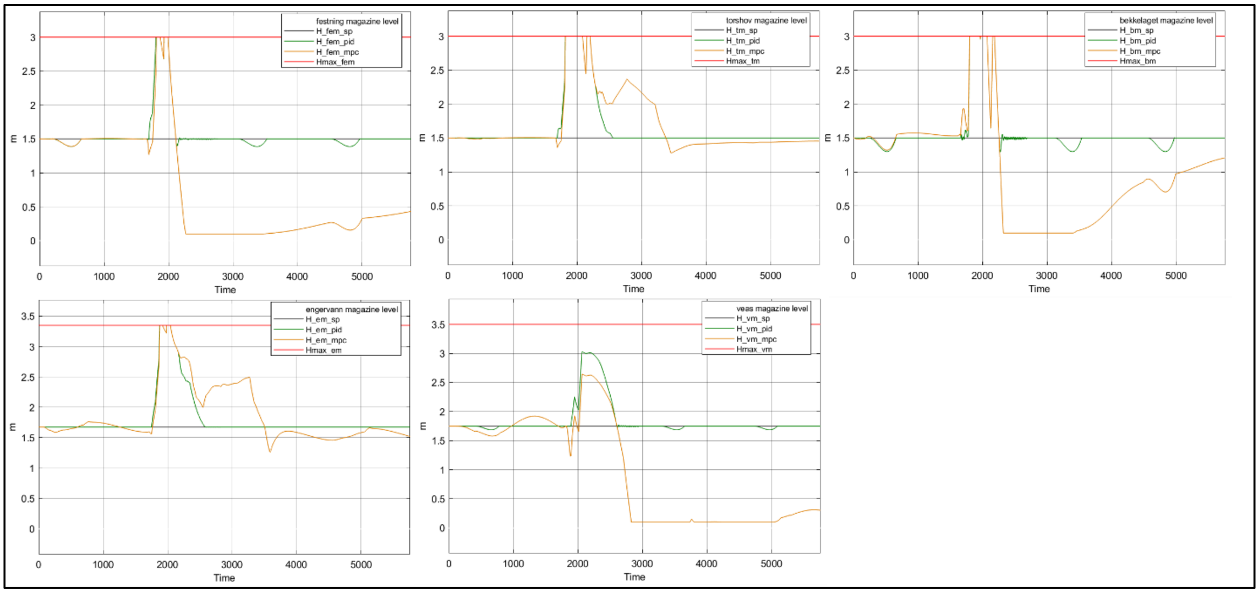

Figure 30 Rain event 2, without forecast, CV results

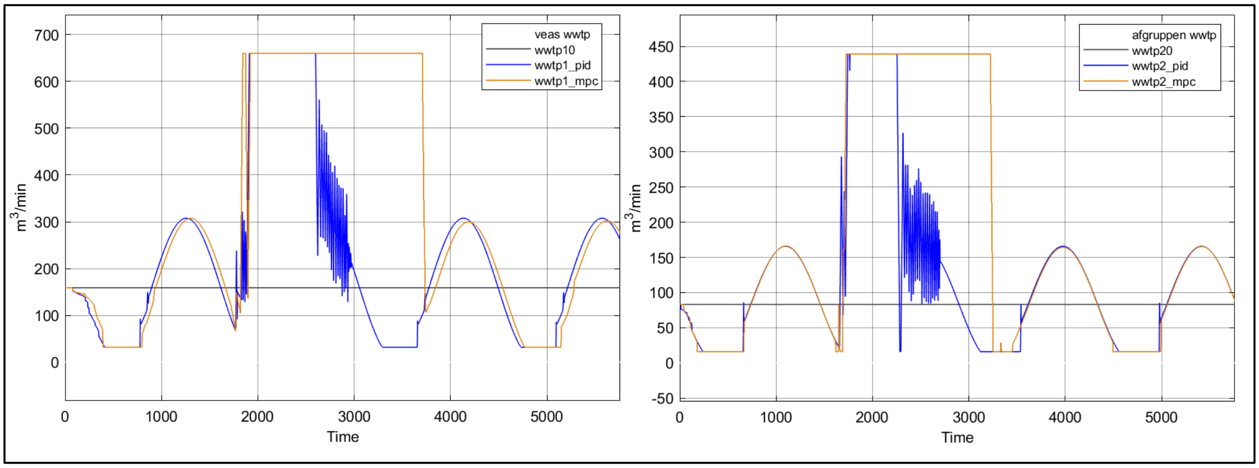

Figure 31 Rain event 2, without forecast, WWTP inflows

10.1.2.3 Rain event 2 with forecast data, controller results

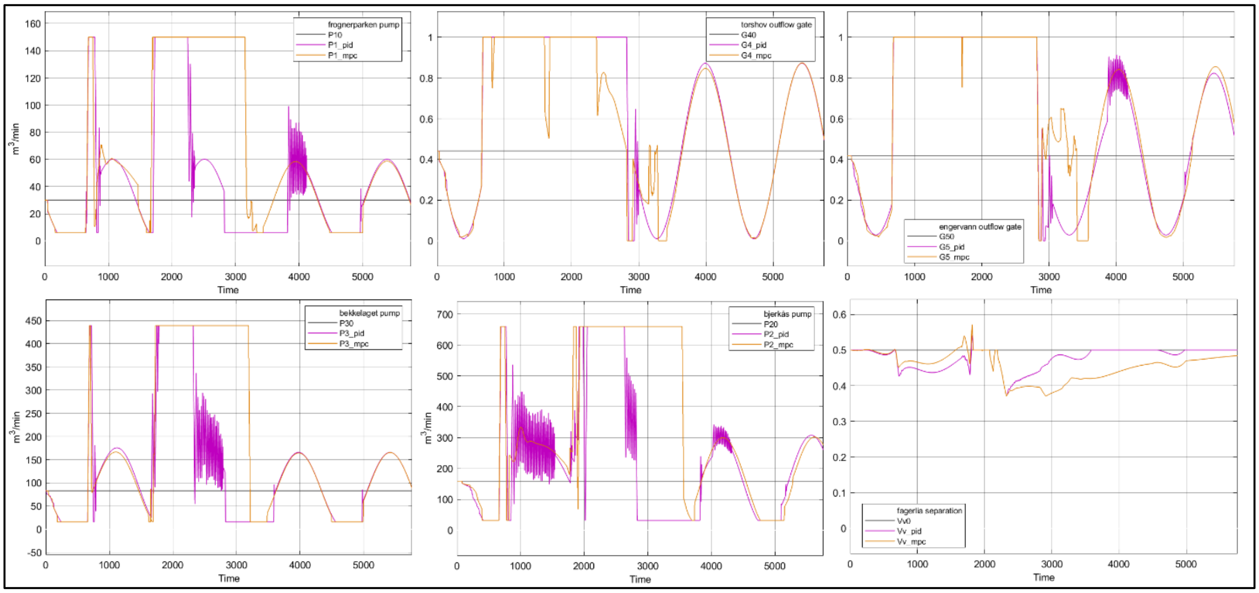

Figure 32 Rain event 2, with forecast, MV results

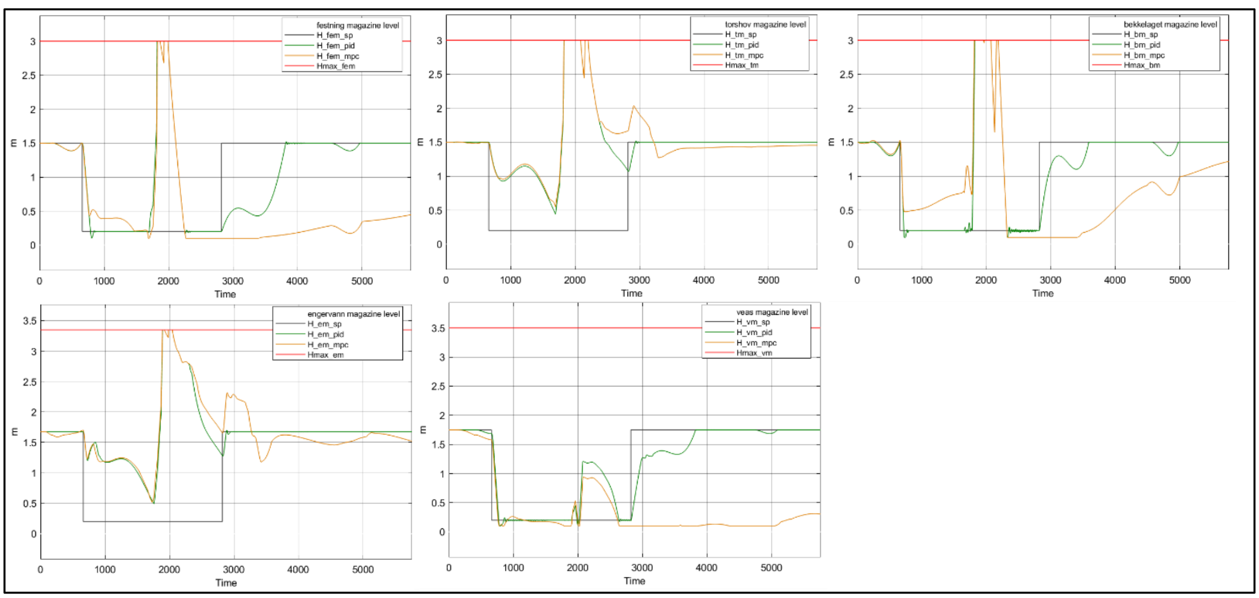

Figure 33 Rain event 2, with forecast, CV results

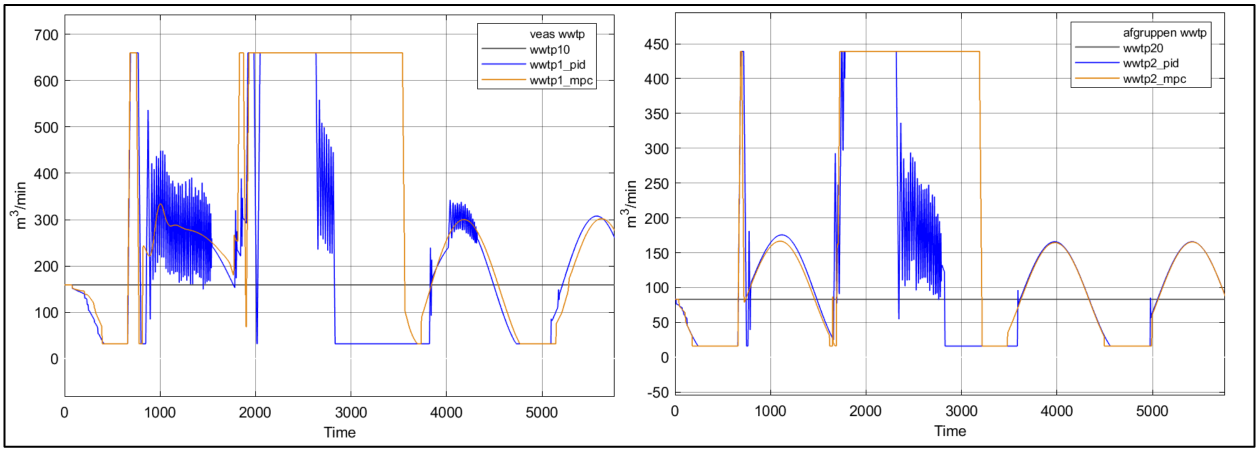

Figure 34 Rain event 2, with forecast, WWTP inflows

10.1.3 Simulation 3

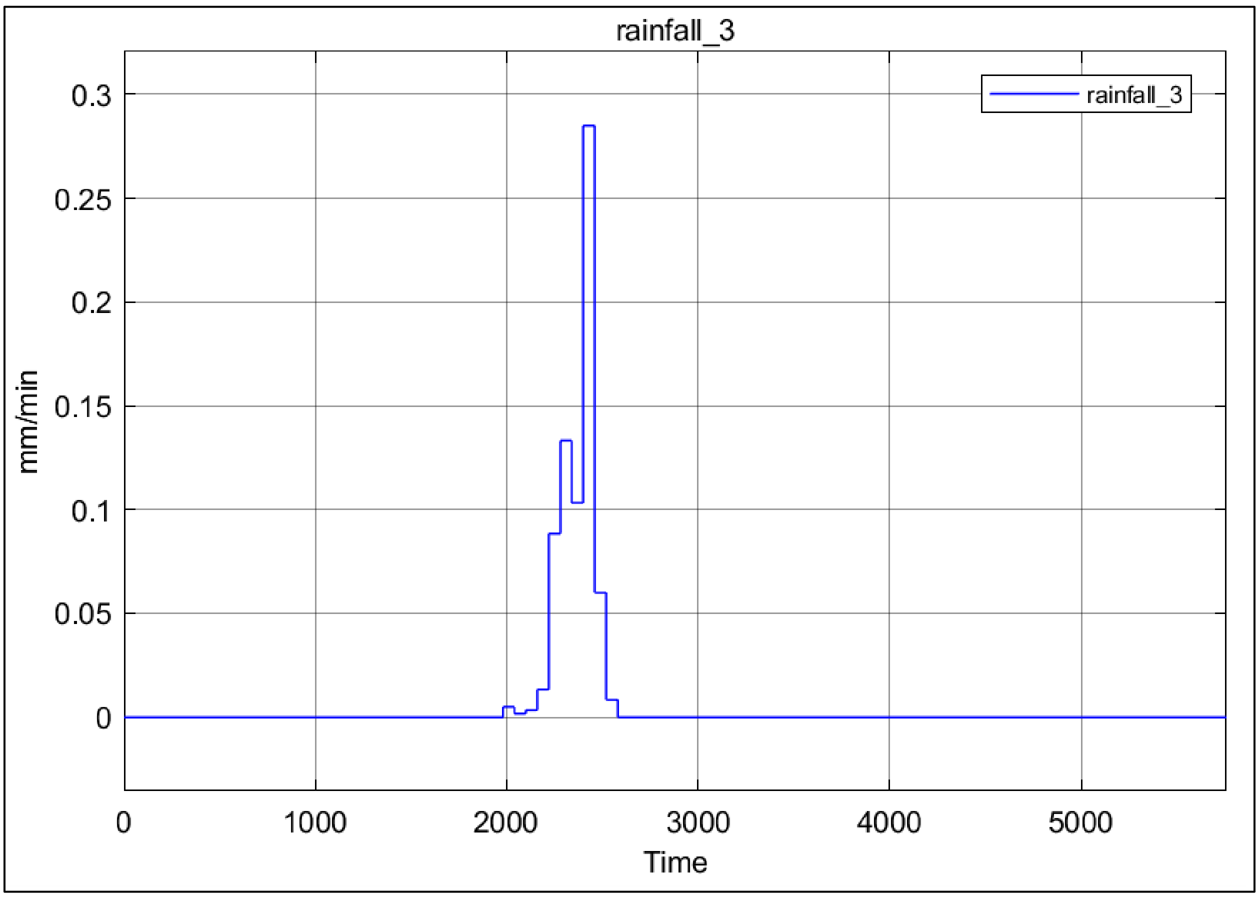

Figure 35 Simulation 3, Rain event 3

10.1.3.1 Input to the model, Rain event 3:

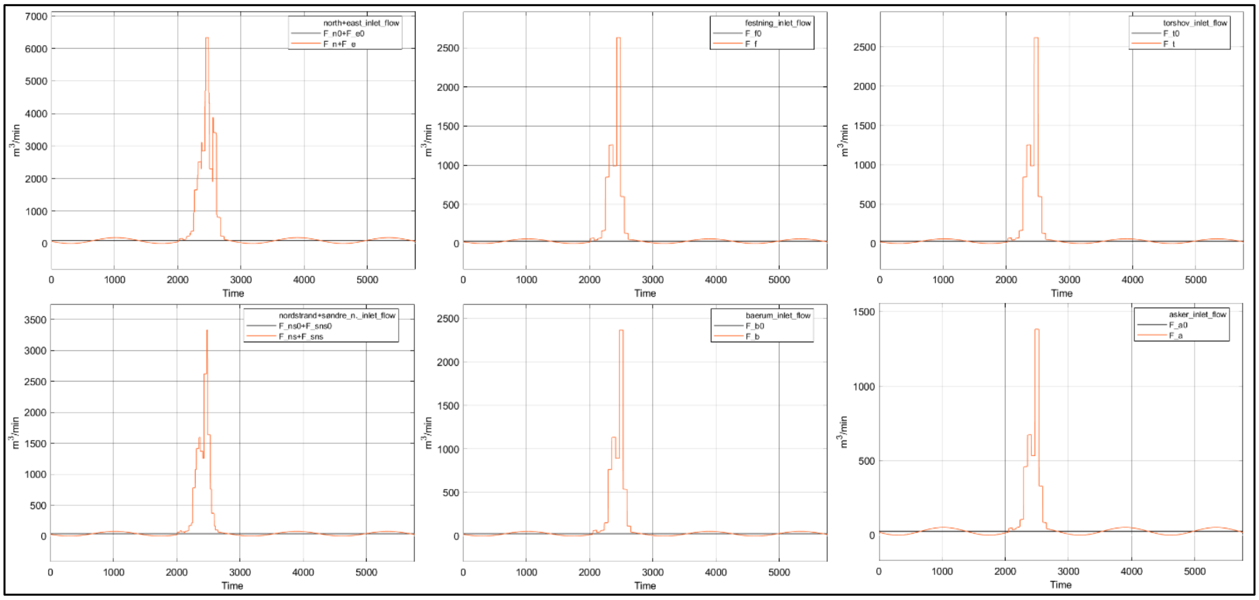

Figure 36 Rain event 3, Inlet flows/DVs

10.1.3.2 Rain event 3 without forecast data, controller results

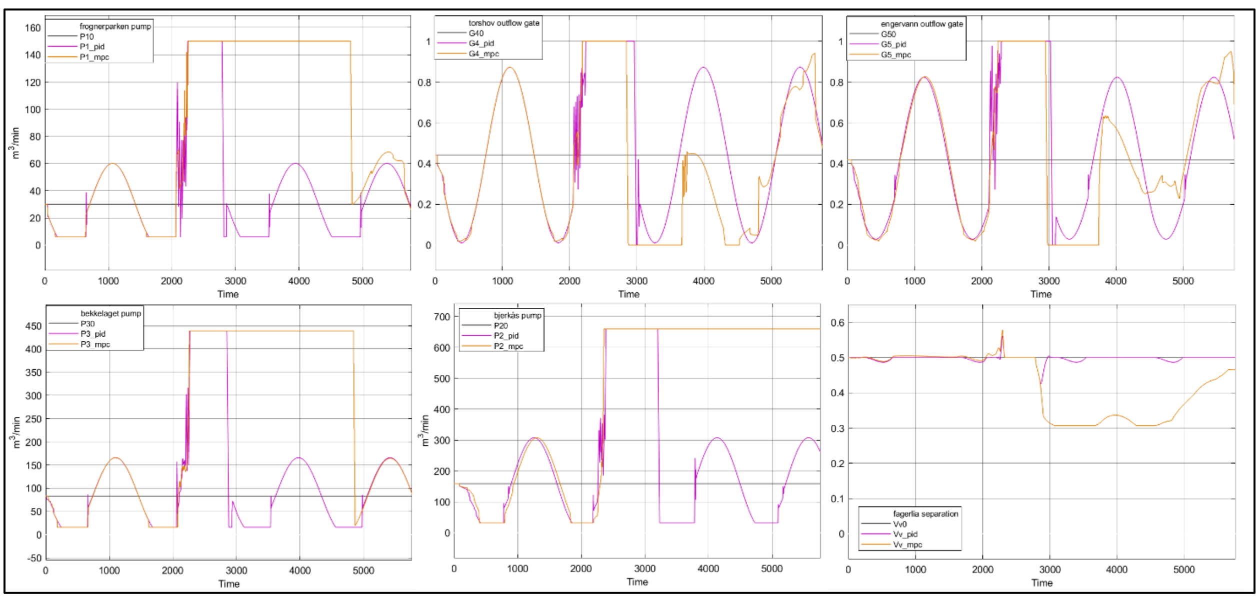

Figure 37 Rain event 3, without forecast, MV results

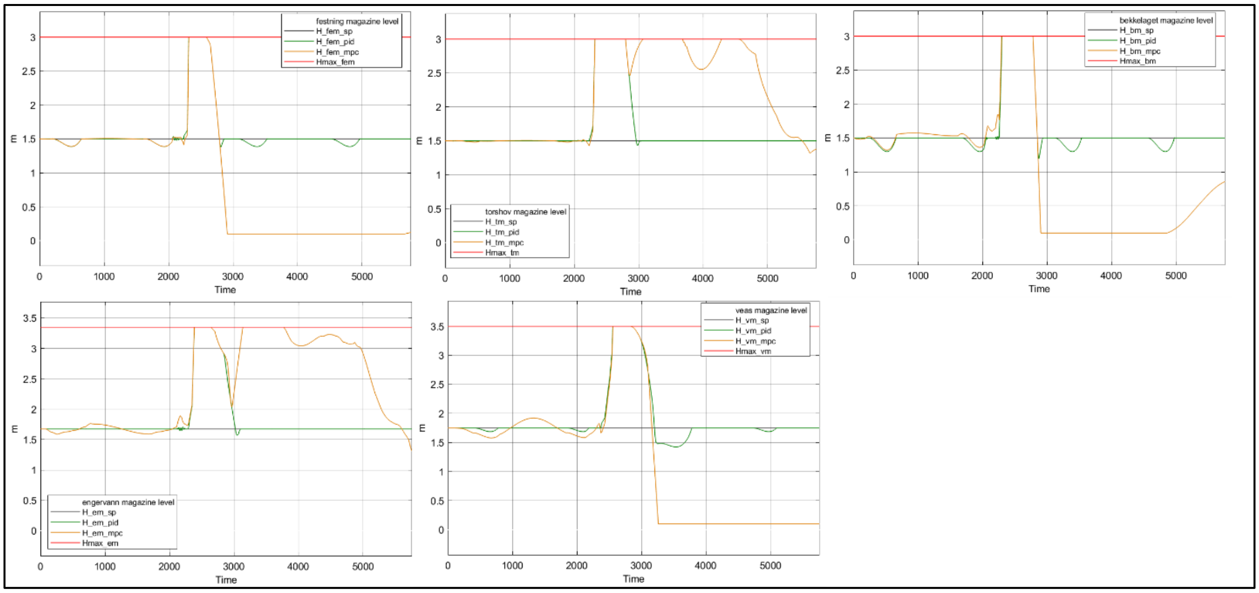

Figure 38 Rain event 3, without forecast, CV results

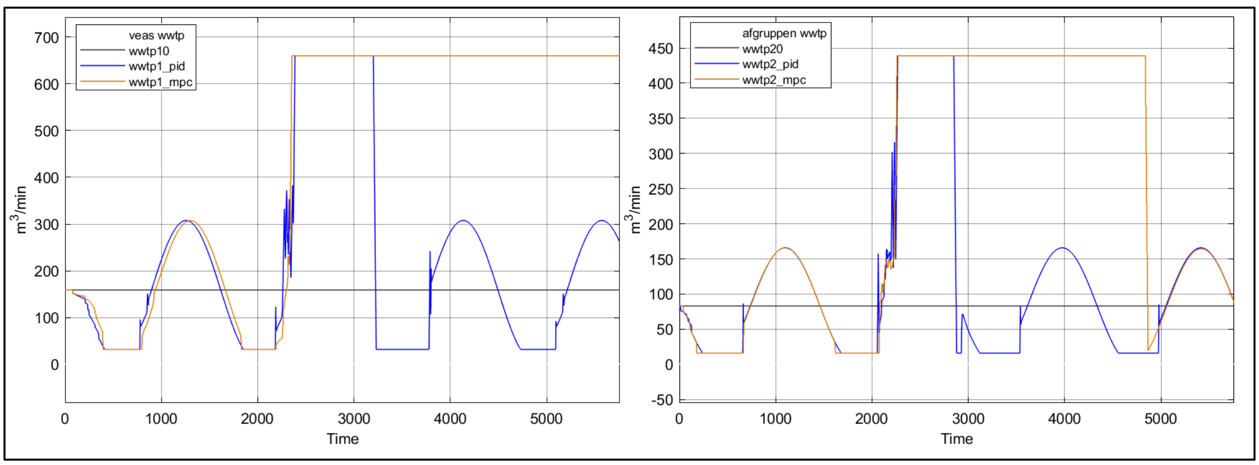

Figure 39 Rain event 3, without forecast, WWTP inflows

10.1.3.3 Rain event 3 with forecast data, controller results

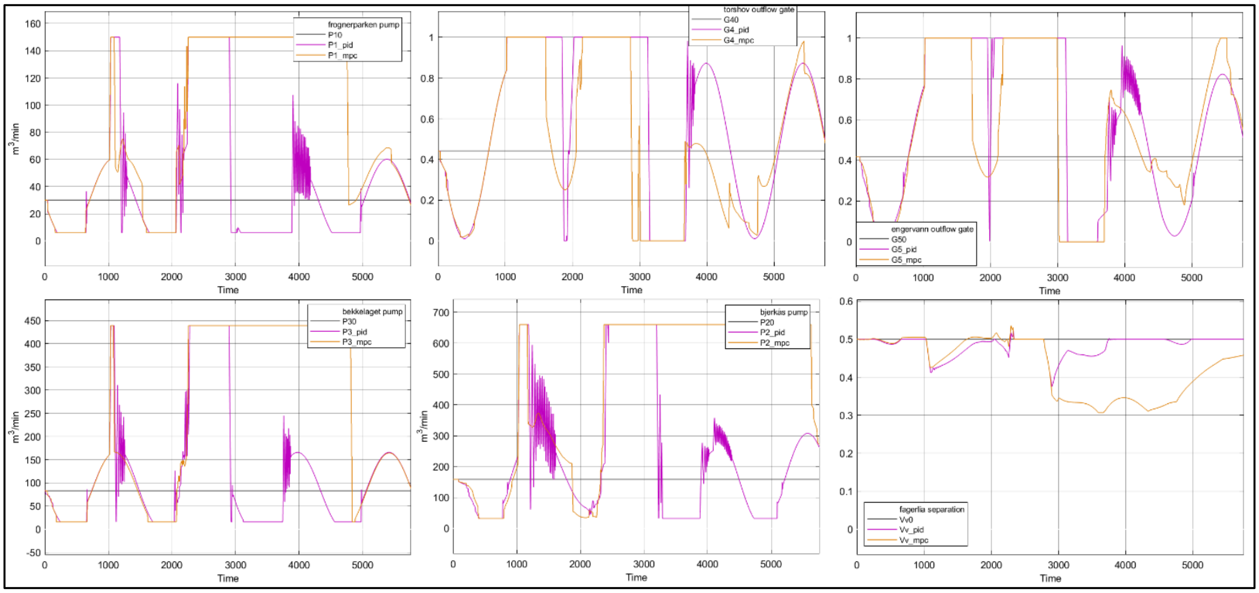

Figure 40 Rain event 3, with forecast, MV results

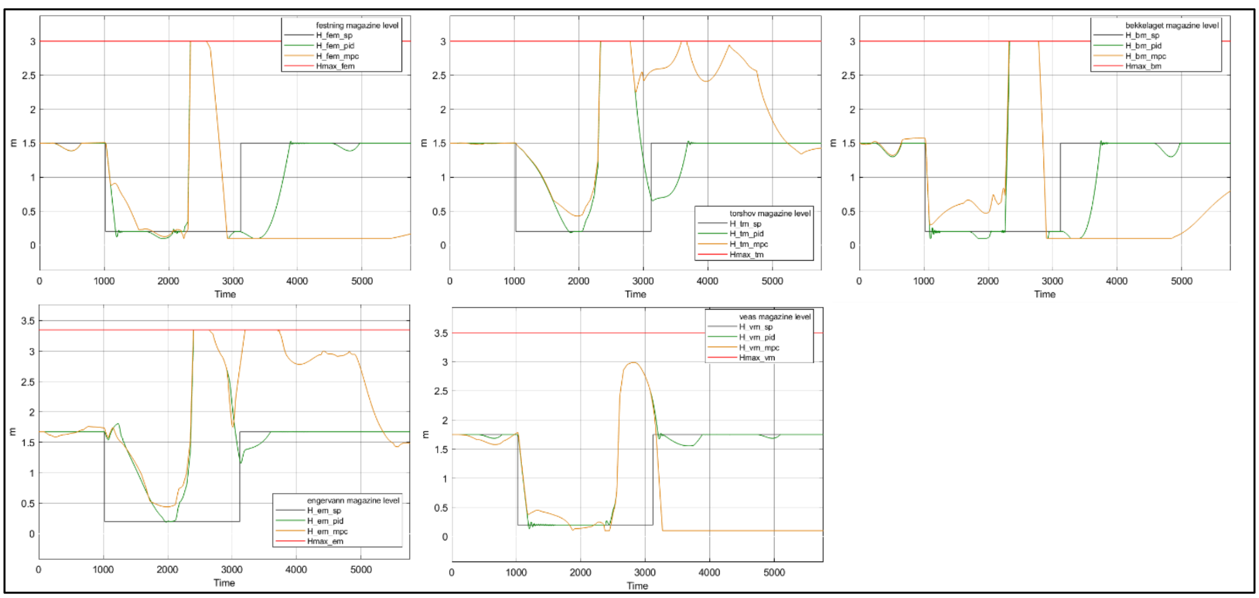

Figure 41 Rain event 3, with forecast, CV results

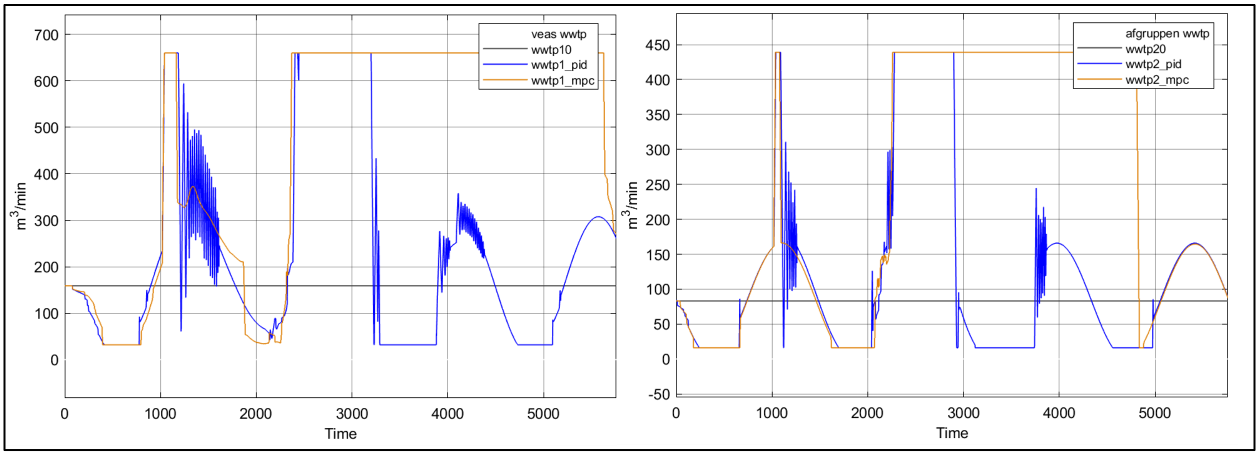

Figure 42 Rain event 3, with forecast, WWTP inflows

10.1.4 Simulation 4

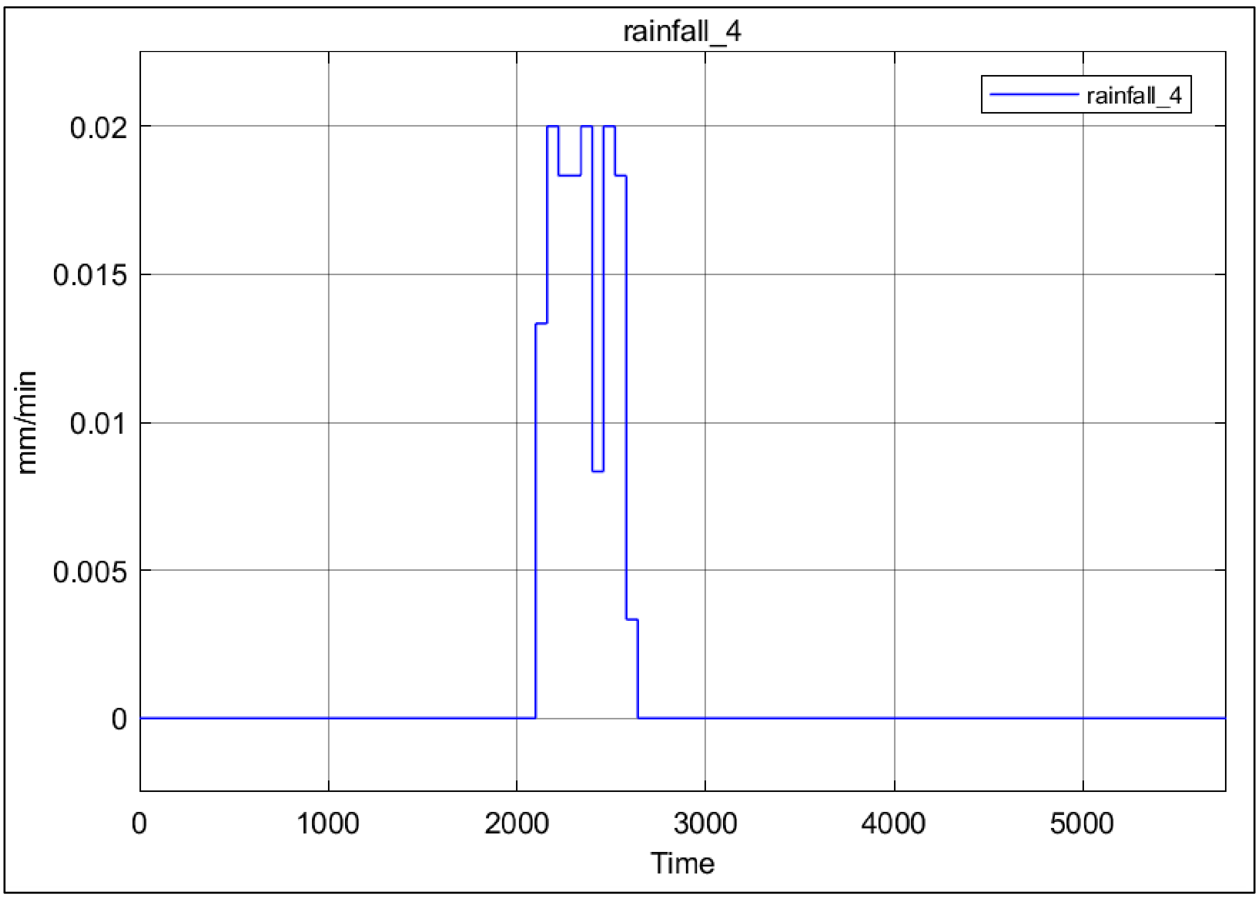

Figure 43 Simulation 4, Rain event 4

10.1.4.1 Input to the model, Rain event 4:

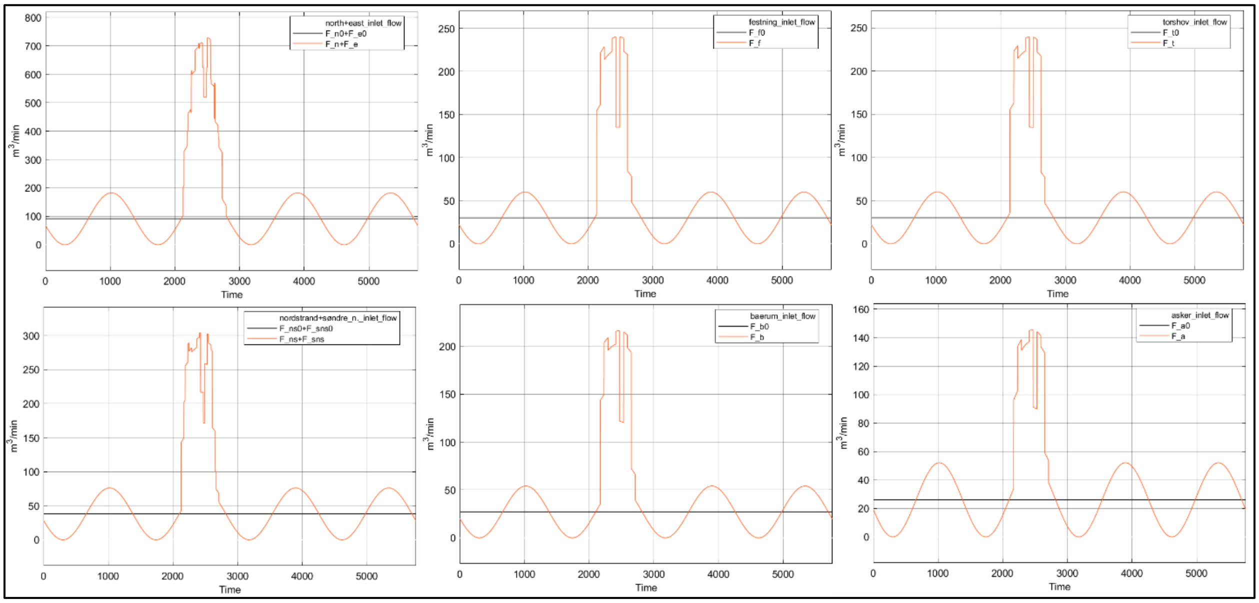

Figure 44 Rain event 4, Inlet flows/DVs

10.1.4.2 Rain event 4 without forecast data, controller results

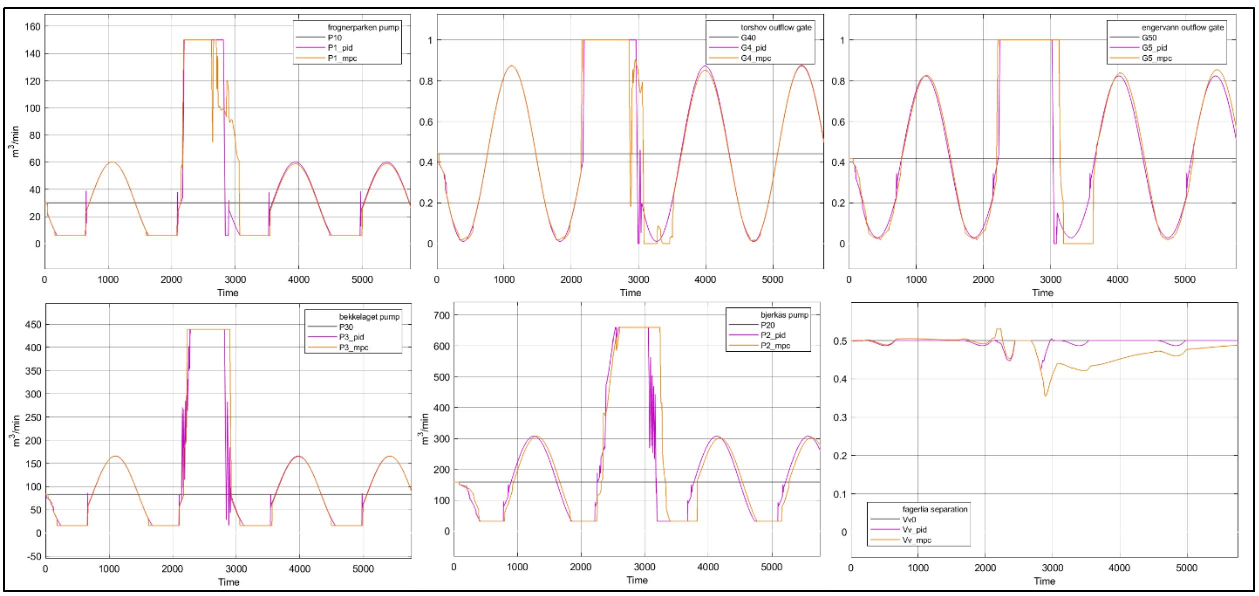

Figure 45 Rain event 4, without forecast, MV results

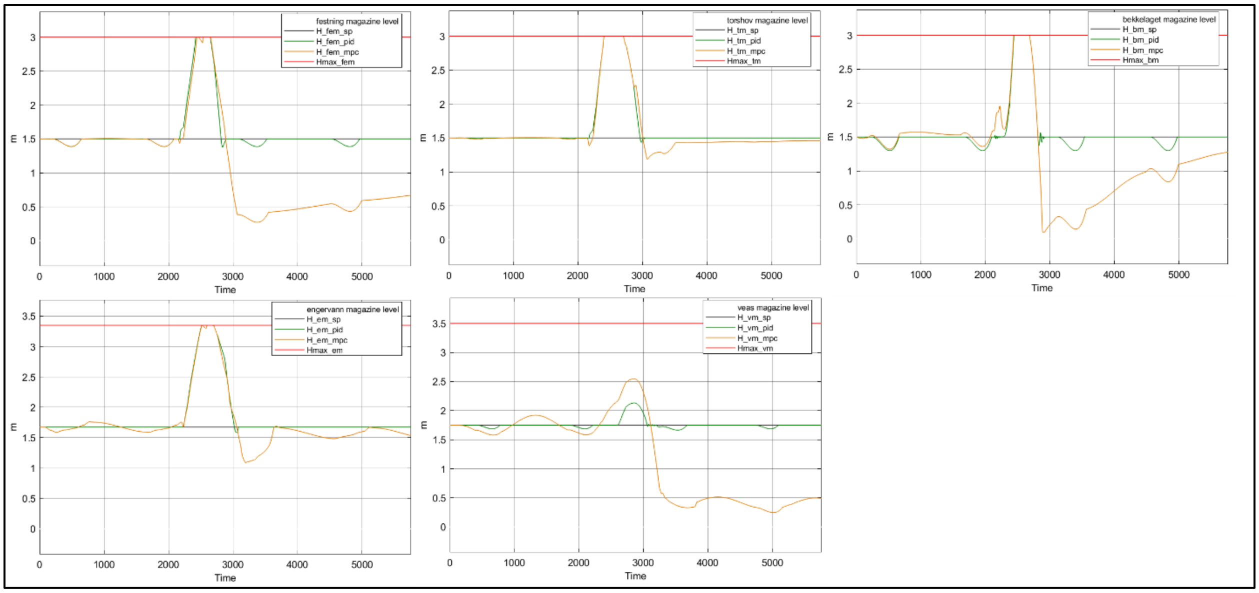

Figure 46 Rain event 4, without forecast, CV results

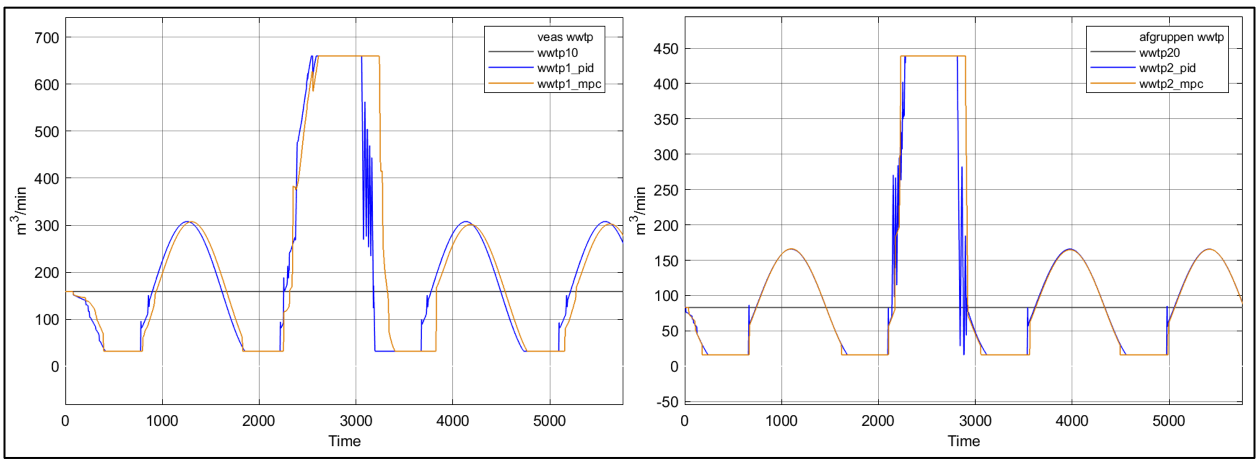

Figure 47 Rain event 4, without forecast data, WWTP inflows

10.1.4.3 Rain event 4 with forecast data, controller results

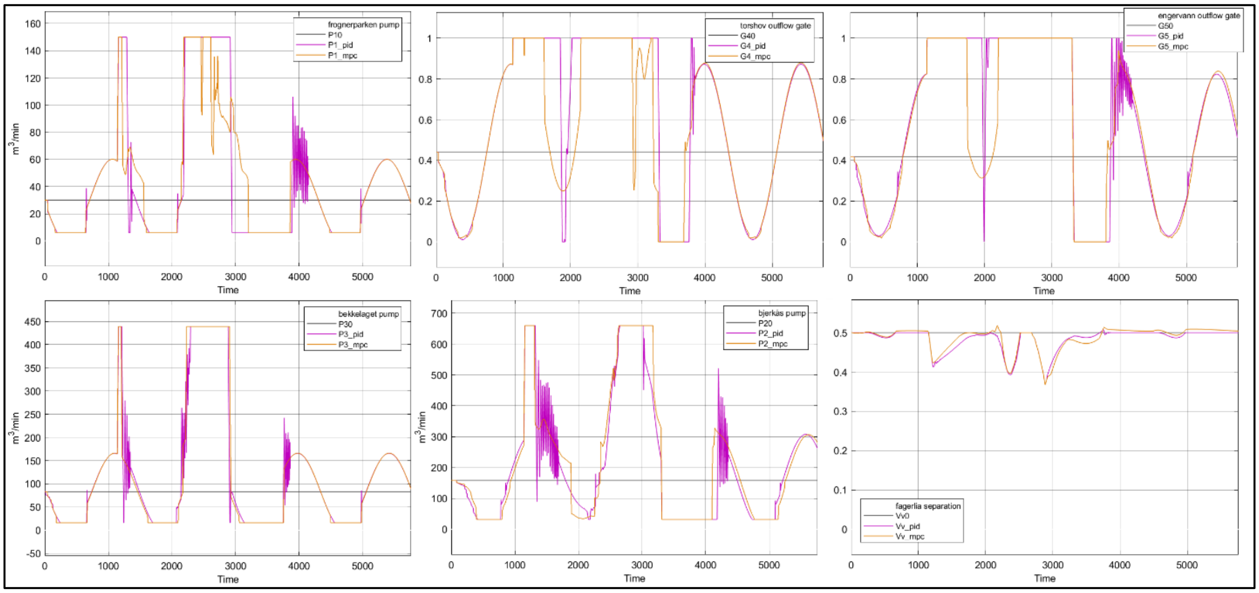

Figure 48 Rain event 4, with forecast, MV results

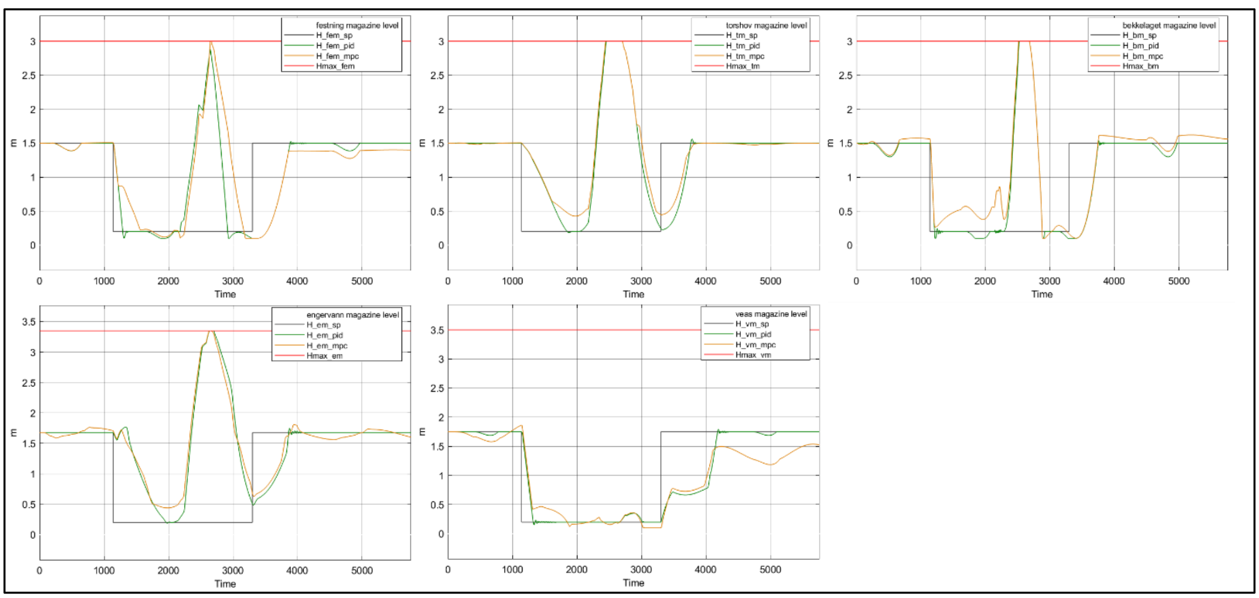

Figure 49 Rain event 4, with forecast, CV results

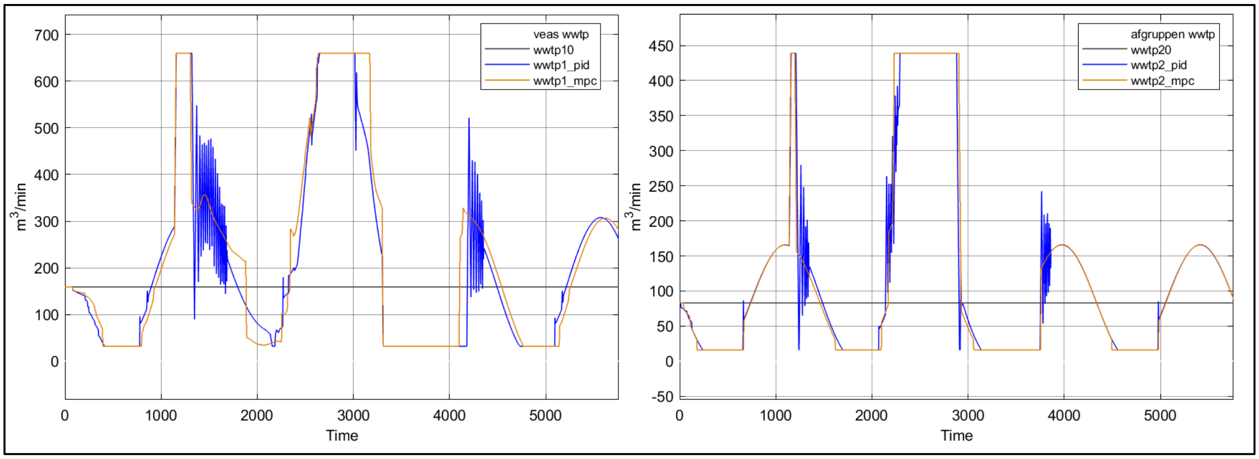

Figure 50 Rain event 4, with forecast, WWTP inflows

10.1.5 Solvers

Automatic solver solution has been utilized in MATLAB and the software has chosen solver ODE23t for all scenarios and controllers. In event 2 and event 3, for some control algorithms, based on MATLABs recommendation, zero crossing control was enabled with the option, adaptive algorithm. Simulation runs' information are shown in table Table 20 MATLAB/Simulink simulation solvers.

The MATLAB/Simulink model in this study has already forced the limitations. Simultaneous PI and MPC control strategy runs in parallel was not applicable because of step size, solver not converging and buffer size problems. Even single simulations took some effort to optimize the solvers and resulted in warnings occasionally. MIMO control alone with 4 days of simulation period involving one rain event took 10 minutes with a personal laptop.

Table 20 MATLAB/Simulink simulation solvers

Rain event	Controller	Solver	Simulation run information
1	PI	Ode23t	-
1	PI+F	Ode23t	-
1	MPC	Ode23t	-
1	MPC+F	Ode23t	-
2	PI	Ode23t	Zero crossing control enabled; algorithm adaptive. Warnings: zero crossings.
2	PI+F	Ode23t	Zero crossing control enabled; algorithm adaptive. Warnings: zero crossings.

2	MPC	Ode23t	-
2	MPC+F	Ode23t	-
3	PI	Ode23t	-
3	PI+F	Ode23t	Zero crossing control enabled; algorithm adaptive. Warnings: zero crossings.
3	MPC	Ode23t	-
3	MPC+F	Ode23t	Zero crossing control enabled; algorithm adaptive. Warnings: zero crossings.
4	PI	Ode23t	-
4	PI+F	Ode23t	-
4	MPC	Ode23t	-
4	MPC+F	Ode23t	-

10.2 Treatment results Overview

Table 21 WWTP treatment results

Rain event	Controller	WWTP Veas treated [10^5 m^3]	WWTP Bekkelaget treated [10^5 m^3]	Total treated water [10^5 m^3]
1	PI	13.04	7.07	20.12
1	PI+F	13.17	7.38	20.55
1	MPC	16.71	9.17	25.88
1	MPC+F	16.72	9.19	25.91
2	PI	13.11	7.14	20.25
2	PI+F	13.27	7.48	20.75
2	MPC	18.81	10.29	29.1
2	MPC+F	18.84	10.28	29.12
3	PI	12.72	6.73	19.45
3	PI+F	13.58	7.0	20.58
3	MPC	25.65	14.09	39.74
3	MPC+F	26.3	14.13	40.43
4	PI	11.99	6.68	18.68
4	PI+F	12.1	6.93	19.04
4	MPC	12.56	6.88	19.44
4	MPC+F	12.66	6.93	19.59

Treatment results are not a good indicator of the performance of the control strategies since the MPC simulations always ended up with less wastewater in the system than the PI controllers. In other words, PI runs had more water to-be-treated in the system when the simulation periods end. Additionally in extreme cases, especially rain event 4, treated water measurements became unreliable. However, overflow model does not get affected by previously explained issues and it is clearly a very strong indicator for the performance of the model as aimed from the start of the work.

10.3 Overflow results

Total overflows and overflow volumes for every rain event with control strategies are presented visually in a compact from. Control strategies are zero control, PI, PI+F, MPC and MPC+F. "+F" notation means the upgrade: real-time optimization with forecast data on PI and MPC control strategies. Zero control means the performance of the system when the pumps and gates/MVs are kept at their dry weather/steady state values. In other words, no control is applied. This can be interpreted as a ground level for control strategies that emphasizes how much overflow can be avoided with control.

Since it may be hard to differentiate the results in figures, numerical results will be presented additionally.

10.3.1 Simulation 1, Rain event 1

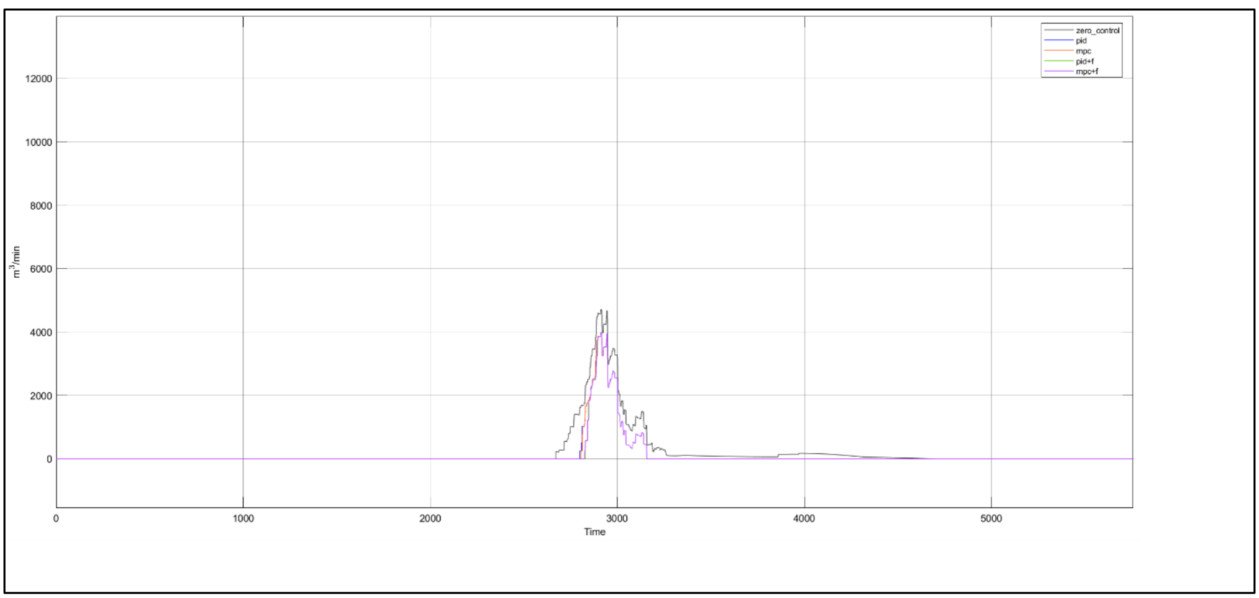

Figure 51 Rain event 1, Overflows

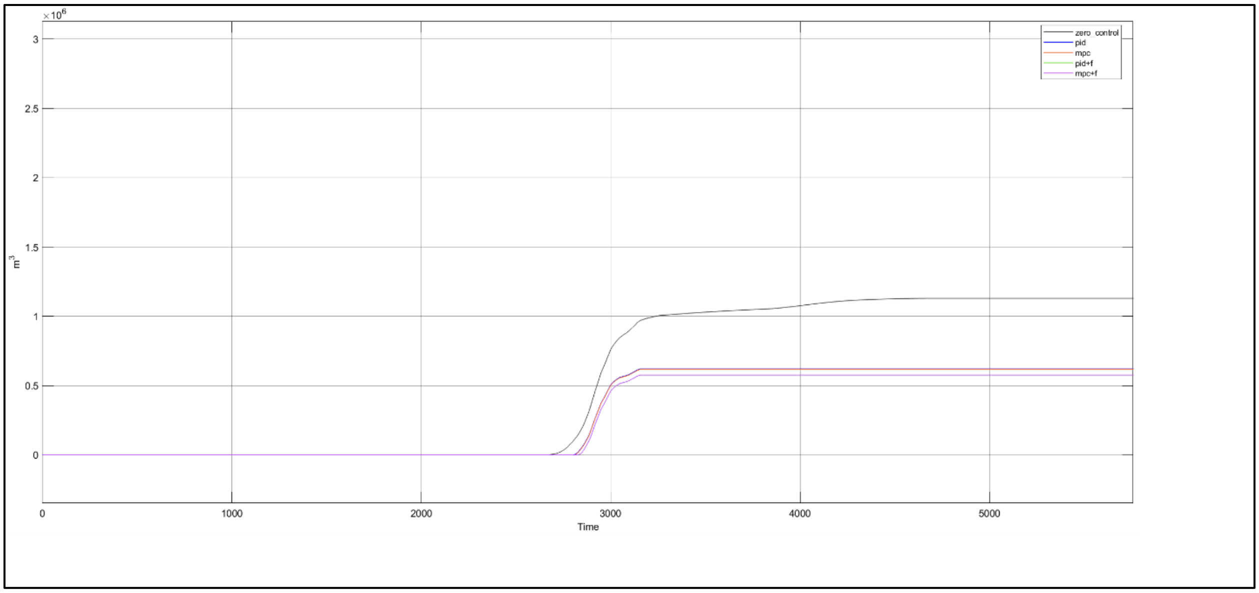

Figure 52 Rain event 1, Overflow volumes

10.3.2 Simulation 2, Rain event 2

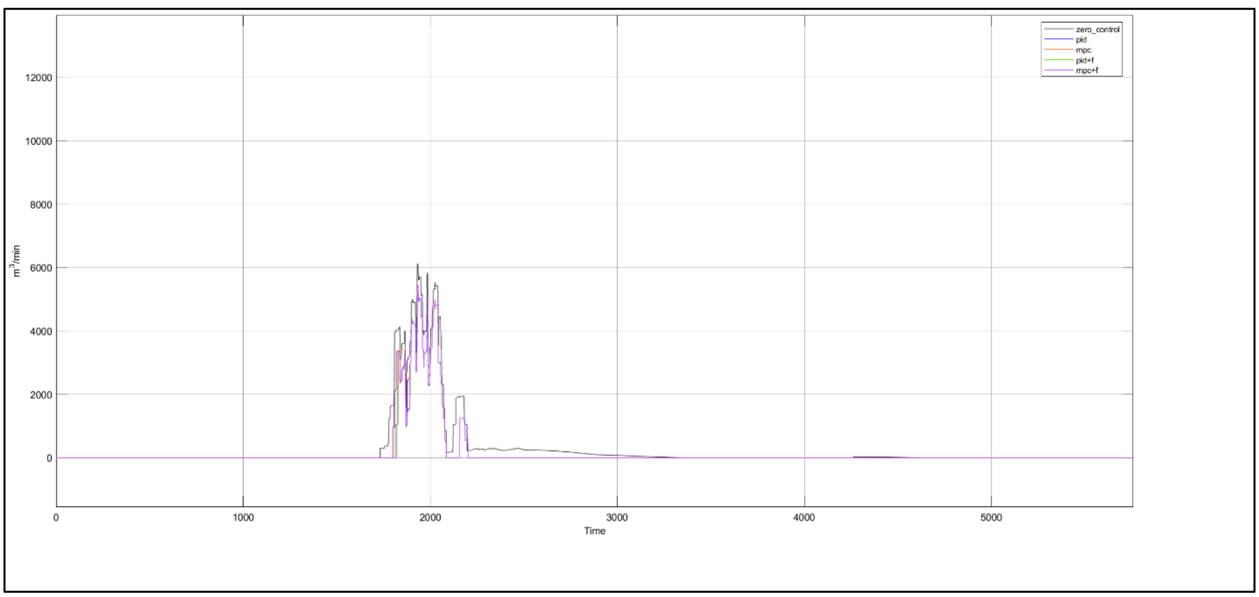

Figure 53 Rain event 2, Overflows

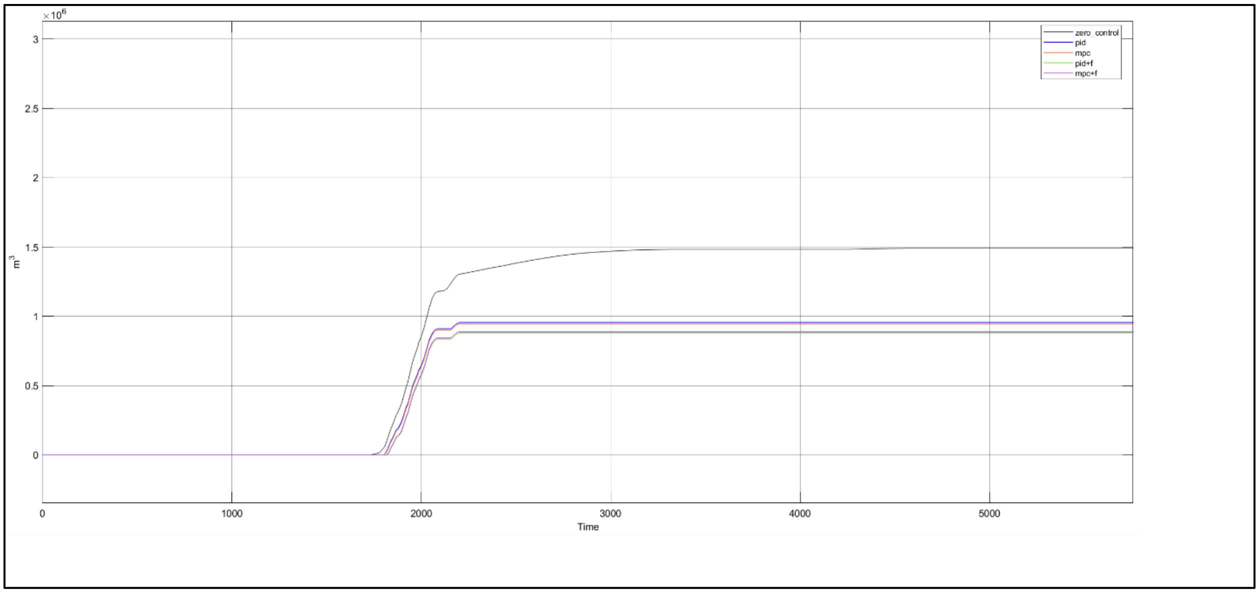

Figure 54 Rain event 2, Overflow volumes

10.3.3 Simulation 3, Rain event 3

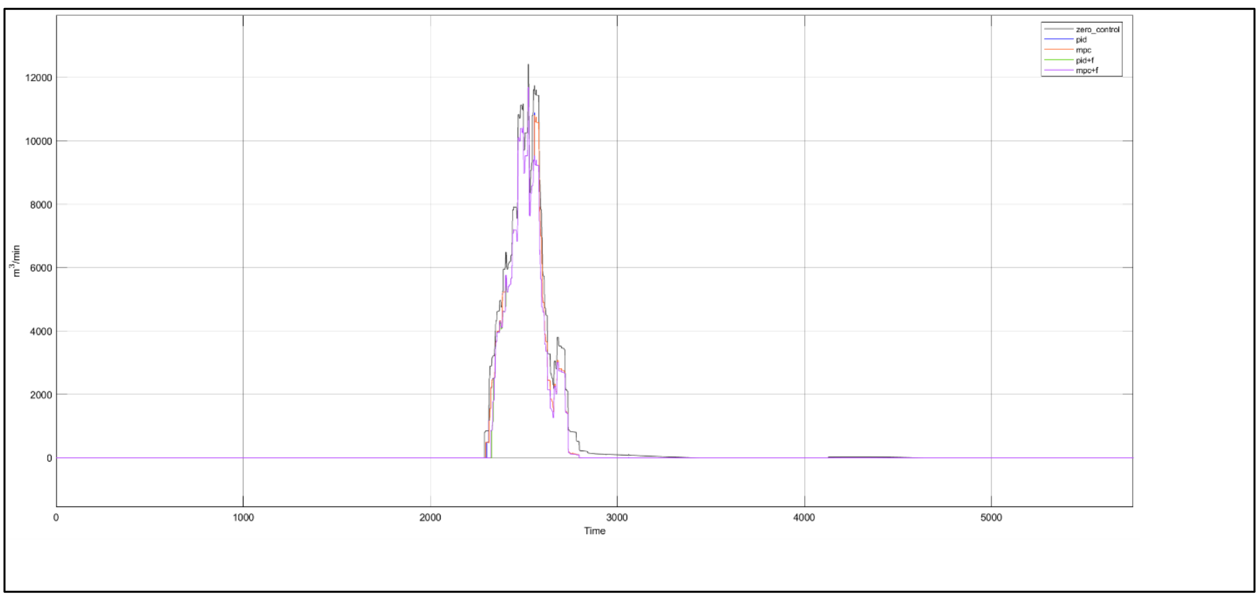

Figure 55 Rain event 3, Overflows

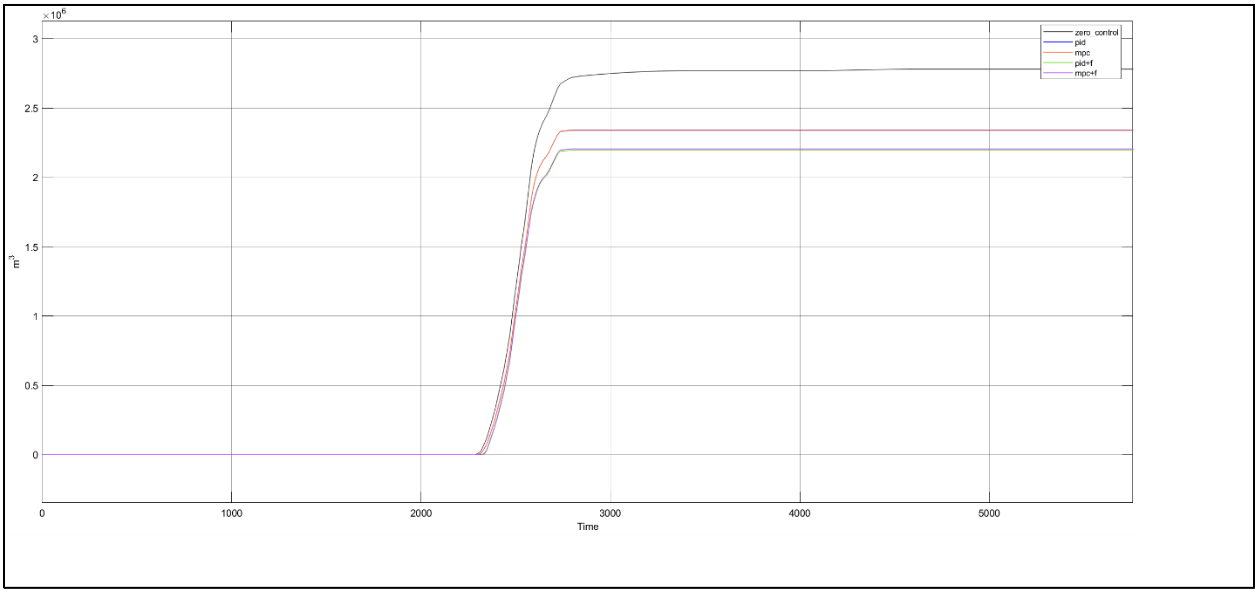

Figure 56 Rain event 3, Overflow volumes

10.3.4 Simulation 4, Rain event 4

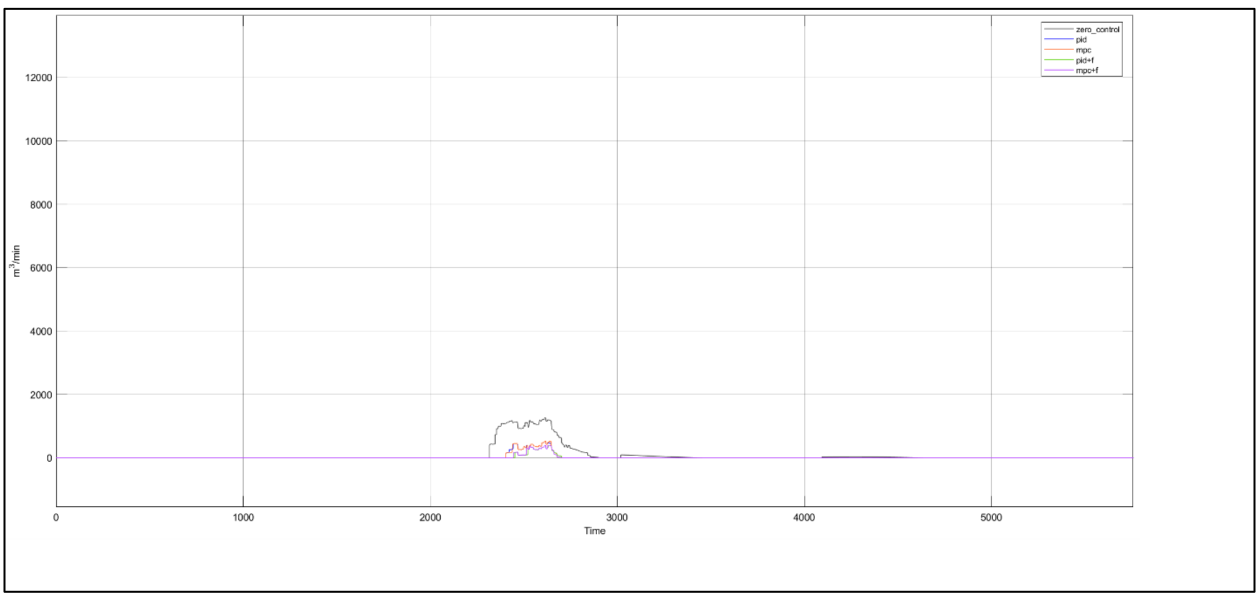

Figure 57 Rain event 4, Overflows

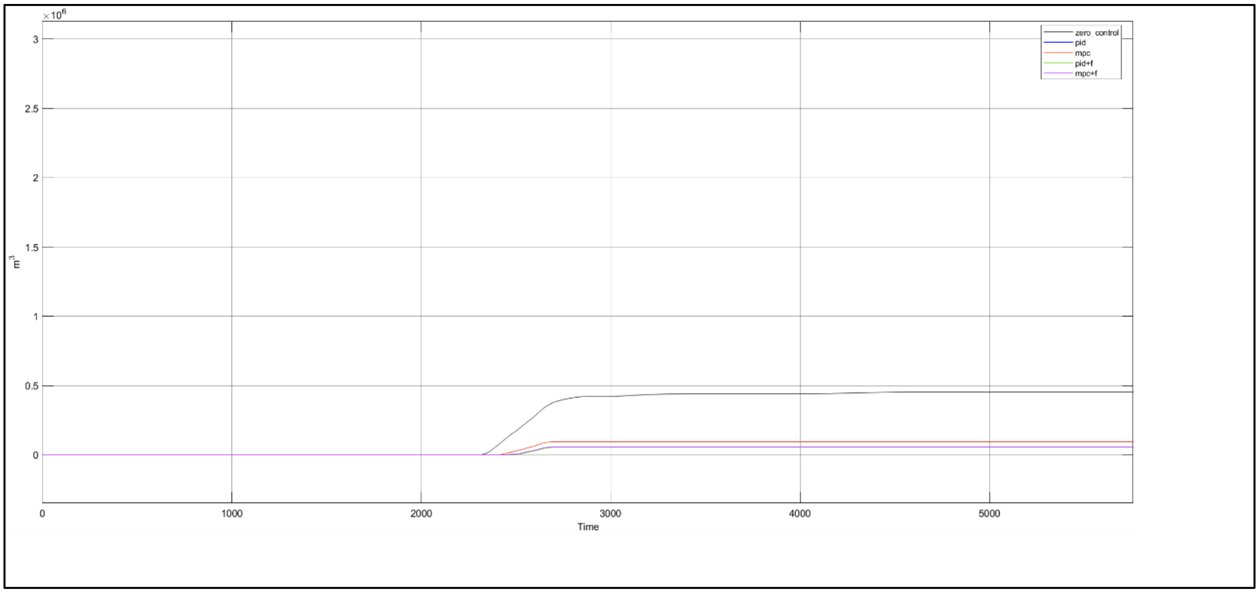

Figure 58 Rain event 4, Overflow volumes

Hard to differentiate the control strategies in the result figures so numerical results are better to clearly analyze the overflows and total overflow volumes.

10.3.5 Total overflows

Table 22 Total overflows

Event	Zero control [10^5 m^3]	PI [10^5 m^3]	PI+F [10^5 m^3]	MPC [10^5 m^3]	MPC+F [10^5 m^3]
1	11.30	6.21	5.76	6.17	5.76
2	14.91	9.55	8.8	9.46	8.9
3	27.82	23.41	21.96	23.4	22.06
4	4.54	0.95	0.55	0.94	0.56

As expected, extreme rain event 3 has substantial amount of overflows and moderate rain event 4 has relatively little overflows. All control strategies have avoided a lot of overflows compared to no control. PI control has more overflow than MPC in all 4 events. However, PI with forecast performed better than MPC with forecast. Real time set-point optimization using forecast data improved PI controllers more than MPC. This might have been because MPC already can account for disturbances in advance since it is a “predictive” control algorithm and forecast data cannot provide the same improvement that it provided to PI controllers.

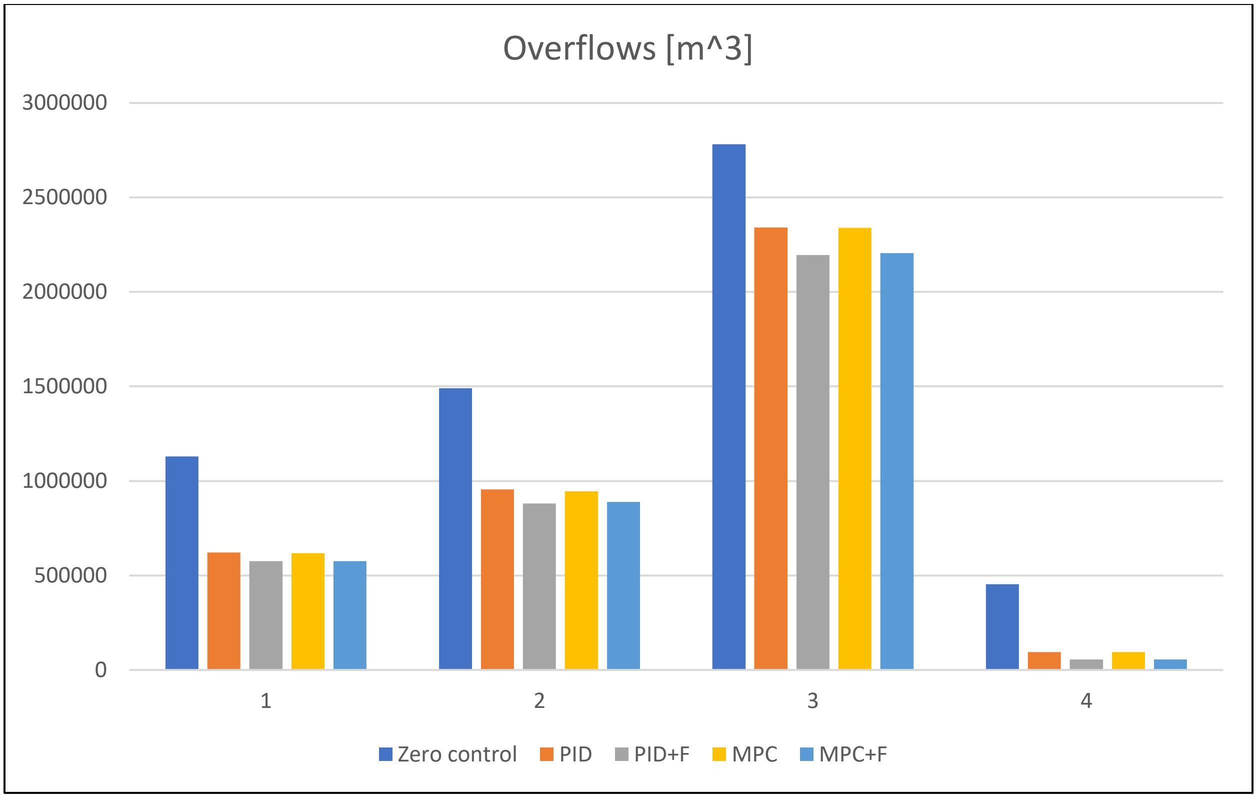

Figure 59 Chart of total overflows

From Figure 59 Chart of total overflows, it can be observed that the real-time optimization with forecast data reduces the overflows more when the rain event is more extreme.

The performance of the PI and MPC strategies are very close and not comparable in this visualization.

Overflow volume difference between the zero-control and the control strategies are similar for all rain events. Control strategies are not perfect but still, this is a strong indicator of the limited capacity of the system itself. Maximum capacity of the system is what really determines the overflows under heavy rain events (for example rain event 1,2 and 3).

RTC seems it cannot contribute much to the extreme events where the capacity of the system is nowhere near enough. However, advanced RTC may really shine with moderate/light rain events where it can optimize the capacity of the system.

10.4 Operational cost analysis

Overflow amount is very critical, however there are many parameters when evaluating the performance of an urban drainage system. Oslo city's large urban drainage system has many powerful actuators which use a lot of energy. Accordingly, operational cost is not a factor to be ignored in urban drainage systems.

In this work, and in all simulations, pump loads are measured and presented. If a control strategy achieves a similar performance with less energy consumption, it can easily affect the final verdict.

Pump load is basically the integration of the MV pump signal for whole simulation period. There are no loads defined for gates since it is assumed that they consume no energy to maintain a position. Energy consumption for gate operations is not included in this study. However, for Torshov and Engervann magazines outflow gates in PI and PI+F controls (figures 24, 29, 32, 37, 40, 48) oscillations were observed. Deviation caused by oscillations would result in more energy consumption for gate operations.

Table 23 Pump loads

Event	Controller	P1 [10^5]	P3 [10^5]	P2 [10^5]
1	PI	2.46	7.07	13.04
1	PI+F	2.61	7.38	13.17
1	MPC	3.26	9.17	16.71
1	MPC+F	3.28	9.19	16.77
2	PI	2.36	7.14	13.11
2	PI+F	2.48	7.47	13.27
2	MPC	3.63	10.29	18.81
2	MPC+F	3.65	10.29	18.86
3	PI	2.32	6.73	12.72
3	PI+F	2.45	7.01	13.58
3	MPC	4.97	14.09	25.65
3	MPC+F	5.01	14.13	26.30
4	PI	2.35	6.68	11.99
4	PI+F	2.48	6.94	12.10
4	MPC	2.44	6.88	12.56
4	MPC+F	2.48	6.93	12.68

Even though the PI and PI+F controls had lower pump loads, they had more oscillations than MPC and MPC+F. It is important to point out that based on how loads are defined, MV oscillations that specifically the PI control exhibited do not directly influence the pump loads shown in Table 23 Pump loads. However, oscillations would naturally have a very negative impact on pumps.

10.5 Controller comparison

Table 24 Controller comparison, numerical

4 events, 16 days	Controller	Total overflow [10^5 m^3]	Total pump load [10^5]
	PI	40.12	89.97
	PI+F	37.07	90.94
	MPC	39.97	125.46
	MPC+F	37.28	129.57

Table 25 Controller comparison, relative

4 events, 16 days	Controller	Relative overflow [%]	Relative pump load [%]
	PI	100	69
	PI+F	92	70
	MPC	97	97
	MPC+F	93	100

Table 25 Controller comparison, relative provides a concise comparison of all control strategies and a nice overview on this master's thesis work. Results are based on all four events and a total of 16 days of simulation period combined.

A common and frequent event like rain event 4 alone can be more appropriate to be assumed as all-time results of the system more than the combined results of the 4 rain events. Therefore, same results format will also be applied to the rain event 4 only.

Table 26 Controller comparison, numerical, rain event 4

Rain event 4, 4 days	Controller	Total overflow [10^5 m^3]	Total pump load [10^5]
	PI	0.95	21.02
	PI+F	0.55	21.52
	MPC	0.94	21.88
	MPC+F	0.56	22.09

Table 27 Controller comparison, relative, rain event 4

Rain event 4, 4 days	Controller	Relative overflow [%]	Relative pump load [%]
	PI	100	95
	PI+F	58	97.4
	MPC	99	99
	MPC+F	59	100

As it can be seen on Tables 25 and 27, both for all simulations and the event 4 alone, MPC performed slightly better than PI control. Pump load of MPC is higher than PI yet the difference is smaller for rain event 4.

For all scenarios, real-time optimization using forecast data have significantly improved the performance of both control strategies. PI control with forecast has performed slightly better than MPC with forecast. Additionally, PI with forecast had lower pump loads than MPC with forecast.

11 Further Work

Specialized high-fidelity modeling software's have gained a lot of ground in the field of urban drainage modeling. Initially they were used for design and planning and considered too complex and computationally heavy for advanced RTC. Today, fast progress in computational power and consistent upgrades to the high-fidelity software's make them the way to go even for modeling advanced applications like RTC. Situation has gone beyond research. Currently in business, these systems (modeling and the implementation) are open for negotiations for any customer that has a drainage system in hand.

General modeling software's such as MATLAB/Simulink can be used to model drainage systems. Control algorithms are rather more established yet, the model must be much simpler because it will not be possible to model hydrodynamics with full extent. Regardless, the model can be relevant and very useful according to purpose of modeling and expected accuracy. Accordingly, in this work, a modeling work of Oslo SN, testing and comparison of PI and MPC controls under rain scenarios and the control improvements with real-time optimization using forecast data are presented.

Throughout this study, initial collaboration between Oslo VEAS, DHI and Oslo Metropolitan University have been gradually established. In later phases of the work, structural data and measurements for Oslo SN from VEAS as well as the Oslo SN high-fidelity MIKE model from DHI made accessible to me. Oslo MIKE model is a calibrated model with the data provided from VEAS. Accordingly, catchment parameters had been adopted from the Oslo MIKE+ models catchment parameters. Yet, overall calibration of the MATLAB/Simulink Oslo SN model used in this study should be done against the VEAS measurements and the simulations of the MIKE model. Being aware of this eventual calibration necessity, flexible parameters have been defined to calibrate the MATLAB/Simulink Oslo SN model fast and efficiently. Unfortunately, time left for this calibration was evaluated insufficient. Suggested first future work is to finalize the calibration of the Oslo SN model.

In this study, all four rain events under all simulations have been assumed having the same rainfall density among all Oslo region catchments. These historical rain events' measurements are from Oslo/Blindern meteorological station which is at Oslo centrum. This point lies between the WWTPs and is roughly in the middle of Oslo region of the model. Originally, method was to find various measurements around Oslo region for the same events and to model the rain scenarios more accurately with varying density across the model. However, there were not enough measurement data available to implement realistic and uneven rain among catchments. Although it has not been implemented in this study, an alternative idea to the insufficient rain measurement can be to create uneven rain scenarios artificially. Accordingly, one of the four rain events could have been chosen and two uneven scenarios of that event could have been created. In the first one, rain density for eastern catchments could have been increased while reducing it for the western catchments and vice versa for the second uneven scenario. While doing so, it is important to keep the total rainfall over entire region unchanging between the original event and two artificial ones. This would validate the comparison between the three events and reveal if control algorithms can perform better under uneven rain scenarios or not. It may also indicate if the Oslo SN is more vulnerable to rain from east or west side. Rainfall event 4 is an appropriate candidate for this because it is a moderate event unlike other events which are extreme and rare.

In this study a basic ratio model for rainfall-runoff with a simple conversion to the inlet flows has been utilized. Moisture for catchment areas and hydrological processes were not included. Such processes are not very suitable to include in MATLAB/Simulink modelling approach. For that purpose, a high-fidelity model such as MIKE from DHI can be used. DHI included that the control strategies in this study are not likely to be directly applicable in Oslo MIKE model since two models inherently function different and the complexity is very distinct. In a possible future work, a control strategy to be deployed in Oslo SN MIKE model should probably be developed and tested in MIKEs own control toolbox.

Although MPC was the supposedly the ideal control solution in the initial discussions and in the literature review, in this study, MIMO MPC strategy performed similar to the SISO PI control strategy. Both strategies had their advantages and disadvantages. Still, it should be kept in mind that a linear MPC was deployed in a non-linear model with long delays. Even the linear MPC took about 10 minutes to finalize a 4-day simulation with my personal Lenovo laptop. Previous attempts to run a PI and an MPC model in parallel did not work since the solvers could not converge and giving warnings of buffer sizes. As a result, PI and MPC models were run separately, their results were logged and visualized in another MATLAB/Simulink model. In this perspective, next step to improve the control could be to deploy a non-linear MPC for Oslo SN. Although they have higher computational loads, solutions such as predicting a fixed number of iterations and the improvements in computational capacity enabled them to be utilized effectively in urban drainage systems. For future work, transition to non-linear MPC and other advanced controls should be, in my opinion, in parallel with a transition to a high-fidelity detailed and realistic model specialized in urban drainage systems.

As for the real-time optimization with forecast data used in this study, DHI mentioned a similar strategy within the Future City Flow project. For future work, real time optimization can be improved to be in par with real implementations. Real-time optimization would use NWP or radar estimations and the optimization in the model would be more advanced than “rainy/not rainy” strategy with fixed set-point changes used in this study. Set points should change continuously based on the real-time forecast and its certainty.

To simulate a realistic outcome from an RTC implementation, runs should cover longer periods for example a complete year. Period should be historical data. In historical data, common rain events will be many and extreme events will be very rare. An implementation of an RTC is therefore should be evaluated based on not only the events’ severity but also based on their frequency.

Extreme rain events easily hit the maximum capacity of the Oslo SN. Under such circumstances, even with perfect control, overflows cannot be further reduced. Running the system at full capacity under heavy rain can be as well done by the current operators.

Under moderate rain events however, an advanced RTC can distinguish. It can effectively utilize the available volume, minimize the actuator loads and seek steady flow to the WWTPs continuously without deploying many operators. Efficiency can further increase under non-equally distributed rain between catchments because the system has the Fagerlia separation weir and 2 WWTPs. It should be pointed out that moderate/light non-equally distributed rains are in the majority throughout a year and the implementation of a control strategy should be evaluated accordingly.

11.1 Comments from collaboration partners

Included people and surface area from Oslo region in the modelling was based on the available information at the start of the thesis work. Assumed people and the area for modelling is thoroughly defined in the report and can be changed for any further work with the model. Later feedback from VEAS was that for catchments, Røyken municipality should have been included instead of Lier municipality. Also, Raelingen, Skedsmo and Nittedal municipalities should have been partially included. These mentioned outer catchments already had a lower impact to the model since their imperviousness and population densities were quite low. Overall, feedback revealed that the area and the people included in the model should have been lower by a very little margin. These changes would result in a little bit lower overflows in the model. Still, it is suspected that the relative performance between the control algorithms would stay almost the same.

In this study and in general, a very critical point about the urban drainage overflows should be pointed out. Unlike a pervasive misunderstanding among politicians, environmentalists and public, urban drainage overflows caused by intense rains are highly diluted. VEAS states that an overflow to the Oslo fjord can be 90% rainwater and 10% municipal wastewater from households and other places. Accordingly, it can be assumed that even though the very intense rains cause higher overflow amounts, the lower the wastewater percentage becomes in the overflow water. More diluted water may have less impact on the water quality of the receiving water body.

VEAS emphasizes that the occasional overflows are not the only issue regarding water quality in the fjord. Regular release of treated water from the WWTPs does still play a critical role since the quality of the treated water is not ideal. Treated water amount should not be underestimated since it is a continues release and it adds up with time. For example, it is noted that daily amount of nitrogen in the "cleaned water" to Oslo fjord can easily be larger than the amount of nitrogen in a seldom overflow. It is an issue that they have recently focused on finding a solution to in the treatment process. Other factors not directly related to the sewer network can also be named on the water quality subject such as pollution and agriculture. Modelling and tracking of water quality based on the density of various substances was out of the scope of this study.

Valuable discussions with DHI revealed that the first rain wash-off of the accumulated pollutants on the run-off surface areas as well as in the interiors of the drainage network are quite impactful on the water quality of the initial overflows. Time accumulation and wash-off of such pollutants can be modelled in MIKE software yet the scope of this study did not cover these accumulative factors.

Although overflows can be used for decision making and alerting public for bad water quality in Oslo fjord, since overflows are not the solely decisive factor, a need for an environmental decision-making system inclusive of all significant factors of water quality became evident in the meeting with OsloMet, VEAS, Oslo VAV, and DHI. A holistic decision-making system could combine the overflows, surface wash-off, treatment process, temperature, circulation in and out to the fjord to name among many. DHI stated that such systems exist and are in operation today.

These systems alert the water quality of the beaches near to the overflow outlets. A system is currently active in Copenhagen and can be seen on the web. (Group, 2022) The system was previously proposed by DHI for Oslo. There are also other suppliers that can deliver such systems, yet currently, it was evaluated unnecessary.

A holistic model for the Oslo Fjord would not only track the water quality for alerting the public but could possibly create and efficient and robust system that tracks the health of the Oslo fjord. It could investigate the water quality factors and reveal insights to the roots of problems, simulate scenarios and possible alterations to empower future decisions. That could create a basis for a powerful operation team starting from this collaboration with OsloMet, VEAS, VAV, and DHI.

12 References

Congcong Sun, L. R.-D. (2021). Control-oriented quality modelling approach of sewer networks. *Journal of Environmental Management, 294*(113031).

Dale E. Seborg, T. F. (2004). *Process Dynamics and Control.* USA: John Wiley & Sons Inc.

Department, O. M. (2020). *Climate Change Vulnerability Analysis for Oslo.* Oslo.

DHI. (2022). *Decision-support system for integrated stormwater management*. Retrieved from Future city flow: https://www.dhigroup.com/operational-services/future-city-flow

Group, D. (2022). *Badevandsudsighten*. Retrieved from https://kbh.badevand.dk/

gruppen, A. (2022, 5 10). *Bekkelaget Renseanlegg*. Retrieved from https://afgruppen.no/prosjekter/anlegg/bekkelaget-renseanlegg/

Haugen, F. A. (2018). Simulations and real applications of PI and MPC averaging level control in a water resource recovery facility. *SIMS-2018.*

Inc., T. M. (2021). MATLAB version 2021b. Natick, Massachusetts.

J. Sitterson, C. K. (2018). An Overview of Rainfall_Runoff Model Types. *International Congress on Environmental Modelling and Software.* Colorado: BYU ScholarsArchive.

Kjell Terje Nedland, B. P. (2005). Oslo: Aquateam - Norsk vannteknologisk senter A/S.

Lorenzo Benedetti, J. L. (2013). Modelling and monitoring of integrated urban wastewater systems. *Water science and Technology*, 1203-1215.

Manfred Schuetze, J. A. (2021). Real time control of sewer systems - a convenient approach to MPC in practice. *15th International Conference on Urban Drainage.* (Online).

Meteorologisk institutt, N. (2021). *Oslo (Blindern) Meteorological Station*. Retrieved from YR: https://www.yr.no/en/statistics/graph/5-18700/Norway/Oslo/Oslo/Oslo%20(Blindern)?q=2019-06-11

N. D. Sto Domingo, A. R. (2010). Flood analysis in mixed-urban areas reflecting interactions with the complete water cycle through coupled hyrologic-hydraulic modelling. *Water Science & Technology, 62.6*, 1386-1392.

Nadia Schou Vorndran Lund, A. K. (2018). Model predictive control of urban drainage systems: A review and perspective towards smart real-time water management. *Critical Reviews in Environmental Science and, 48*(3), 279-339.

O. Mark, G. S. (2008). Analysis and Adaptation of Climate Change Impacts on Urban Drainage Systems. *11th International Conference on Urban Drainage.* Edinburg, Scotland, UK.

Oslo. (2019). *Application Form for the European Green Capital Award 2019, 9 Wastewater management.* Oslo: European Green Capital.

P. A. Stentoft, L. V.-N. (2020). Integrated model predictive control of water resource facilities and sewer systems in a smart grid: example of full-scale implementation in Kolding. *Water Science & Technology, 81.8*, 1766-1777.

Peter M. Bach, W. R. (2014). A critical review of integrated urban water modelling - Urban drainage and beyond. *Environmental Modelling & Software, 54*, 88-107.

Rosenthal, R. E. (2007). *GAMS - A User's Guide.* Retrieved from GAMS Development Corporation: https://www.un.org/en/development/desa/policy/mdg_workshops/training_material/gams_users_guide.pdf

Skogestad, S. (2002). Simple analytic rules for model reduction and PID. *Journal of Process Control*, 291-309.

Theo G. Schmitt, M. T. (2004). Analysis and modeling of flooding in urban drainage systems. *Journal of Hydrology, 299*, 300-311.

VEAS. (2022, 5 10). *Vann*. Retrieved from En renere Oslofjord: https://www.veas.nu/produkter/vann

Wolfgang Rauch, J.-L. B.-K. (2002). Mathematical modelling of integrated urban drainage systems. *Water Science & Technology, 45*(3), 81-94.